NTNU

Norwegian University of
Science and Technology

Modeling and Characterization of Liquid Vapor Equilibrium of N-methyl-1,3-Propanediamine for CO2 Capture

Using the Extended UNIQUAC Framework

Christian Morten Jens

Chemical Engineering and Biotechnology
Submission date: June 2011
Supervisor: Hallvard Fjøsne Svendsen, IKP

Norwegian University of Science and Technology
Department of Chemical Engineering

NTNU
Norwegian University of Science and Technology

Faculty of Natural Sciences and Technology
Department of Chemical Engineering

MASTER THESIS 2011

Title: Modeling and characterization of liquid vapor equilibrium of N-methyl-1,3-Propanediamine for CO_2 capture	**Subject (3-4 words):** CO_2 capture N-methyl-1,3-Propanediamine Thermodynamic modeling Extended UNIQUAC model
Author: Christian Morten Jens	**Carried out:** 24.01.2011 – 04.07.2011
Supervisor: Hallvard F. Svendsen	**Number of pages** **Main report:** 87 **Appendix:** 37

ABSTRACT

Goal of work:
- Thermodynamic characterization of the phase- and chemical equilibrium of N-methyl-1,3-Propanediamine and CO_2 through VLE experiments
- Model development based on the determination of the interaction parameters from the extended UNIQUAC activity coefficient framework.

Conclusions and recommendations:
In this work the loaded MAPA system has been thermodynamically characterized. This was done by measuring the phase- and chemical equilibrium in the laboratory, as vapor - liquid - equilibrium data. A thermodynamical model that was based on the extended UNIQUAC activity coefficient framework was used in an attempt to model these data. The parameters of the extended UNIQUAC model and the unknown carbamate equilibrium constants were determined in an regression analysis where the experimentally determined data were used. The parameters and equilibrium constants found are able to predict the experimental data accurately below loadings of one.

I declare that this is an independent work according to the exam regulations of the Norwegian University of Science and Technology

Date and signature: .Trondheim 29.06.2011.....

Contents

List of Figures

LIST OF FIGURES

LIST OF FIGURES

List of Tables

Glossary

A	= Volume %.
$\mathbf{a_i}$	= Group effect parameter.
B	= Second virial coefficient [mol/m^3].
C	= Third virial coefficient [mol^2/m^6].
$\mathbf{B^{HS}}$	= Hard sphere volume.
$\mathbf{\bar{b}_i}$	= Reduction variable = $\left(\frac{\partial B}{\partial N_k}\right)$.
$\mathbf{b_i}$	= Group effect parameter.
$\mathbf{c_i}$	= Group effect parameter.
$\mathbf{d_i}$	= Group effect parameter.
$\mathbf{e_i}$	= Group effect parameter.
G	= Gibbs free energy [kJ].
H	= Enthalpi [kJ/mol].
i	= summation variable.
j	= summation variable.
K	= Equilibrium constant.
k	= summation variable.
k	= Boltzmanns constant [$m^2kgs^{-2}K^{-1}$].
$\mathbf{l_i}$	= Group effect summation notation variable.
N	= mol.
$\mathbf{N_A}$	= Avogadro's number = $6.0221415 \cdot 10^{23}$.
$\mathbf{n_t}$	= total mol.
$\mathbf{p_i}$	= Partial pressure of component i [kPa].
$\mathbf{\bar{v}_i}$	= Molecular volume of component i [m3/mol].
$\mathbf{Q_i}$	= Van der vaals volum of component i, a UNIQUAC parameter used in the regression.
R	= Universal gas constant [J/Kmol].
r	= Distance between two molecules [m].
$\mathbf{R_i}$	= Van der vaals surface of component i, a UNIQUAC parameter used in the regression.
$\mathbf{T_C}$	= Critical temperature [K].

T	= Temperature [K].
u	= Total energetic interaction parameter u, a UNIQUAC parameter used in the regression.
$\mathbf{u_0}$	= Base energetic interaction parameter u_0, a UNIQUAC parameter used in the regression.
$\mathbf{u_0}$	= Temperature dependent energetic interaction parameter u_t, a UNIQUAC parameter used in the regression.
V	= Volume $[m^3]$.
X	= Plotting variable used in Modfit.
$\mathbf{x_i}$	= Mole fraction of component i in the gas phase [dim. less].
Y	= Responce from the model Modfit runs.
$\mathbf{y_i}$	= Mole fraction of component i, usually in the gas phase [dim. less].
α	= loading [mol CO_2/ mol amine.
$\varphi_\mathbf{i}$	= fugacity coefficient of component i [din. less].
μ	= chemical potential.
$\delta_\mathbf{ij}$	= Notation that is of great use when differentiating complex summation expressions, and especially when the goal is to obtain the differentials denoted by "i" and "j".
ζ	= Extent of reaction.
$\mathbf{\Delta}$	= Symbolizes change, i.e. the difference before - after.
λ	= Lagrangian multiplier.
ϕ	= Intermolecular potential.
ϵ	= Parameter that defines the repulsion between two molecules.
σ	= Radius of a molecule.
γ	= Activity coefficient [dim. less].
MAPA	= N-methyl-1,3-Propanediamine.
UNIQUAC	= *UNI*versal *QUA*si*C*hemical.
NMR	= Nuclear Magnetic Resonance.
DEEA	= N,N-DIETHYLAMINOETHANOL.
BASF	= Badische Anilin- und Soda-Fabrik.
MEA	= Mono Ethanol Amin.
MEA	= Methyl Diethanol Amin.
sat	= saturated.
tot	= tot.
HTA	= High Temperature Apparatus.
HTA	= Low Temperature Apparatus.
VLE	= Vapor Liquid Equilibrium.

est	= estimated.
abs	= absorption.
eq	= equilibrium.
2.vir	= Second virial.

1

Introduction

1.1 Motivation

The world energy demand is projected to rise rapidly, and much of that demand will be met by fossil fuel conversion, predominantly coal. Industrial activity such as iron and steel making, aluminum and cement production, refineries and oil and gas production all produce massive quantities of CO_2 that can be captured and stored. One of the most feasible options regarding removal of CO_2 from a gas stream, whether low pressure, high pressure, power production or industrial origin, is absorption into a chemically reacting systems, e.g. an amine system. This technique is best employed on large point sources such as power plants or other industrial units. 40 % of the world wide CO_2 emissions stem from about 4000 point sources, thus indicating that this technology has the potential to make a significant impact on the global emissions [Hoff 2010 (15)].

In order to evaluate and optimize these processes, models that are capable of simulating the capture processes have to be developed. For the model to be accurate it is critical to have an accurate thermodynamical model, as it describes both the phase equilibrium and the chemical equilibrium in the liquid phase, where the capture reactions take place. This thermodynamical model will lie at the heart of every plantwide simulation done. The accuracy of the thermodynamical model is dependent on the activity coefficient model, i.e. the part of the thermodynamical model that takes into account the deviation from ideality. The framework for the activity coefficient model is a ”proven piece of technology” and nothing new,

but they depend on system specific "interaction parameters". These interaction parameters are unique for each component in the system and for the interaction between the components in the system, and thus have to be determined for each system specifically.

This work deals with the determination of the interaction parameters, of the extended UNIQUAC framework, in a system that captures CO_2 in aqueous N-methyl-1,3-Propanediamine (MAPA), so that it is possible to simulate the behavior of CO_2 capture in this amine system.

1.2 Aim and outline of the thesis

As stated the aim for this work has been to determine the interaction parameters of the extended UNIQUAC model applied on the system that arises when CO_2 is captured in MAPA. This was done by measuring the vapor liquid equilibrium in the laboratory and then regressing the interaction parameters of the extended UNIQUAC model until the model predicted the same experimental data that were measured.

The outline of the thesis is as follows: In chapter 2 the general theory regarding the loaded MAPA system and the model used is presented. Chapter 3 - Materials and Methods - deals with the detailed procedures used in this work, both for the modeling part and for the experimental part. Chapters 4 and 5, Results and discussion, presents the results of the experiments and modeling and the subsequent discussion. The next chapter is Conclusions & Recommendations, and Appendixes A, B and C deal with respectively; the detailed description of the experimental method used, selected matlabcode used in this work and a more detailed description of the chemical equilibrium solver from [Jens 2010 (16)].

2

Theory

2.1 About MAPA

The reason to do this work on MAPA is because it is a interesting compound with regard to CO_2 capture. It is not very volatile [Kim 2009 (17)], which is good as it decreases the amount of amine which will leave the absorber with the cleaned gas, and it is part of the newly discovered two phase system of DEEA and MAPA that increase the CO_2 capture ability. MAPA is also thought to form a very stable zwitterion, as will be discussed later on, and since it is diamine it has increased CO_2 capture capacity at least compared to single amines. MAPA stands for "Methyl Amino Propyl Amin" and its structure is displayed in figure 2.1.

2.1.1 Physical data on MAPA

The data have been found in [BASF (2)].
IUPAC NAME: N-methyl-1,3-Propanediamine
CAS NR: 6291-84-5
Molecular weigth: 88.15 g/mol
Phase at standard conditions: liquid
Color: colorless to yellow
Smell: amin-like
pH: 13.5 for 100 g/l at 20°C

Meltingpoint: -72°C
Boilingpoint: 140-141°C
Flashpoint: -72°C
Density: 0.85 g/cm^3 at 20°C
Other names: (3-Aminopropyl)methylamine, N-Methyl-1,3-propanediamine, 3-Methylaminopropylamine, N-Methyltrimethylenediamine, N-Methyl-1,3-diaminopropane, N-Methyl-1,3-propylenediamine, 1-Amino-3-(methylamino)propane and 3-Amino-1-(methylamino)propane

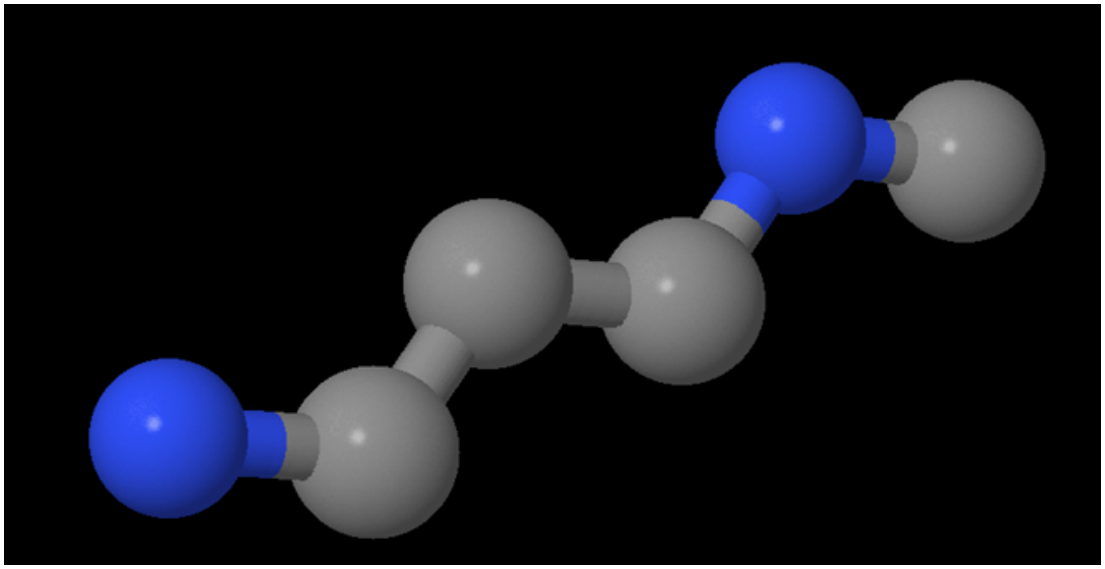

Figure 2.1: Structure of the MAPA molecule - Where the gray atoms are carbon atoms and the blue atoms are the nitrogen atoms. Hydrogen atoms are not shown in this structure. [DIPPR (9)]

2.2 The loaded MAPA system

2.2.1 The reactions

When the pure MAPA is diluted into an aqueous system and then loaded, i.e. CO_2 is "captured", there are several reactions that occur. The reactions that are thought to happen are shown in reactions 2.1a to 2.1i. Where reaction 2.1a is the water ionization, reaction 2.1b is the Bicarbonate - Dicabonate equilibrium,

reaction 2.1c is the first protonation of MAPA, reaction 2.1d is the second protonation of MAPA, reaction 2.1e is the formation of primary carbamate, reaction 2.1f is the formation of secondary carbamate, reacton 2.1g is the formation of primary zwitterion, reaction 2.1h is the formation of secondary zwitterion and reaction 2.1i is the formation of Dicarbamate. The subscripts "p" and "s", mean "primary" and "secondary" and are disscussed in section 2.2.2.

$$2H_2O = H_3O^+ + OH^- \tag{2.1a}$$

$$H_2O + HCO_3^- = H_3O^+ + CO_3^{2-} \tag{2.1b}$$

$$H_2O + MAPAH^+ = H_3O^+ + Mapa \tag{2.1c}$$

$$H_2O + MAPAH_2^{2+} = H_3O^+ + MAPAH^+ \tag{2.1d}$$

$$H_2O + MAPA + CO_2(l) = H_3O^+ + MAPACOO_p^- \tag{2.1e}$$

$$H_2O + MAPA + CO_2(l) = H_3O^+ + MAPACOO_s^- \tag{2.1f}$$

$$H_2O + H^+MAPACOO_p^- + CO_2(l) = H_3O^+ + MAPACOO_p^- \tag{2.1g}$$

$$H_2O + H^+MAPACOO_s^- + CO_2(l) = H_3O^+ + MAPACOO_s^- \tag{2.1h}$$

$$2H_2O + 2CO_2 + MAPACOO_p^- + MAPACOO_s^- = 2H_3O^+ + MAPACOO_p^- + 2MAPA(COO)_2^{2-} \tag{2.1i}$$

2.2.2 On the components of the loaded MAPA system

The molecular structures of the primary and secondary carbamates and zwitter ions are shown in figures 2.3(a) to 2.3(f). The label of primary and secondary carbamate/zwitterion, is meant as an label to distinguish between the two nitrogen groups in the MAPA molecule. The primary, secondary, tertiary label is referring to the number of carbon atoms that are connected with the nitrogen atom. Thus a secondary amine group has two carbon molecules connected to it. A primary has only one and a tertiary has three. Applied on figure 2.3(a), the amine group on the left is the secondary, $C-NH-C$ and the amine group to the right, $C-NH_2$ is the primary group. Normally the zwitterion is an unstable compound [Svendsen & Da Silva (8)], but in the MAPA system it is thought that it can form a stable compound, figure 2.2 shows the idea. Here the whole molecule would bend in such a way that the positive charge of the protonated amine group can come close enough to the negative charged carbamate group to have effect on each other. The molecule would thus form a ring structure which would be stable, thus stabilizing the otherwise unstable zwitterion.

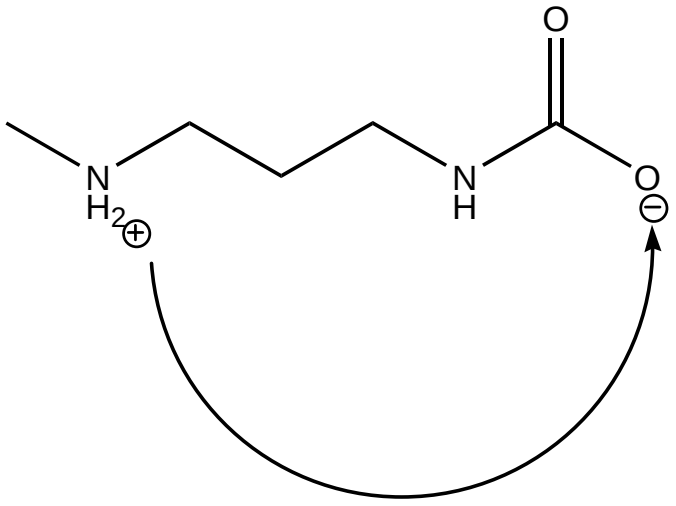

Figure 2.2: Schematic for the stabilization of the MAPA Zwitterion - Where the arrow shows how the molecule could bend so that the two charges become sufficiently close to stabilize the molecule [Svendsen 2011 (7)]

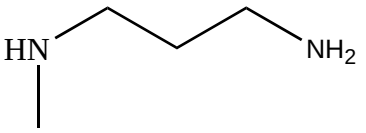

(a) Structure of the MAPA molecule

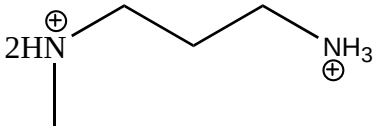

(b) Structure of the fully protonated MAPA molecule

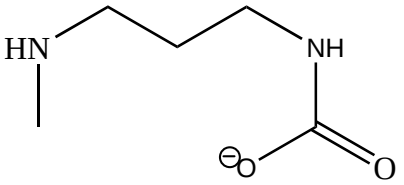

(c) Structure of the primary carbamate

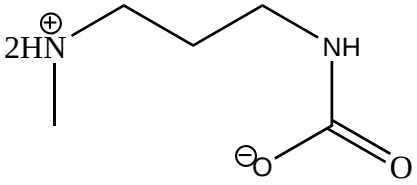

(d) Structure of the primary zwitterion

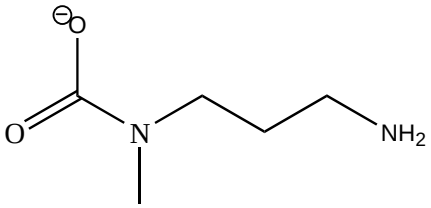

(e) Structure of the secondary carbamate

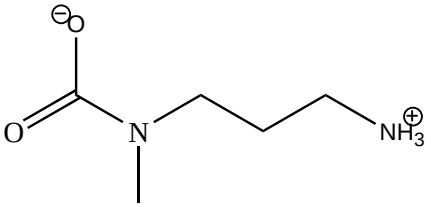

(f) Structure of the secondary zwitterion

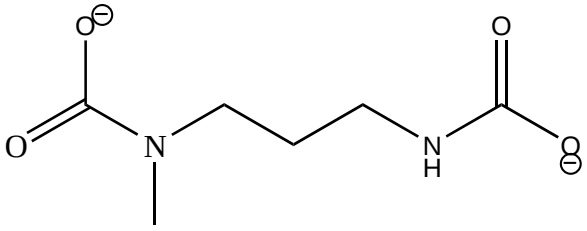

(g) Structure of the dicarbamate of MAPA

Figure 2.3: Molecular structures of the carbamates and zwitterions of MAPA

2.3 Loading calculations

Loading, α, is a way of describing how much CO_2 that has been absorbed by the solution. Equation 2.2 defines how loading is calculated.

$$\alpha = \frac{mol\ CO_2\ absorbed}{mol\ amine} \tag{2.2}$$

This is dependent on how "mol amine" is defined. If it is defined as "when the solution has reached equilibrium", α will be loading dependent as the amount of amine decreases when reacting with CO_2. Another way of defining it could be "the initial amount of amine", this way α becomes loading independent. Either way should in theory be fine as long the choice is consistent. In this work loading has been defined as the latter.

2.4 The model

The model used in this work was originally written by Dr. Erik Hessen (14) for MEA and MDEA, and then expanded by PhD candidate Ugochukwu Edwin Aronu for the MAPA system.

2.4.1 Model structure

The model structure is shown in figure 2.4 where the top level, the installation routine, defines the temperature, concentration of amine and loading. The loading is implemented as a vector with increasing amounts of CO_2 which the layers below work through, yielding equilibrium concentrations of all the species in both the liquid- and gas phase at each point in the loading vector, at the given T and amine concentration. Each of the equilibrium concentration points are found through iteration in the layers below, namely the chemical equilibrium calculation routine and phase equilibrium calculation routine, which in each iteration step draws on the extended UNIQUAC model and fugacity calculation routine. This is the reason for the overlapping layer structure in figure 2.4.

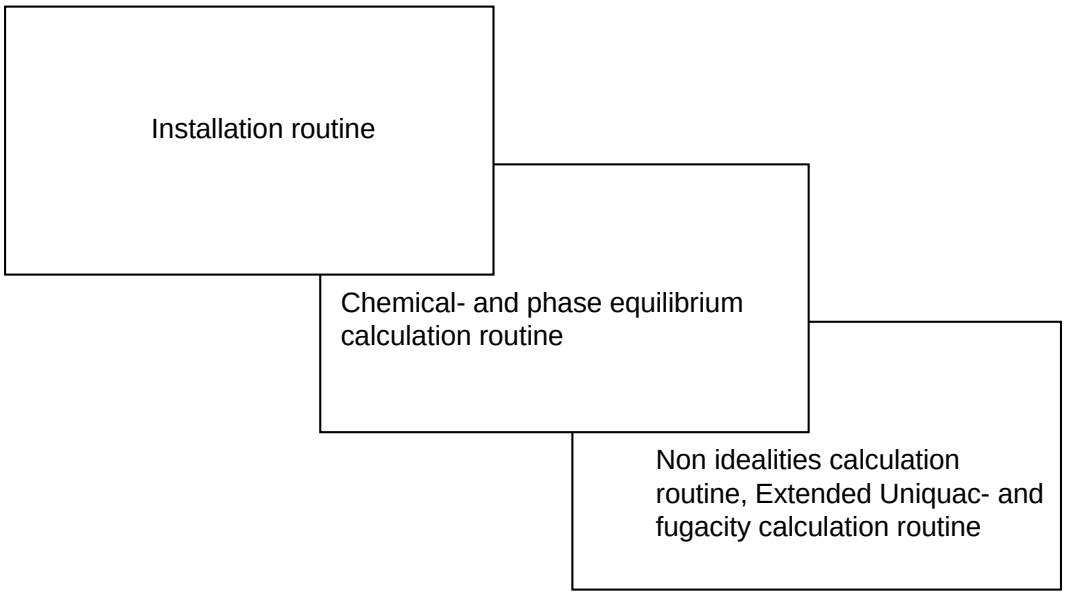

Figure 2.4: Structure of the model - The three blocks in the figure are discussed below

2.4.2 Installation routine

As stated this is a very simple section of the model which writes the parameters of the experiment into a way which can be "understood" by the model. It defines everything needed for the layers below. Temperature, initial concentrations, loading vector, etc.

2.4.3 Chemical- and phase equilibrium calculation routine

The chemical and phase equilbrium is calculated in this part of the model, as the title suggests.

Chemical equlibrium calculation routine

As this model uses a activity coefficient approach to account for the non idealities of the system, it is necessary to use the Gibbs free energy framework. The Gibbs free energy equation is linearized and minimized in order to find the equilibrium. As the minimization is constrained by a mass balance and a electroneutrality

balance, a Lagrangian multiplier approach can be used[1]. The interested reader is referred to [Hessen 2010 (14)] or appendix C, which has been taken from [Jens 2010 (16)], where the chemical equilibrium calculation routine has been discussed at length.

Phase equilibrium calculation routine

The phase equilibrium calculation routine that calculates the composition of the components in the vapor phase, is set up as a traditional vle problem. It is based on the equilibrium criteria, equation 2.3.

$$\mu_i^{vap}(T, P, \mathbf{n}) = \mu_i^{liq}(T, P, \mathbf{n}) \tag{2.3}$$

The distribution of free CO_2 is determined in the model by Henry's law, where the reference state is the solubility of CO_2 at infinite dilution in water at system temperature and pressure. The partial pressures are calculated based on equation 2.4. The equation is the basis of an iteration procedure which iterates until the correct gas phase concentrations, i.e. partial pressures have been determined.

$$y_i \varphi_i p_{tot} = x_i \gamma_i \varphi_i^{sat} p_i^{sat} exp\left(\frac{1}{RT}\int_{p_i^{sat}}^{p_i} \bar{v_i}\ dp\right) \tag{2.4}$$

Where, $\mathbf{p_i}$, p_i^{sat} [kPa] is the partial pressure and the saturated partial pressure, $\varphi_\mathbf{i}$, φ_i^{sat} [dimm. less] is the fugacity coefficent and the fugacity coefficient at saturated pressure, $\mathbf{x_i}$, $\mathbf{y_i}$ [dim. less] is the mole fraction of the component "i" in the liquid- and gas phase, γ_i [dim. less] is the activity coefficient, $\bar{\mathbf{v}}_\mathbf{i}$ [mol/m^3] is the partial molar volume of component "i", T [K] is the temperature and R is the gas constant [J/Kmol]. For CO_2 the reference state is at infinite dilution of CO_2 in water. This reference state naturally doesen't work for for water, as water cannot be diluted to infinite dilution in water. Thus the reference state of water is for pure water at system temperature and pressure. Equation 2.4, which is on the general form, has to be modified accordingly.

Since the total pressure is not known in the model, it is necessary to estimate it, on the basis of the Henry's coefficient, the mole fractions in the liquid phase, x_i and the activity coefficients, γ_i. This is another critical part of the model as it

[1]The Lagrangian multiplier is used for optimization/minimization of constrained systems

describes the link between the gas phase and the liquid phase. Equations 2.5a, 2.5b and 2.5c show the procedure.

$$p_i = x_i \gamma_i K_i \tag{2.5a}$$

$$p_{tot} = \sum_i p_i \tag{2.5b}$$

$$error = \left| \frac{\left(p_{tot}^k - p_{tot}^{k-1}\right)}{p_{tot}^{k-1}} \right| \tag{2.5c}$$

Where "K_i" is the "transfer function" from the liquid- to the gas phase for each component "i". For Water it would be the saturation pressure of water at the given temperature and for MAPA it would be the saturation pressure of MAPA at the given temperature. For CO_2 it would be Henry's coefficient at infinite dilution at given temperature. For the rest of the species it is set to 0, as it is assumed that all the reaction takes part in the liquid phase. This is thought to be a valid assumption as MAPA is a very non volatile compound, and its reaction compounds are thought to be even less volatile [Kim 2009 (17)]. One point worth mentioning is that when estimating the total pressure, it is contrary to expectation, dependent on the fugacity. This because as the partial pressures are found by iteration, which then are summed to find the total pressure. So that an fugacity calculation routine is needed even when calculating the total pressure.

2.4.4 Non idealities calculation routine

Activity coefficient calculation routine

The activity coefficient which accounts for the non idealities in the liquid phase was calculated using the extended UNIQUAC equation [Thomsen and Rasmussen (29)]. The difference between the "extended" and the "regular" UNIQUAC equation is a Debye Hückel term which was added by Thomsen and Rasmussen. This term accounts for the non idealities which originate from ionic interactions, while the traditional Uniquac terms, the combinatorial- and residual term, accounts

for respectively the non idealities based on size and temperature. The extended Uniquac model will not be discussed in detail in this thesis, again the interested reader is reffered to [Hessen 2010 (14)], [Jens 2010 (16)] and [Thomsen and Rasmussen (29)] or appendix C as it has been discussed to great length there. What however is important for this thesis is how the parameters of the extended UNIQUAC model are defined. The Debye Hückel term is based on standard electrostatic calculations, which are based on the ionic charge that the molecule has. The combinatorial and residual terms are based on three parameters, $\mathbf{R_i}$,$\mathbf{Q_i}$ and u. R and Q are thought to be size parameters and are defined to be the "van der waals area and volume" respectively, and there is one r and q for each component. The last parameter, "**u**", is taking into account the "energetic interaction" between two molecules, which makes for a lot of u's since there are 14 components in the liquid phase. In addition the "u" has two components, one temperature dependent term,$\mathbf{u_0}$, and one base term, $\mathbf{u_0}$, which make up u, as shown in equation 2.6.

$$u = u_0 - u_t \left(T - 298.15\right) \tag{2.6}$$

Fugacity coefficient calculation routine

When the model was received, the gas phase was described as a Peng Robinson equation of state, where the effect of amine in the gas phase appeared to be neglected. It was decided to investigate this and to develop an gas phase non ideality description based on the second virial equation of state. Because this is the only equation that can be derived from statistical thermodynamics [Haug-Warberg (12)]. In the end, as will be discussed later, the original gas phase representation was kept. However the developed method could be powerful method for describing the gas phase for any loaded amine system, and therefore it is described in this thesis at considerable detail. Fugacity[1] is defined in equation 2.7.

$$RTln\varphi_i = \mu_i^{r,p}\left(T, p, \mathbf{n}\right) \tag{2.7}$$

[1]In this case the pressure residual, $\mu_i^{r,p}$, is used, but also $\mu_i^{r,v}$, volume residual could be used

A method for finding $\mu_i^{r,p}$ was provided by [Warberg 2006 (12)], which is based on the virial equation of state, equation 2.8.

$$\frac{Pv}{RT} = 1 + \frac{B(T)}{v} + \frac{C(T)}{v^2} + ... \tag{2.8}$$

In theory the sequence can go on to infinity but for most practical purposes including the second- and third virial coefficients, $B(T)$ and $C(T)$, are enough. Typically when the second virial coefficient is included the equation of state is adequate to describe the deviation from ideallity up to about 10 bar, and when including the third it is adequate up to 100 bar [Laurendeau 2005 (20)]. When only $B(T)$ is included equation 2.8 is reduced to equation 2.9. Figure 2.5 shows the behavior of B(T) as a function of temperature, where it is very non ideal at low temperatures since repulsive forces are dominant, then it flattens out and finally it drops a bit toward zero at very high temperatures.

$$pV^{2.vir} = NRT + Bp \tag{2.9}$$

When using the Gibbs framework, equation 2.10, the difference between the real

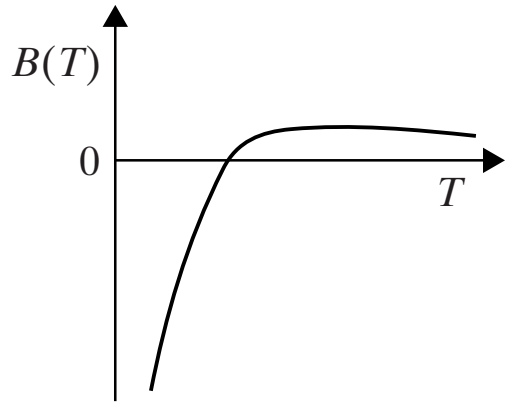

Figure 2.5: Temperature effect on B(T) - The second virial coefficient

volume and the ideal volume is defined as the basis for the residual gibbs energy with regard to pressure.

$$G^{r,p,2.vir} = \int_0^p \left(V^{2.vir} - V^{ig}\right) dp = \int_0^p \left(\frac{NRT}{p} + B - \frac{NRT}{p}\right) dp = Bp \tag{2.10}$$

Thus

$$\mu_i^{r,p} = \left(\frac{\partial G^{r,p}}{\partial N_i}\right)_{T,p} = \left(\frac{\partial Bp}{\partial N_i}\right)_{T,p} \tag{2.11}$$

The differentiating of equation 2.11 is non trivial even though B can be defined as a relatively simple mixing rule, equation 2.12

$$B = N \sum_i \sum_j x_i x_j B_{ij} \tag{2.12}$$

Where $B_{ij} = B_{ji}$. To make the expression easier to differentiate, equation 2.12 is rewritten as $NB = \sum_i \sum_j N_i N_j B_{ij}$. Now expression 2.11 can be rewritten as equation 2.13. The assumption that $B_{ij} = B_{ji}$ is thought to be valid as it seems logical that for example Water has the same interaction with CO_2 as CO_2 has on Water.

$$\left(\frac{\partial NB}{\partial N_k}\right)_T = \sum_i \sum_j \left(\frac{\partial N_i N_j}{\partial N_k}\right) B_{ij} \tag{2.13}$$

Kronecker's delta is introduced, where $\delta_{ii} = 1$ when $i = j$ and $\delta_{ij} = 0$ when $i \neq j$, and the equation is differentiated yielding equation 2.14. Kronecker's delta is a mathematical notation form that is of great use when differentiating complex summation expressions, and especially when the goal is to obtain the differentials denoted by "i" and "j".

$$B + B\left(\frac{\partial B}{\partial N_k}\right)_T = \sum_i \sum_j (\delta_{ik} N_j + N_i \delta_{jk}) = \sum_j N_j B_{kj} + \sum_i N_i B_{ik} \tag{2.14}$$

The complexity of the right hand side of equation 2.14 can be reduced significanty by changing one of the summation variables from "i" to "j"using $B_{kj} = B_{jk}$, yielding equation 2.15

$$\bar{b_i} = \left(\frac{\partial B}{\partial N_k}\right) = 2 \sum_i \frac{N_i}{N} B_{ik} - \frac{B}{N} \tag{2.15}$$

Thus equation 2.16 sums up the derivation of the fugacity coefficient based on the second viral equation.

$$RTln\varphi_k^{2.vir} = \left(\frac{\partial G^{r,p,2.vir}}{\partial N_k}\right)_{T,p} = p\left(\frac{\partial B}{\partial N_k}\right) = p\bar{b_i} \tag{2.16}$$

Where $B = N\sum_i \sum_j x_i x_j B_{ij}$. The framework for estimating the fugacity coefficient based on the 2 cross virial coefficient, B_{ij}, has been presented in this section. The problem now becomes how to find find the coefficients, B_{ij}, needed to solve the specific problem at hand, how this is handled is shown in section 3.2.3

2.5 Solubility

When large amounts of CO_2 have been captured in the amine solution, and the CO_2 partial pressure in the gas phase is still high, more CO_2 will force itself into the liquid phase. This CO_2 might appear as physically solved free CO_2. The amount of this physically bound CO_2 is determined by the solubility or Henry's coefficient $[kPa\ m^3\ mol^{-1}]$. As it is not feasible to measure the solubility of CO_2 in the amine solution since it would react "away", the N_2O analogy has been developed. This analogy states that since N_2O is similar to CO_2 in terms of structure, electron configuration, etc, N_2O can be used to measure the solubility of CO_2 in systems where the CO_2 would react away. Mathematically, equations 2.17 and 2.18 define the analogy.

$$H_{CO_2}^{MAPA} = \frac{H_{N_2O}^{MAPA}}{H_{N_2O}^{H_2O}} H_{CO_2}^{H_2O} \tag{2.17}$$

$$H_{CO_2}^{MAPA} = \gamma_{CO_2}^{*} \cdot H_{CO_2}^{H_2O} \tag{2.18}$$

In the model used in this work, equation 2.18 is used to calculate the real solubility of CO_2 in the loaded MAPA solution based on the experimentally measured solubility of CO_2 at infinite dilution at system temperature and pressure ,$H_{CO_2}^{H_2O}$. As the equation shows it is assumed that the activity coefficient can take care of the difference between the CO_2 in the pure water and in the amine solution.

2.6 Heat of Absorbtion

Heat of absorbtion of CO_2 $[kJ\ mol^{-1}]$ is defined as the heat that is needed to absorb a given moles of CO_2 in the liquid alkanolamine solution. Equation 2.19 shows how it is calculated.

$$H_{abs} = \sum_i \zeta_i \Delta H_i \tag{2.19}$$

Where ζ_i and ΔH_i are the extent of reaction $[mol]$ and the heat of reaction, or enthalpy of reaction $[kJ/mol]$ of reaction "i". Heat of absorption can be related to the equilibrium constants via Gibbs Helmholtz equation, equation 2.20. Thus this model can be used to predict the heat of absorption. There are other ways of predicting this than Gibbs Helholtz equation, the interested reader is referred to [Hessen 2010 (14)].

$$\frac{\mathrm{d}lnK_a}{\mathrm{d}T} = \frac{\Delta H_a}{RT^2} \tag{2.20}$$

3

Materials & methods

3.1 Experimental method

3.1.1 VLE measurements

The basic idea of the VLE[1] measurements is to measure, as the name suggests, the vapor liquid equilibrium of the specific loaded amine system. Thus the gas phase concentration of CO_2, or the total pressure depending on the apparatus used, is measured as a function of temperature and loading. The VLE measurements in this work were performed in two apparatuses, one for the low temperatures at atmospheric total pressures, "The low temperature apparatus or LTA", where equilibrium at 40 °C, 60 °C and 80 °C was measured. The experiments at high temperatures 80 °C, 100 °C and 120 °C, and up to 10 bar total pressure, were carried out in another apparatus, "The high temperature apparatus or HTA". For 80 °C the lower loading experiments were carried out in the LTA and the higher loading experiments were performed in the HTA, as high partial pressure of CO_2 is needed to reach the high loadings. The experiments were mainly performed for 2M MAPA solution, but some 5M experiments were carried out to augment the experimental data available. The liquid samples taken were titrated for Amine and CO_2 content. The detailed procedure follows in appendix A.

[1] Vapor-Liquid-Equilibrium

Low temperature and pressure VLE measurements

The flowsheet of the low temperature apparatus, LTA, is shown in figure 3.1. As

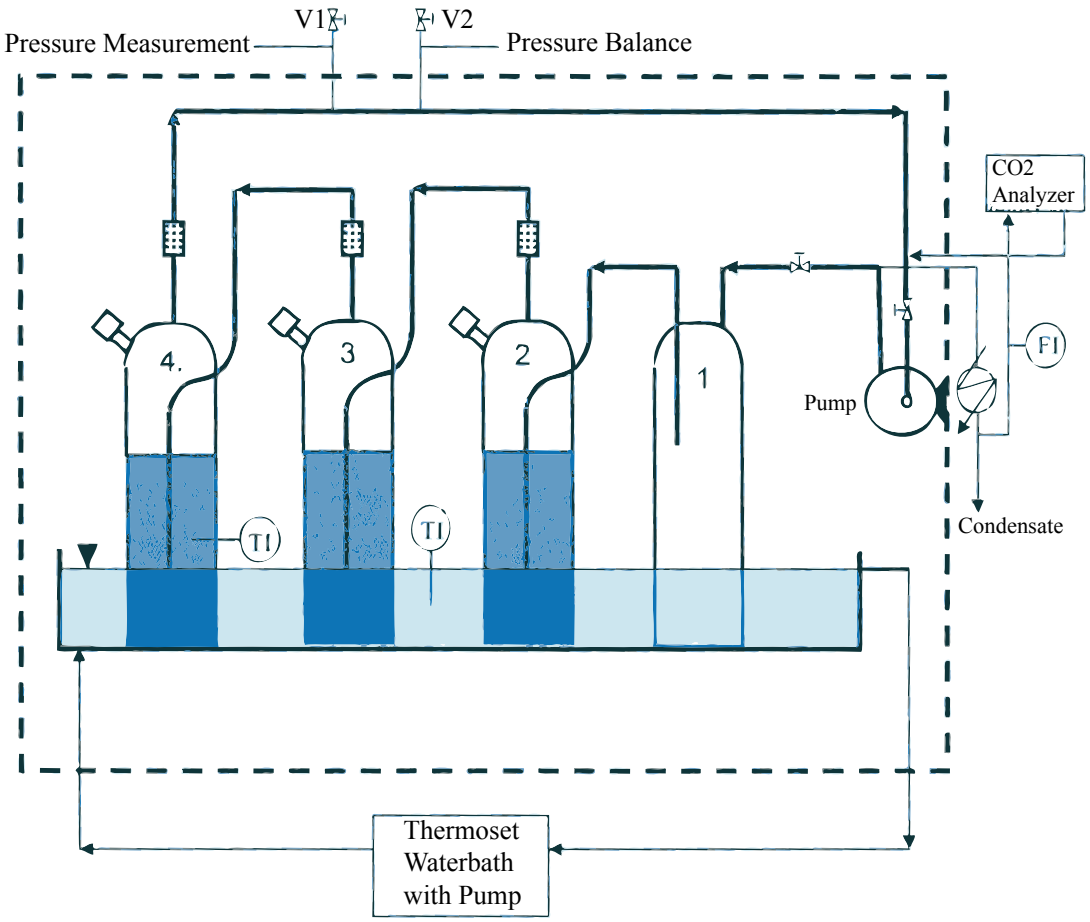

Figure 3.1: Flowsheet of the LTA - Where the amine is placed in the flasks and the gas phase is circulated through the CO_2 analyzer

can be seen from figure 3.1, there is no way to add CO_2 during the experiment, thus the Amine solution had to be loaded before the experiment was started. Preloading was done by simply pressurizing the amine solution with CO_2 until the solution stopped gaining weight, i.e. there was no more CO_2 being absorbed. The gas phase CO_2 analyzer could only measure concentrations of maximum 20 vol. %, and since it was not known how much the solution had to be preloaded to get this point, the solution was preloaded to the maximum. The solution was then tested in the apparatus to see if it yielded gas phase concentrations of CO_2

above 20 vol %, if it did the loaded solution was removed from the apparatus and carefully diluted by unloaded amine to get the loading down and tested again. This way the first point that could be precisley measured was found. Then about 150 mL of loaded solution was then placed into each flask. The desired temperature was set, and after reaching it, the circulation pump was turned on so that the closed atmosphere in the system could be analyzed by the CO_2 analyzer. A liquid sample was taken from the first flask after the CO_2 content of the atmosphere was determined. The mixture in the flasks was extracted via a manual pump, and then diluted by mixing the original mixture with unloaded amine solution to get the next lower loading point to test. The new mixture was then filled into the flasks and the experiment was repeated. Before the experiment was started each day the CO_2 analyzer had to be calibrated with known gas mixtures.

High temperature and pressure VLE measurements

The flow sheet of the high temperature apparatus, the HTA, is shown in figure 3.3. The HTA is called "the tilting apparatus"[1], because the whole autoclave tilts 180 degrees, to ensure good mixing of the solution and gas phase inside the stainless steel autoclave. The tilting has a frequency of 20 seconds, and temperature and pressure can be set between 80 to 150°C and 1 to 20 bar. The high pressures means that high loading areas can be reached. The tilting autoclave is located inside a thermostat cabinet which can be seen on figure 3.2, where the temperature is controlled by a heater and a fan. The temperature of the autoclave itself is maintained by an oil bath where the oil circulates on pipes directly on the autoclave. As this apparatus has the possibility to add CO_2 during the experiment, 200 mL of *unloaded* solution is fed into the autoclave via a piston pump, and not preloaded solution as with the LTA. The inside of the autoclave is filled with a packing material, which ensures good contact between the two phases, thus reducing the time required to reach equilibrium. Total pressure and temperature inside the autoclave is displayed on a computer which is connected to the apparatus.

[1] In Norwegian: "Vippecellen"

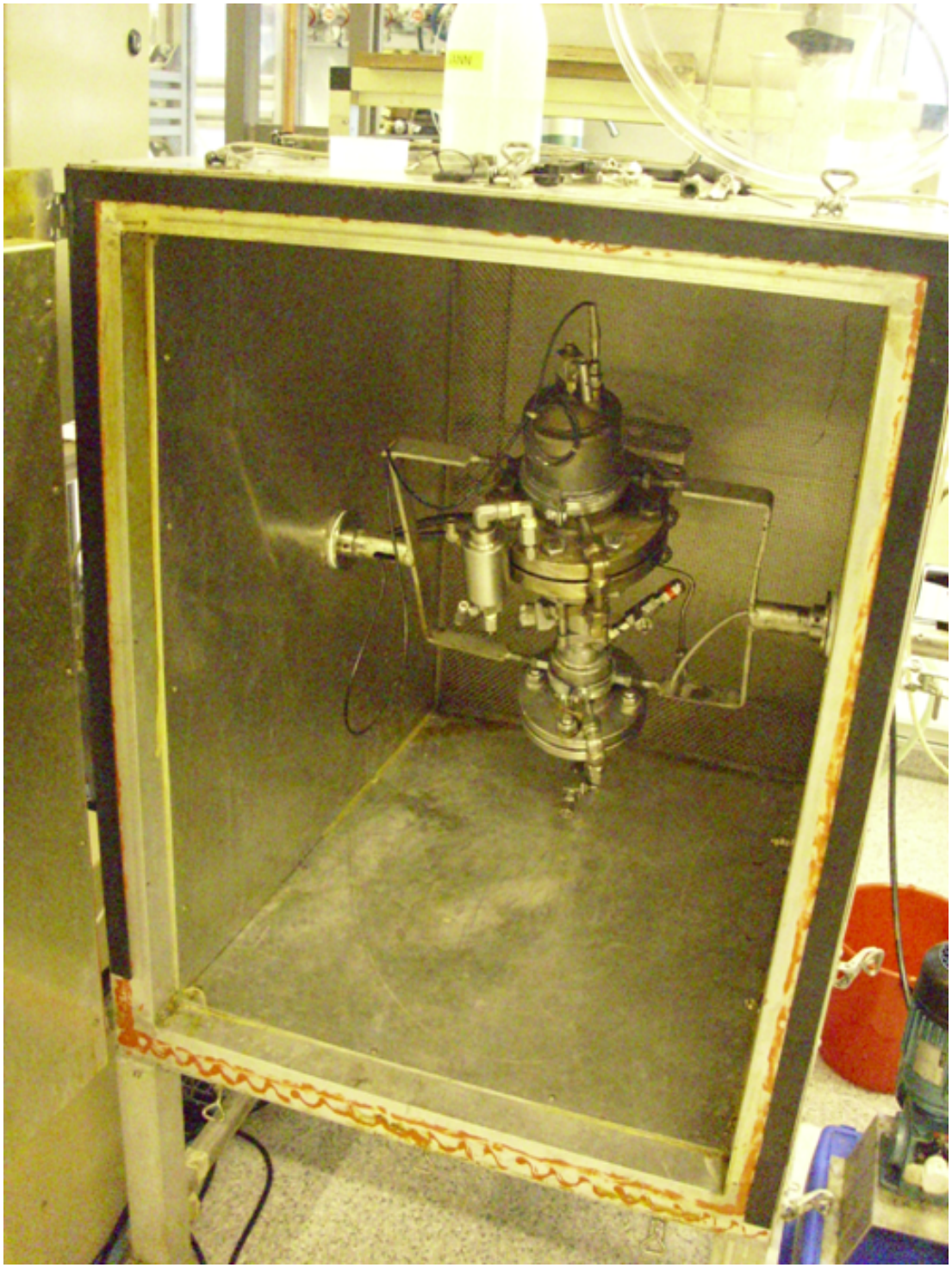

Figure 3.2: The HTA - Depicted in its thermostat cabinet. The autoclave itself is barely visible, it is the small cylindrical shaped vessel in the middle of the tilting part of the apparatus

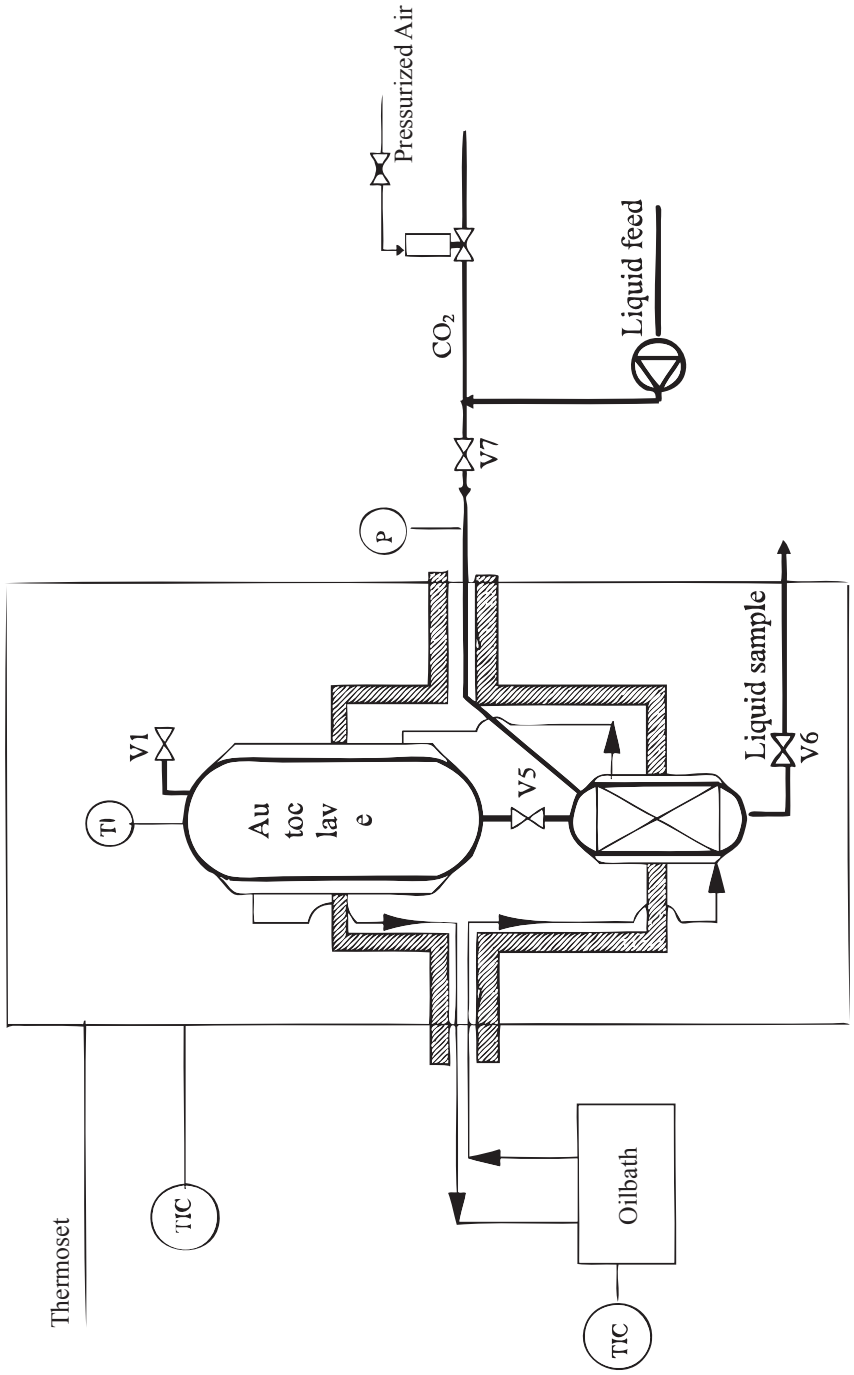

Figure 3.3: Flow sheet of the HTA -

3.1.2 Analysis of liquid samples

Two tests were used to analyze the liquid samples taken from the two apparatuses, one to determine the CO_2 amount and one to determine the amine amount. The two proceduers are discussed in the following section.

CO_2 analysis

The goal of this analysis is to determine how much CO_2 is in the liquid phase, to do this the reactions that form the components that "store" the CO_2 have to be reversed. This is done by adding Bariumhydroxide, $Ba(OH)_2$, and heat which then will result in the precipitation of CO_2, as shown in reaction equation 3.1.

$$Ba^{2+} + CO_2 + 2OH^- = BaCO_3(s) + H_2O \tag{3.1}$$

Barium and NaOH will be added in excess so that all CO_2 will precipitate. The precipitated $BaCO_3$ will then be removed from the liquid phase by means of filtration. Then the precipitated $BaCO_3$ is transferred to a new aqueous solution. Through addition of hydrocloric acid, as shown in equation 3.2, the precipitated $BaCO_3$ is dissolved.

$$BaCO_3(s) + 2HCl = BaCl_2 + CO_2 + H_2O \tag{3.2}$$

Now that the CO_2 "storage reactions" have been reversed the new solution does not contain any amine, which would influence the final step of the analysis, the solution is ready for titration against NaOH. Finally equation 3.3 yields the final CO_2 concentration.

$$CO_2\left(\frac{mole}{kg}\right) = \frac{1}{20}\cdot\frac{\text{HCl(gm)} - \text{NaOH(ml)} - \text{[Blank HCl(gm) - Blank NaOH(ml)]}}{\text{Sample(gm)}} \tag{3.3}$$

Amine analysis

Instead of having to extract the CO_2, as was done in the CO_2 analysis, here the procedure is much more simpler as the samples are titrated against H_2SO_4. The detailed procedure is described in appendix A, and equation 3.4 shows how the amine concentration is calculated.

$$\text{Amine (mole/liter)} = \frac{H_2SO_4\,(\text{ml}) \cdot 0.2}{Sample(ml)} \tag{3.4}$$

3.1.3 Experimental calculations

In this section the procedure for calculation loading and partial pressure of CO_2 is described. Example experimental calculations are shown in appendix A.

Low temperature calculations

For the experimental points found in the low temperature apparatus, as described in section 3.1.1, P_{CO_2} was found by the following procedure. From the LTA the gas phase volume % of CO_2 is known, but it has to be corrected for by the calibration results. After that, to find the partial pressure of CO_2, it is necessary to calculate the saturated partial pressure of water and MAPA above the sample in the flasks at the current temperature. Also the pressure of water above the condensate at the condensate temperature has to be calculated. The assumption here is that there is no MAPA present in the condensate. This assumption is considered valid since MAPA is very nonvolatile, and thus very little of it leaves the sample flasks. In fact, the condensate was tested for amine at uneven intervals, and almost no amine was found. To find P_{CO_2} then equation 3.5 was used.

$$P_{CO_2}(T)\,[\text{kPa}] = A \cdot \Big(P_{tot}(T) - P_{H_2O}^{Cell,sat.}(T) - P_{MAPA}^{Cell,sat.}(T) + P_{H_2O}^{Cond.,sat.}(T) \Big) \quad (3.5)$$

Where A is the volume percent of CO_2 in the gas phase. The saturated pressures were found using the Antonine equation with parameters from [Kim 2009 (17)]

High temperature calculations

As the principle of finding P_{CO_2} in the HTA is the same as in the LTA, the equation used, equation 3.6, is the similar to the equation used in the LTA, equation 3.5.

$$P_{CO_2}(T)\,[\text{kPa}] = P_{tot} - P_{MAPA}^{sat} - P_{H_2O}^{sat} \quad (3.6)$$

It should be noted that in the LTA this form of equation is thought to be accurate enough to calculate the partial pressures since it operates at atmospheric conditions and only up to 80°C. In the HTA however there are much higher pressures and temperatures, thus to accurately calculate P_{CO_2} based total pressure measurements, fugacity should be included in the equation. Since there is no clear way

to calculate the fugacities accurately for this system in the regression analysis, the total pressure was used as the regression "target" for the data from the HTA

3.2 Modeling Method

In the following section the authors modifications to the existing model are described.

3.2.1 Model modifications

When the model was received, it was optimized for a set of equilibrium constants that favored a high zwitterion stability, equationset 3.7, this constellation of equilibrium constants gave a relatively good fit with regard to VLE data points for loading beneath 1. The equations in equationset 3.7 are in the same order as the reactions in reactionset 2.1. The extended UNIQUAC model was not used as its use made the whole model crash. To avoid using the extended UNIQUAC model, all the activity coefficients were set to 1, as would be the case for the ideal system. In this work the author spent a lot of time to make the model converge when the extended UNIQUAC model was turned on[1]. First it was thought that there was an inconsistency in the chemical equilibrium calculation algorithm, since the algorithm uses a combination of two different numerical methods, as shown in figure 3.4. The inner loop uses a linerization of ideal Gibbs energy iterated on with a

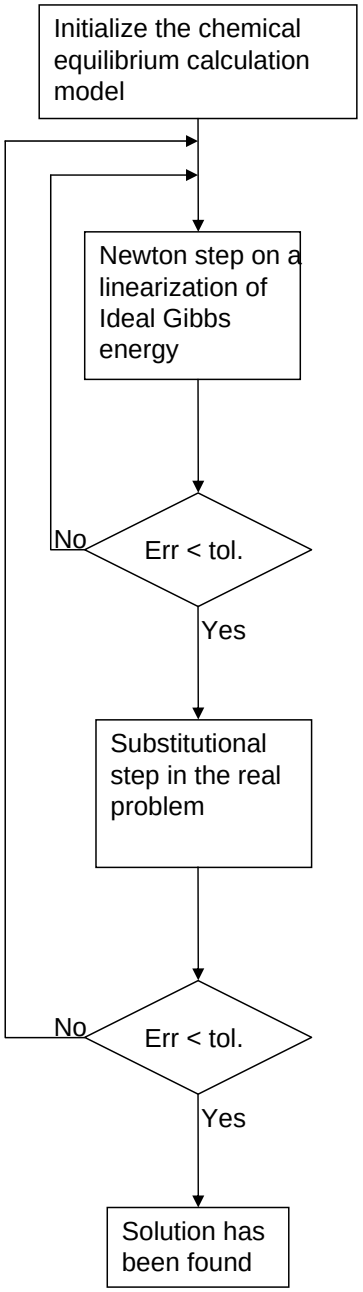

Figure 3.4: Flowsheet of the chemical equilibrium solver algorithm

[1]i.e. the activity coefficients were $\neq 1$

newton method, which means that it is not nec-
essary to find the gradient of the activity coefficient with regard to the iteration variables, lambda λ and total mole n_t. To find this gradient is very time consuming, as there is no analytical derivative of the activity coefficients in the extended UNIQUAC model, so that it is necessary to perturbate[1] the extended UNIQUAC model to find the gradients. To avoid this time consuming pertubation, the non idealities are implemented in an outer loop trough an substitutional routine, this method of handling the problem is described in [Michaelsen and Mollerup 2007 (24)], the result of this approach is to make the model very fast. Problems arise when assessing why the model does not converge, as there are two different numerical methods with different convergence criteria. This makes it hard to judge from observing the iteration procedure if the model is converging.

It also makes it harder to implement schemes that could ensure convergence. For example if a newton method has convergence problems it is easy to introduce a step length reduction method[2]. This approach was tried and some initial success was made, however this approach was discontinued, after correspondence with the chemical equilibrium calculation routines author Erik Hessen(5), it was concluded that the problem was the the handling of the non idealities and did not lay in the linearization. In fact the model should not have problems as long as the system that is modeled is not very very unideal(5). The focus in the convergence work now changed to the parameters of the extended UNIQUAC model, R,Q and u as described in section 2.4.4. It was thought that they produced activity coefficients that were to small or large for the algorithm to converge. The method employed to reach conversion was very simple, one after another the parameters were "opened", i.e. changed from the ideal case, 1, to the value that the extended UNIQUAC model calculated. By doing it this way it is always known which

[1] Perturbation theory comprises mathematical methods that are used to find an approximate solution to a problem which cannot be solved exactly

[2] In essence this method checks if the iteration is going in the right direction, using the convergence criteria for the newton method, and if it does not, the last "safe" answer is reloaded and the iteration step is shortened so that the next result is nearer to the solution and does not overshoot it.

of parameters that caused problems. In the end the model converged for all concentrations and temperatures.

$$lnK_{Water\ ionization} = 132.899 - \frac{13445.9}{T} - 22.4773 \cdot lnT \tag{3.7a}$$

$$lnK_{Dissociation\ of\ carbondioxide:} = 231.465 - \frac{-12092.1}{T} - 36.7816 \cdot lnT \tag{3.7b}$$

$$lnK_{Dissociation\ of\ bicarbonate} = 216.049 - \frac{12431.7}{T} - 35.4819 \cdot lnT \tag{3.7c}$$

$$lnK_{Primary\ protonation} = -4.0304125 - \frac{6074.82}{T} \tag{3.7d}$$

$$lnK_{Secondary\ protonation} = -0.3846832 - \frac{5878.91}{T} \tag{3.7e}$$

$$lnK_{MAPACOO_p^-} = 2.57380 + \frac{9607.1}{T} - 7.43890 \cdot lnT \tag{3.7f}$$

$$lnK_{MAPACOO_s^-} = 2.26 + \frac{9607.1}{T} - 7.43910 \cdot lnT \tag{3.7g}$$

$$lnK_{H^+MAPACOO_p^-} = 1250.9 - \frac{60885.00}{T} - 188.54 \cdot lnT \tag{3.7h}$$

$$lnK_{H^+MAPACOO_s^-} = 1251.5 - \frac{60885.0}{T} - 188.54 \cdot lnT \tag{3.7i}$$

$$lnK_{MAPA(COO^-)_2} = 4569.30 - \frac{218550.0}{T} - 676.770 \cdot lnT \tag{3.7j}$$

The last five of these equilibrium constants are unknown, and thus had to be included in the regression analysis.

3.2.2 How to modify the model for a new amine/amine system

The goal of this section is to provide a quick guideline, in order to ease the potential problems that might arise when trying to modify this model for use in another amine system. There are a number of parameters that have to be changed, the list is provided below in table 3.1, and below a short description of the parameters that are not self explanatory.

c.Z

The electronic charge, [C], of the components of the system.

c.nrx

The number of reactions in the system.

c.Akeq

The equilibrium constants for the reactions in the system. As described in equation C.40, the initialization routine needs standard state chemical potentials for each specie in the system. Equation C.40 shows how they are calculated from the equilibrium constants. However sometimes there are more species than equilibrium constants, and thus some of the standard state potentials that are not known from literature have to be set to zero, this is explained in more detail in section C.1.3.

c.A

The element conservation matrix. This matrix contains all the elements of all the compounds. An example would be equation 3.8 where the element conservation matrix of a system containing only water,MAPA and CO_2. In the matrix the first row is the number of Hydrogen atoms, the second is the number of carbon atoms, the third row is the number of Nitrogen atoms and the fourth row is the number of oxygen atoms. The columns show how many atoms of each compound they include, respectively the columns represent water MAPA and CO_2

$$c.A = \begin{bmatrix} 2 & 12 & 0 \\ 0 & 4 & 1 \\ 0 & 2 & 0 \\ 1 & 0 & 2 \end{bmatrix} \begin{matrix} H \\ C \\ N \\ O \end{matrix} \tag{3.8}$$

c.N

The stoichiometric matrix, which accounts for the changes that occur during the reactions. For a system with the two reactions 2.1a and 2.1b the stoichiometric matrix would look like equation 3.9

$$c.N = \begin{bmatrix} -2 & -1 \\ 1 & 0 \\ 1 & 1 \\ 0 & -1 \\ 0 & 1 \end{bmatrix} \begin{matrix} H_2O \\ OH^- \\ H_3O^+ \\ HCO_3^- \\ CO_3^- \end{matrix} \tag{3.9}$$

Where the rows represent the individual specie and the columns represent the change in species that happens as a result of the reactions, the columns represent respectively reactions 2.1a and 2.1b.

RPAR, QPAR, u0 and ut

The parameters of the UNIQUAC equation have been discussed in section 2.4.4, however in this section a quick example number of parameters needed for a system of 2 species, Water and CO_2. For each specie one r and q parameter is needed, thus giving R_{CO_2}, Q_{CO_2}, R_{H_2O} and Q_{H_2O}. The u parameter as defined in equation 2.6 $u_{CO_2-CO_2}$, $u_{H_2O-H_2O}$ and $u_{H_2O-CO_2}$. As u consists of both u0 and ut, the simple system of only water and CO_2 already gives 10 parameters.

3.2.3 Approximation of the Cross viral coefficient

The theory for calculating the fugacity coefficient based on the second virial coefficient is described in section 2.4.4. When implementing the theory on the loaded MAPA system, the cross virial coefficients $B_{CO_2-H_2O}(T)$, $B_{MAPA-H_2O}(T)$ and $B_{CO_2-MAPA}(T)$ had to be determined. By the therm "cross" the interaction between two species is meant. Only these three coefficients are necessary since it is assumed that only water, MAPA and carbon dioxide is present in the gas phase. This section describes how these coefficients are found.

Table 3.1: Parameters that have to be changed for the model for to be used in another amine system

Parameter	Where	What is its physical meaning
c.Mw	data.m	Molecular weights of the species
c.Z	data.m	Electron charge of the species
c.nrx	data.m	Number of reactions
c.Akeq	data.m	Equilibrium constants
c.A	data.m	Element conservation matrix
c.N	data.m	Stoichiometric matrix
c.tci	data.m	Critical temperature
c.pci	data.m	Critical pressure
c.vci	data.m	Critical volume
c.pscoeff	data.m	Saturated partial pressures
c.vs_am	data.m	Molecular volume
RPAR	uniquac.m	R parameter in the Uniquac model
QPAR	uniquac.m	Q parameter in the Uniquac model
u0	uniquac.m	u0 parameter in the Uniquac model
ut	uniquac.m	ut parameter in the Uniquac model

The first of these cross second virial coefficients has been experimentally measured and was found in the literature [Springer Materials (21)]. Since MAPA is a less common compound than water or carbon dioxide, the two latter coefficients were not found in the literature. Thus a method [McCann and Danner (23)] to predict the *pure* second virial coefficient of MAPA, $B_{MAPA}(T)$ was found. This could together with $B_{H_2O}(T)$ and $B_{CO_2}(T)$ be used to determine the two latter cross virial coefficients. The *pure* second virial coefficients of water and carbon dioxide, $B_{H_2O}(T)$ and $B_{CO_2}(T)$, were also found in the literature [Springer Materials (22)]. Thus all that is needed for the approximation of $B_{MAPA-H_2O}(T)$ and $B_{CO_2-MAPA}(T)$ had been found.

The idea for the estimation of the cross coefficients, $B_{MAPA-H_2O}(T)$ and $B_{CO_2-MAPA}(T)$, was to regress the pure coefficients temperature dependent polynomial into the form of the square well potential representation for B(T), equation 3.17. This determined the component specific parameters B^{HS}, λ and ε. It was assumed that the second *cross* virial coefficient could be represented on the same form, thus the *cross* specific parameters B^{HS}_{cross}, λ^{cross} and ε^{cross} had to be determined. These parameters were determined using different averaging techniques based on the pure parameters. Which averaging technique to be used on which parameter was determined by testing the method against different known experimentally determined second cross virial coefficients.

Estimation of the pure second virial coefficient, B_{MAPA}

The method found [McCann and Danner (23)] is a group contribution method. The basic idea of the group contribution method is to divide a molecule into different parts, so called functional groups as shown in figure 3.5, and stating that each of these groups has a different influence on the physical properties. The effect of each of these groups are quantified and multiplied with the number of times the group occur, the sum of these products yields the physical property that is estimated. The estimation method of Mcann and Danner (23) uses the second order scheme of Benson and Buss(3), which is one of many different schemes developed. In the second order scheme, a group is defined as " a polyvalent

atom[1] together with its ligands, at least one of which also must be polyvalent"(23). Thus the method is simple, for each group a number of group specific parameters, as shown in equation 3.10, are needed to estimate the 2 virial coefficient for a pure substance. What is special about this method are the special correction terms that had to be introduced to improve the accuracy for substances with multiple occurrences of the following three groups, $C-(C)_2(H)_2$, $C_b-(F)$ and $C_b-(F)_2(C)_2$. Thus for each of these three groups there are two contributions, the primary and the secondary as shown in equation 3.11. The procedure is described below.

$$\Delta B_i = a_i + \frac{b_i}{T_r} + \frac{c_i}{T_r^3} + \frac{d_i}{T_r^7} + \frac{e_i}{T_r^9} \tag{3.10}$$

$$B = \sum_{pri} n_i \Delta B_i + \sum_{sec} (n_i - 1)^2 \Delta B_i \tag{3.11}$$

Detailed procedure:

1. Draw the molecular structure of the desired molecule.
2. Draw blocks around the individual groups.
3. Make a list of the groups and the number of occurrences of each.
4. For each equation constant add up the values for all of the primary group contributions multiplied by their respective number of occurrences as equation 3.12

$$\sum_{pri} n_i \Delta B_i = \sum_i n_i a_i + \frac{\sum_i n_i b_i}{T_r} + \frac{\sum_i n_i c_i}{T_r^3} + \frac{\sum_i n_i d_i}{T_r^7} + \frac{\sum_i n_i e_i}{T_r^9} \tag{3.12}$$

5. Similarly for all the groups having secondary contributions, sum each constant multiplied by $(n_i - 1)^2$ as equation 3.13 shows.

$$\begin{aligned} \sum_{pri} (n_i - 1)^2 \Delta B_i = \sum_i (n_i - 1)^2 a_i + \frac{\sum_i (n_i - 1)^2 b_i}{T_r} + \\ \frac{\sum_i (n_i - 1)^2 c_i}{T_r^3} + \frac{\sum_i (n_i - 1)^2 d_i}{T_r^7} + \frac{\sum_i (n_i - 1)^2 e_i}{T_r^9} \end{aligned} \tag{3.13}$$

[1] $A^{\pm a}$ where A is polyvalent if $a > 1$

6. Calculate the second virial coefficient at the desired reduced temperature using equation 3.11.

As an example the estimated second virial coefficient for tri-n-propylamine has been calculated in table 3.2, based on the groups in picture 3.5. In table 3.3 the method is used to calculate B_{MAPA} based on the functional groups of the MAPA molecule as shown in figure 3.6, which resulted in the polynomial in equation 3.14. B_{H_2O} and B_{CO_2} were found in Springer materials (22).

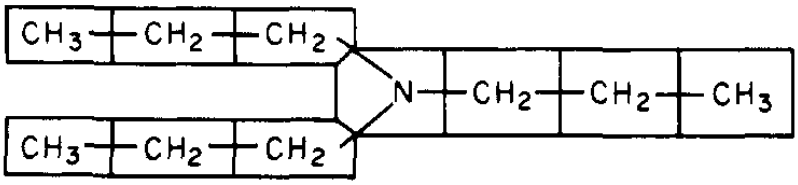

Figure 3.5: The structure of tri-n-propylamine split up according to the second virial coefficient prediction method - Figure from [McCann and Danner (23)]

$$B_{MAPA}(T_r) = 189.18 - \frac{458.19}{T_r} - \frac{251.46}{T_r^5} - \frac{11.87}{T_r^7} \tag{3.14}$$

As the attentive reader has noticed equations 3.14, 3.13, 3.12, 3.11 and 3.10 all are dependent on *the reduced temperature*, T_r, and not temperature T. Reduced temperature is defined as $T_r = T/T_C$. Since the critical temperature T_C for MAPA is not known, it also had to be estimated. A method was found [Riazi et al (27)] which did this, in addition to estimating the critical pressure and volume. The method is based on a polynomial which uses molecular mass [g/mol], density of the pure component at 20°C, and boiling point at atmospheric pressure [K]. Section B.2.2 in appendix B shows it's implementation in matlab.

Table 3.2: Example estimation of $B_{tri-n-propylamine}$

group	n_i	a_i	b_i	c_i	d_i
Primary contribution					
$C-(C)(H)_3$	3	41.33	-103.27	-22.80	-0.0506
$C-(C)_2(H)_2$	3	31.32	-69.14	-41.01	-1.058
$N-(C)_3$	1	25.87	-28.83	-44.02	-2.1184
$C-(N)(C)(H)_2$	3	28.63	-72.51	-27.057	-0.428
$\sum_{pri} n_i l_i$		329.71	-763.39	-316.62	-6.7282
Secondary contribution					
$C-(C)_2(H)_2$	3	0.277	2.363	-2.406	-0.298
$\sum_{sec}(n_i-1)^2 l_i$		1.108	9.452	-9.624	-1.192
Total contribution					
$B_{tri-n-propylamine}(T_r)$		330.82	-753.94	-326.24	-7.9202

Table 3.3: Estimation of B_{MAPA}

group	n_i	a_i	b_i	c_i	d_i
Primary contribution					
$C-(C)_2(H)_2$	1	31.32	-69.14	-41.01	-1.058
$C-(N)(H)_3$	1	41.33	-103.27	-22.8	-0.0506
$N-(C)_2(H)$	1	25.87	-61.76	-68.84	-3.871
$N-(C)(H)_2$	1	33.4	-79	-64.7	-6.04
$C-(N)(C)(H)_2$	2	28.63	-72.51	-27.057	-0.428
$\sum_{pri} n_i l_i$		189.18	-458.19	-251.45	-11.87
Secondary contribution					
$C-(C)_2(H)_2$	1	0.277	2.363	-2.406	-0.298
$\sum_{sec}(n_i-1)^2 l_i$		0	0	0	0
Total contribution					
$B_{MAPA}(T_r)$		189.18	-458.19	-251.45	-11.87

Estimation of the cross virial coefficient

Now that the pure second virial coefficient of all the components in the gas phase were determined, the next step was to decide how to approximate the cross virial coefficient. With all pure coefficients available one obvious possibility was to just take the geometric mean of the two pure coefficients. However this does not always give the best results, a better approach is to use is to regress the found pure coefficients into the equation for the square well potential, equation 3.17, determining the pure parameters B^{HS}, λ and ε. To find the second cross virial coefficient it was assumed that the cross coefficient could be described by the same equation. Thus the cross parameters could be found by different averaging techniques as described.

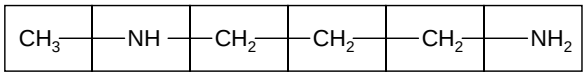

Figure 3.6: The structure of MAPA split up according to the second virial coefficient prediction method from [McCann and Danner (23)]

The following is a quick theoretical part on how equation 3.17 is derived. The theory states that the equation for the second virial coefficient can be written as equation 3.15 [Laurendeau 2005 (20)]

$$B(T) = 2\pi N_A \int_0^\infty \left[1 - e^{\phi(r))/kT}\right] r^2 dr \tag{3.15}$$

Where N_A is avogadro's number, r is the distance between the molecules, σ is the molecular diameter, T [K] is the temperature, k is Boltzmann's constant and $\phi(r)$ is the intramolecular potential. Here integration to ∞ is mathematically sound as the intermolecular potential, drops to zero when the distance between the molecules becomes greater than a few molecular diameters. It can be stated that, in general, the second virial coefficient can easily be derived from equation 3.15 given a suitable model for $\phi(r)$. In this work the square well potential model for $\phi(r)$ was chosen, due to it being a relatively accurate model of B(T) for low to medium-high temperatures [Laurendeau 2005 (20)]. Figure 3.7 displays

the schematic of the Square well potential, and equation 3.16 its mathematical definition.

$$\phi(r) = \begin{cases} \infty & r \leq \sigma \\ -\varepsilon & \sigma < r \leq \lambda\sigma \\ 0 & r > \lambda\sigma \end{cases} \tag{3.16}$$

Equation 3.16 says that if the distance between the molecules, r, is smaller than the molecular radius, σ, the repulsion is infinite which makes sense. When the distance between the molecules is above a set number of times the molecular radius, $\lambda\sigma$, the repulsion becomes zero. And between these extremities the repulsion is defined by a parameter ε. When integrating equation 3.15 while using the square well potential, equation 3.16, the result is equation 3.17.

$$B(T) = B^{HS}\left[1 - \left(\lambda^3 - 1\right)\left(e^{\varepsilon/kT} - 1\right)\right] \tag{3.17}$$

Where B^{HS} is the hard square volume, λ is the parameter that defines the number of atomic radiuses before before the repulsion is set to zero and ε is the parameter that defines the strength of the repulsion. All of these parameters are system specific when equation 3.17 is used to represent the second virial cross coefficient, and thus need to be found for the new mixed system. For B^{HS} the new mix or "cross" parameter is found through a geometric mean, the same for ε, λ however is found through a 3rd order mean. Section B.2.1 shows the Matlab code that implements the outlined method.

The method outlined provides a powerful tool for finding and predicting the properties of the gas phase of more or less any amine system. Of course the method is only a crude approximation, but in the authors opinion a no less valid method than assuming an ideal gas phase, i.e. that all the fugacity coefficients are set to 1, or assuming that there is no amine present in the gas phase, thus solving the gas phase using an SRK or Peng Robinson equation of state. In the end the original fugacity coefficient calculation routine that was incorporated into the model when it was received was used. Due to reasons discussed in section 5.2.3.

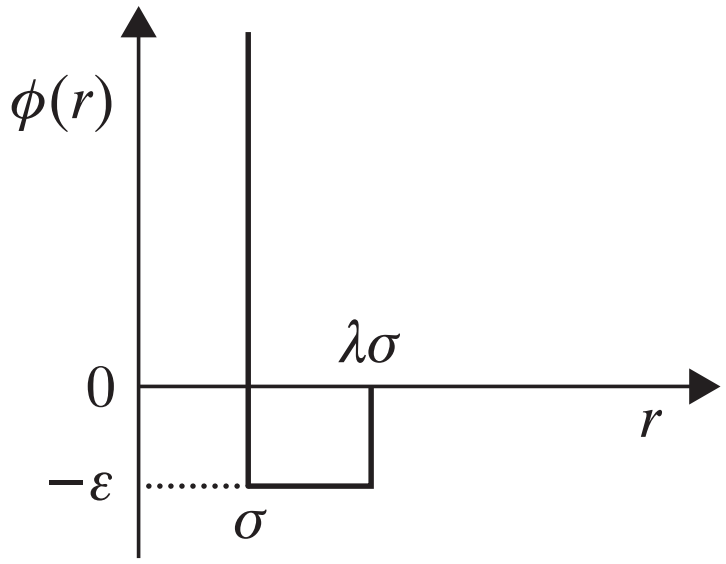

Figure 3.7: The schematic of the square well potential - where the graph shows the repulsion as a function of distance between the molecules, r, [Laurendeau 2005 (20)]

3.3 The regression procedure

3.3.1 Manual fitting

Manual fitting is done as the title suggests, by changing the parameters of the extended UNIQUAC model and equilibrium constants by hand. This is a very tedious process and in hindsight the author should have developed tools for doing this automatically instead of trying to do it by hand. The parameters regressed were the unknown carbamate equilibrium constants, equations 3.7f to 3.7j, the r and q parameters and the energetic interaction terms, u_0 and u_t. Experimentally determined CO_2 partial pressures, total pressures for the unloaded and loaded solution, C^{13} NMR data and loadings were used for the parameter regression. The fitting procedure was as follows.

Firstly the unknown temperature dependent carbamate equilibrium constants were regressed to reproduce the experimental data when only the ionic long range

term were used for activity coefficient calculation. A sensitivity test was performed on the r,q and u parameters, yielding the parameters with the highest influence on the prediction of the experimental data. These parameters were carefully changed until a good first fit was found that could be used as a starting point for the automatic regression in Modfit. The values of the R and Q parameters should be between 0 and 15, and the values of the u_0 and u_t parameters can vary between -5000 and 10^{10} (6).

3.3.2 Modfit

Modfit is an inhouse parameter regression tool, where it is possible to regress a large number of parameters, in this case the parameters of the extended UNIQUAC equation and equilibrium constants, to a large number of data, in this case experimental- VLE data and NMR data (13). The setup of the model is straight forward enough, the following is a quick guide. First Modfit has to "installed" into matlab, this is done by opening matlab, then choosing "file" and then "set path". Then "add folder" and then select the folder where Modfit lies, then press "ok".

The matlab files needed to run Modfit are shown in section B.3. Three files are needed, one main file to govern Modfit, one file to define the data that Modfit is regressing against and one to initiate the model. The file uniquacmodMAPA.m governs Modfit, the file MAPAdata.m defines the data which Modfit is regressing against and the file uniquacmodMAPA.m initiates the model by starting the function eqmodelMAPA.m. UniquacmodMAPA.m is thus the link between Modfit and the model proper. The procedure is then to define the parameters Modfit is regressing against, defining which parameters Modfit is free to change and defining its upper limit (BMAX), lower limit(BMIN) and the initial guess(B0). In the governing file uniquacmodMAPA.m, the responses of the model is designated as Y. Y would be whatever Modfit uses as its target for the regression analysis. It could be P_{CO2} or P_{tot} or the mole fractions from an NMR analysis. X is the input to the model, temperature, weight percent amine, etc. The file MAPAdata.m transforms the experimental data into this framework. As can be

seen in the matlab code the variable beta is included in the the eqmodelMAPA.m function. This is a vector with the new values for the parameters Modfit is allowed to change. To implement this change some code has to be pasted into the the model proper so that the values of the vector beta will overwrite the original parameters in the model proper. Below is the code necessary shown that has to be pasted into the extended Uniquac equation of the model proper for the given Modfit configuration in section B.3.

In file uniquacmodMAPA.m and MAPAdata.m the variable "FLAGG" determines if Modfit is using total pressure or partial pressure as regression target, thus the variable "FLAGG" gives Modfit great flexibility to use different types of experimental data in the same regression. Remember to change the length of the vectors BNL, BNK and BIN to the same length as B0. The ones and zeros in BIN designate which variables Modfit is free to change. A one designates that Modfit can change the variable in the regression and a zero designates it to be fixed. Modfit is based on Levenberg & Marquardt minimization which minimizes the objective function 3.18 [Aronu et al (1)].

$$F = \sum_{i=1}^{n} \left(\frac{P_{CO_2}^{exp} - P_{CO_2}^{cal}}{P_{CO_2}^{exp}} \right)^2 + \sum_{i=1}^{n} \left(\frac{P_{tot}^{exp} - P_{tot}^{cal}}{P_{tot}^{exp}} \right)^2 \tag{3.18}$$

```
 % IF PARAMETER ESTIMATION RUN
   % Checks if parameter est. run or not.
if ~isempty(varargin{:}{:}{:}{:}{:})
    parnew = varargin{:}{:}{:}{:}{:};

       u0(3,4) = parnew(1);
       ut(3,4) = parnew(2);
       u0(3,5) = parnew(3);
       ut(3,5) = parnew(4);
       u0(3,6) = parnew(5);
       ut(3,6) = parnew(6);
       u0(3,8) = parnew(7);
       ut(3,8) = parnew(8);
       u0(3,10) = parnew(9);
       ut(3,10) = parnew(10);
       u0(3,14) = parnew(11);
       ut(3,14) = parnew(12);
end
```

4

Results

4.1 Data available for the MAPA system

The data available for the loaded MAPA system is presented in table 4.1. Roughly half of the VLE data available for the loaded MAPA system were measured in this work.

4.2 Method verification

4.2.1 VLE measurement verification

In order to familiarize the author with the experimental methods and to check the validity of the experiments to be performed a series of verification experiments were carried out, both for the HTA and LTA. The low temperature verification experiments were performed with a 5M MAPA solution at 40°C and the results are shown in figure 4.1. The HTA validation was done by testing a solution of 45 wt % MEA. The results were compared with 45 wt% MEA data from [Gondal]. The results are shown in figure 4.2 and show excellent agreement with the data from Gondal.

Data	C [M]	T [K]	loading	Source
VLE	5M	313.15	$0.125 - 1.1$	Measured by Peter Bruder & Shahla Gondal & in this work
		333.15	$0.6 - 1.1$	Measured by Peter Bruder
		353.15	$0.5 - 1.4$	Measured by Peter Bruder & in this work
		373.15	$0.8 - 1.3$	Measured by Peter Bruder
		393.15	$0.6 - 1.1$	Measured by Peter Bruder
VLE	2M	313.15	$0.6 - 1.1$	Measured in this Work
		333.15	$0.5 - 1.2$	Measured in this Work
		353.15	$0.3 - 1.4$	Measured in this Work
		373.15	$0.9 - 1.3$	Measured in this Work
		393.15	$1 - 1.4$	Measured in this Work
NMR	5M	273.15	$0 - 0.56$	(4)
$H_{N_2O}^{MAPA}$	5 M	273.15	$0 - 0.94$	(4)
H_{abs}	3 wt%	313.15	$0.2 - 2.5$	[Kim, I. (17)]
		353.15	$0.2 - 1.6$	[Kim, I. (17)]
		393.15	$0.3 - 1.6$	[Kim, I. (17)]
H_{abs}	8 wt%	313.15	$0 - 0.4$	[Kim and Svendsen (18)]
		333.15	$0 - 0.4$	[Kim, I. (17)]
		333.15	$0 - 0.4$	[Kim and Svendsen (18)]

Table 4.1: The data available for the loaded MAPA system

4.2.2 Boiling test

Due to scatter observed in the vle data, figures 4.13, 4.14 and 4.15, an "boiling test" was performed to see if this was the reason for scatter in the data. It was thought that the reason that the samples with scatter could have been unknowingly left to boil for a longer/shorter time period than others during the CO_2 titration procedure. This could lead to the the capture reactions not being completely reversed and thus the method would yield an incorrectly amount of CO_2 captured. The same sample was titrated eight times, two parallels were boiled for one hour, two were boiled for thirty minutes, two were boiled for 5 minutes and two samples were just boiled up once and then immediately removed from the heater. The results are shown in table 4.2. The reason why the results of the parallels are compared to the one hour parallels is because it was assumed that at one hour all the CO_2 would have been released from the amine mixture.

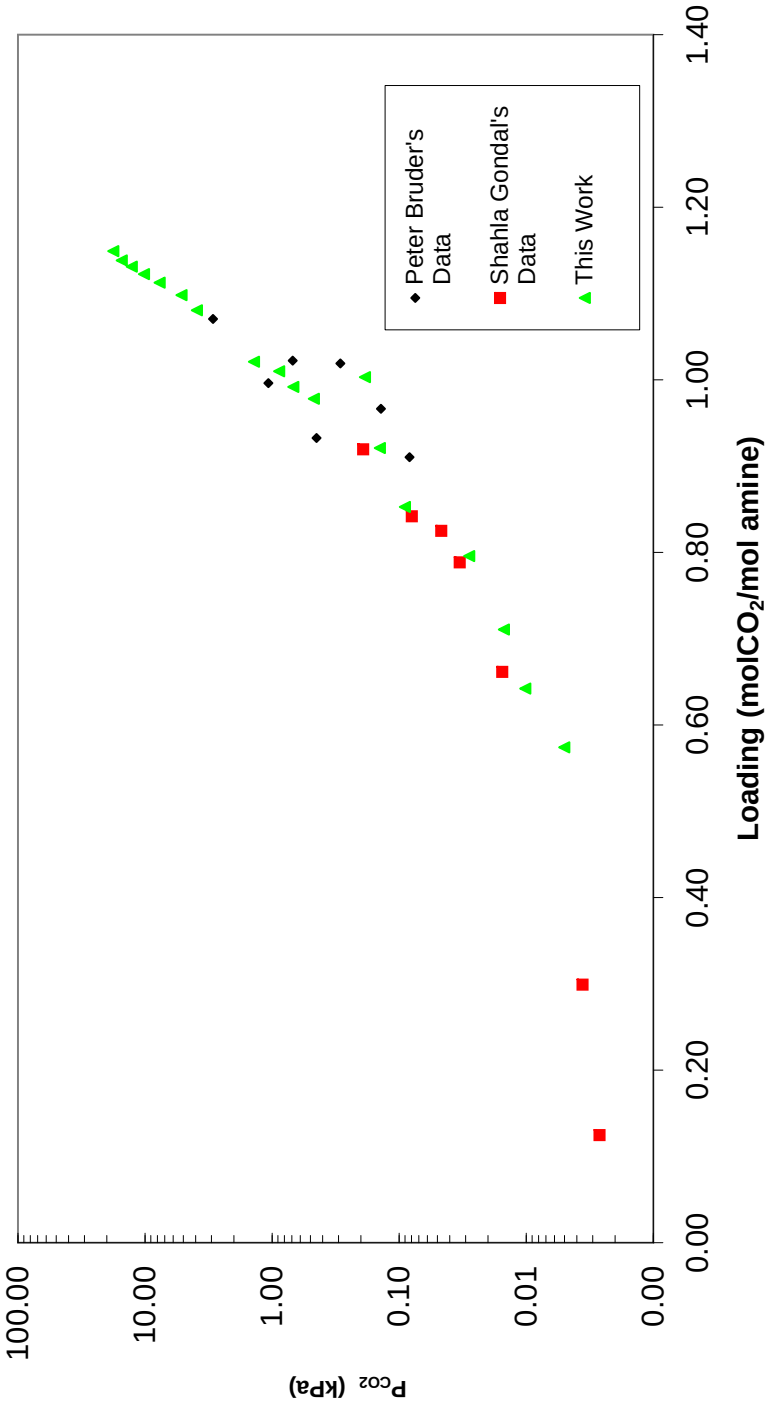

Figure 4.1: VLE data for the loaded 5 M MAPA system - Done for verification purposes

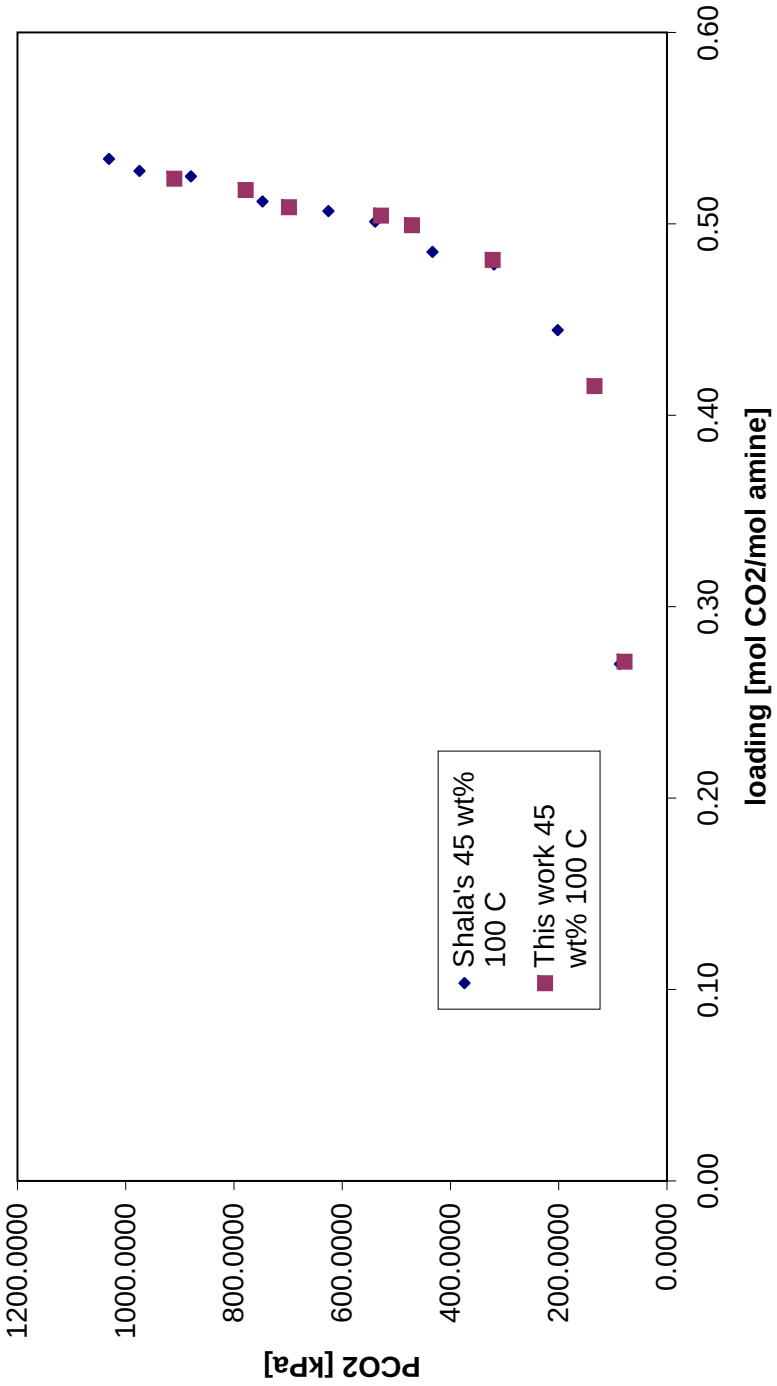

Figure 4.2: VLE data for the loaded 45 wt % MEA system - Where the pink points are the data of this work and the blue points are the data of Gondal.

Table 4.2: Results of the boiling time experiment - The parallels are displayed in pairs and the numbers are the average of the pair

Paralell nr.	Boiling time [min]	CO_2 amount determined [mol CO_2/l]	Deviation from 60 min case [%]
1 and 2	0	1.726	0
3 and 4	5	1.726	0
5 and 6	30	1.727	0.1
7 and 8	60	1.726	NA

4.2.3 Fugacity calculation routine verification

As the fugacity calculation routine is based on a set of predictions, namely the critical temperature prediction, B_{pure} prediction and B_{cross} prediction. Each of the steps had to be tested and validated. The validating results are shown in this section. The prediction power of the B_{pure} prediction method was tested with three amines of varying complexity. The critical temperature was predicted and used in the B_{pure} prediction, therefore the figures 4.3, 4.4 and 4.5 are a measure of the combined prediction power of T_c^{est} and B_{pure}^{est}. Unfortunately no experimental B_{pure} values for a diamines were found in the literature, which limits the methods use for MAPA somewhat. As can be seen in the figures 4.3, 4.4 and 4.5 the method is capable of predicting B_{pure} within the experimental uncertainty most of the time. The next step was to test the prediction power for cross coefficient, B_{cross}^{est}. The results are shown in figures 4.6, 4.7, BenzeneCO2, 4.9 and 4.10. The two figures 4.11 and 4.12 show the prediction of the two coefficients $B_{MAPA-CO_2}$ and B_{MAPA-H_2O}.

4.3 VLE Results

The VLE data for the 2M loaded system are shown in figure 4.13, the 5M VLE data are shown in figure 4.14 and the 2M and 5M data are shown together in figure 4.15.

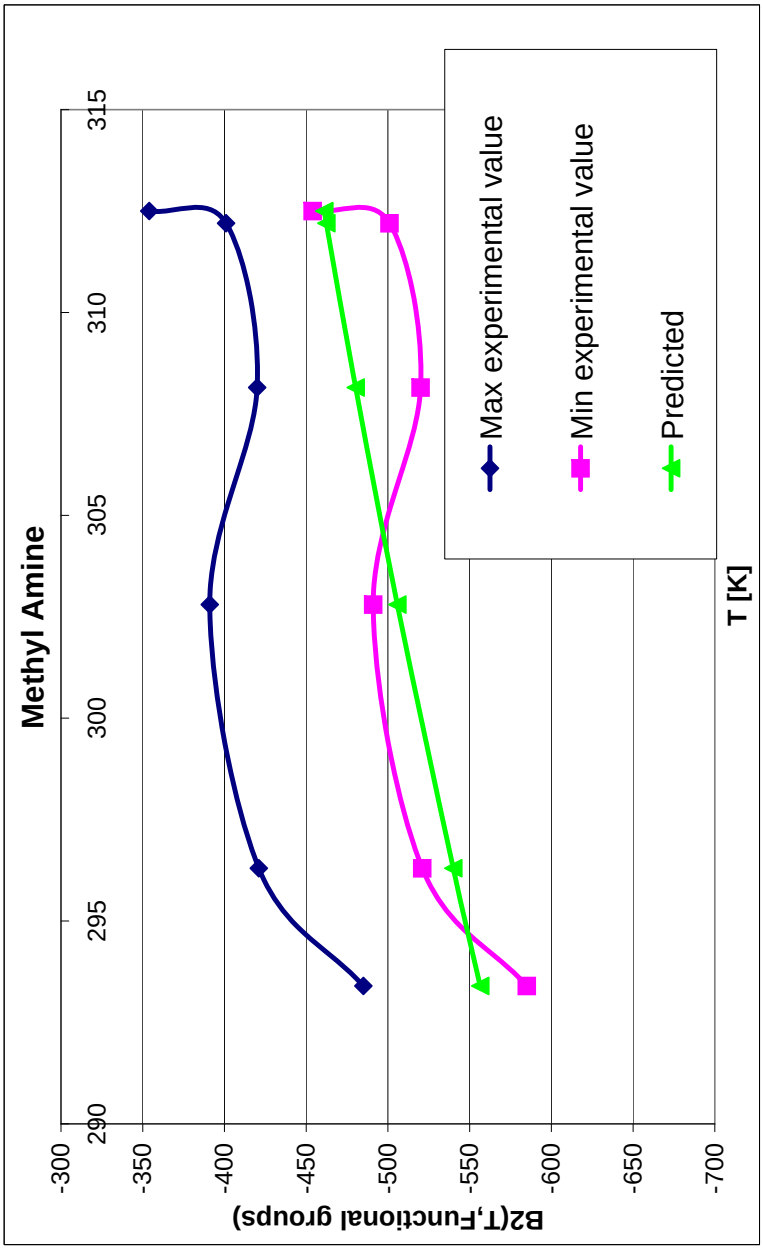

Figure 4.3: Prediction of Second virial coefficient for Methylamine - where the blue line shows the experimental value pluss max uncertainty, the pink line shows the experimental value minus the max uncertainty and the green line shows the prediction. The experimental values were found in Springer materials (22)

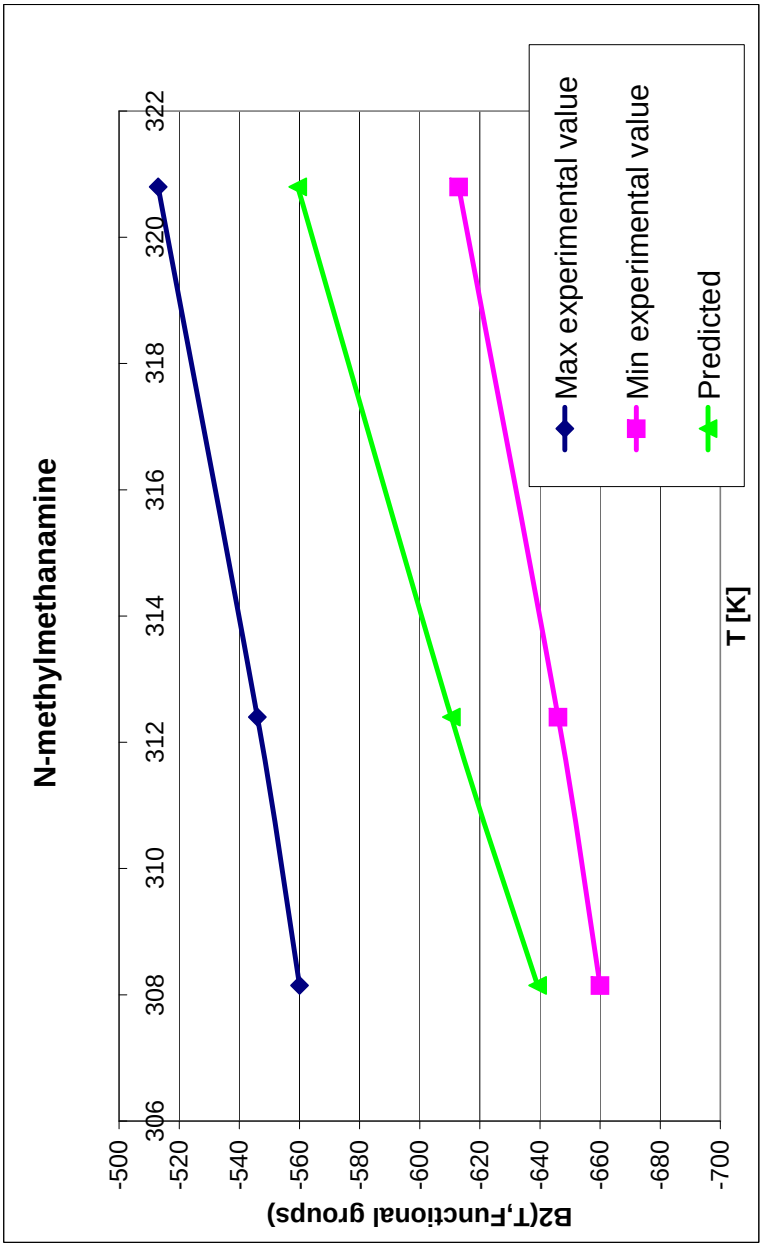

Figure 4.4: Prediction of Second virial coefficient for N-methylmethanamine - where the blue line shows the experimental value pluss max uncertainty, the pink line shows the experimental value minus the max uncertainty and the green line shows the prediction. The experimental values were found in Springer materials (22)

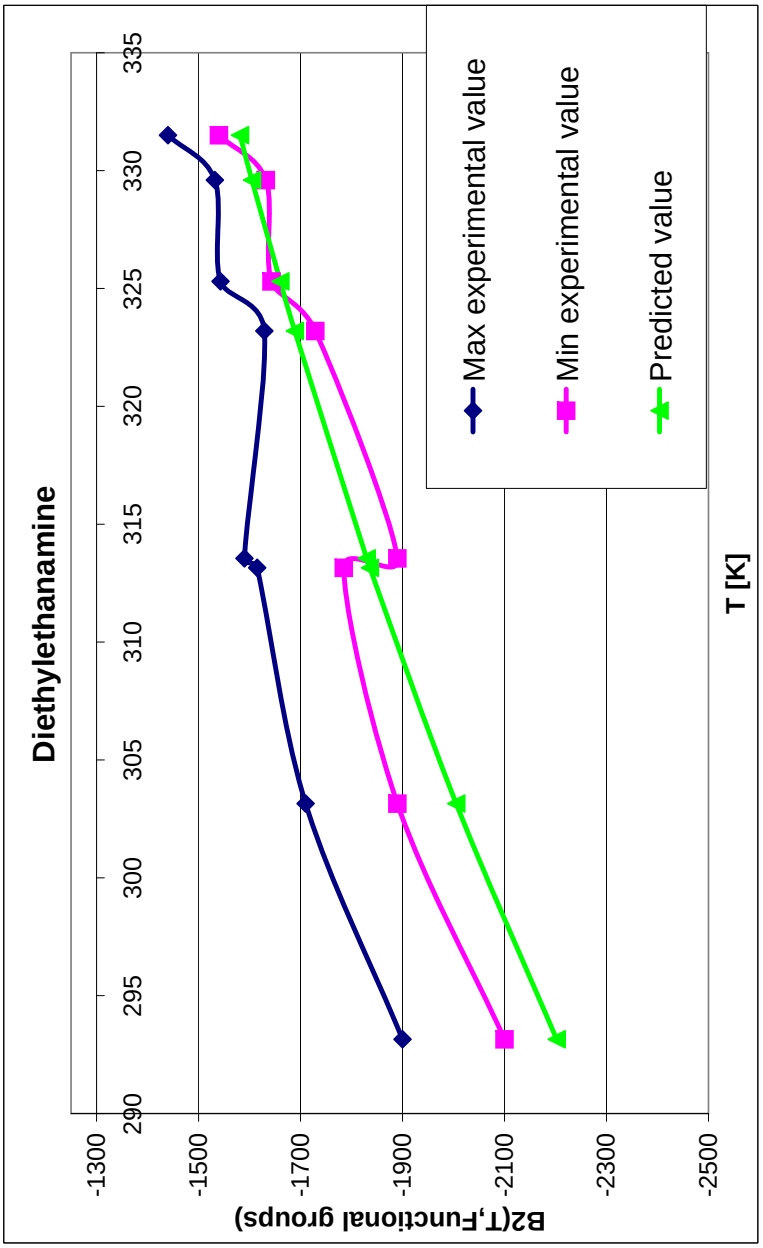

Figure 4.5: Prediction of Second virial coefficient for Diethylethanamine - where the blue line shows the experimental value pluss max uncertainty, the pink line shows the experimental value minus the max uncertainty and the green line shows the prediction. The experimental values were found in Springer materials (22)

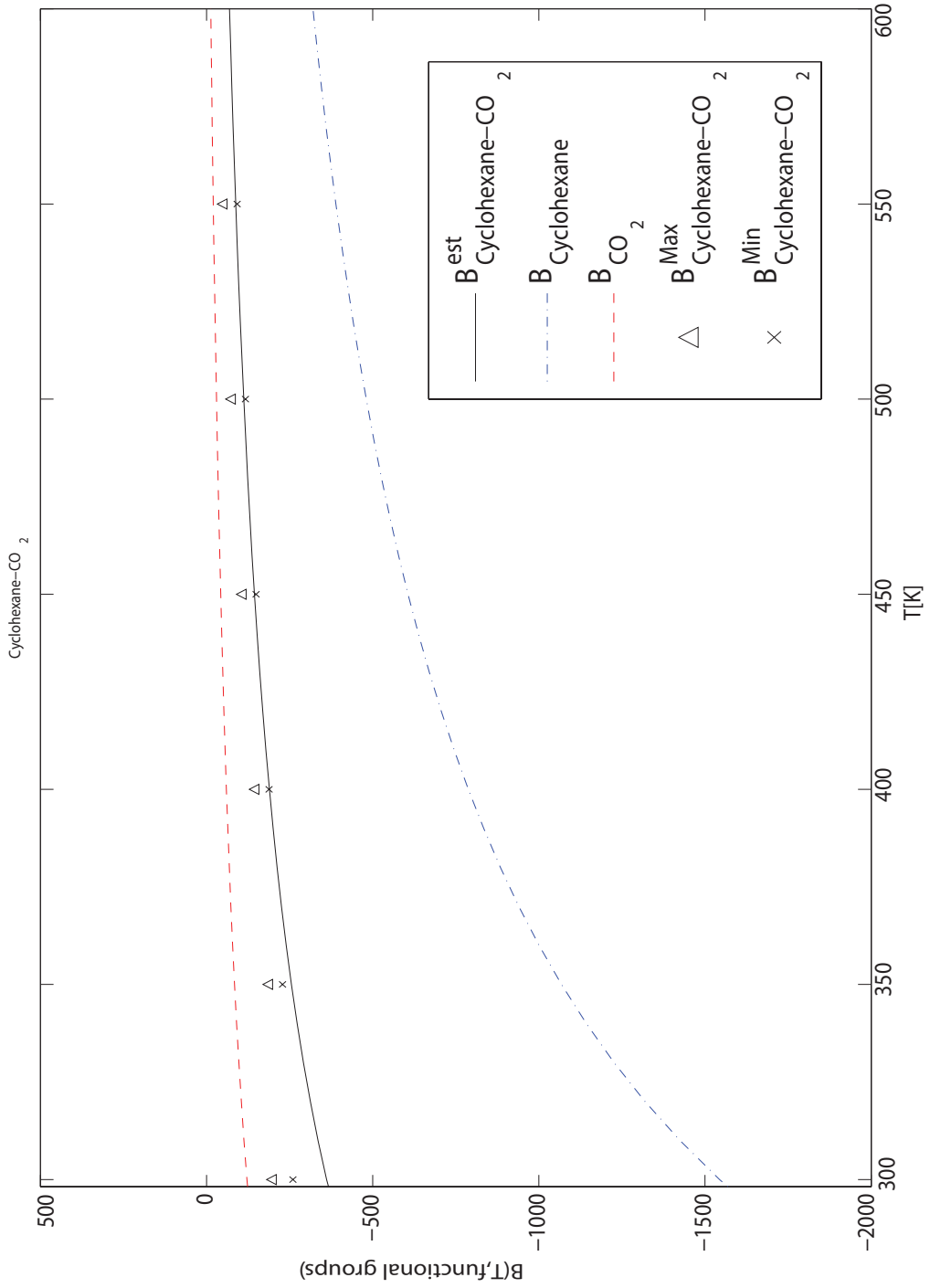

Figure 4.6: Prediction of Cross Second virial coefficient for the mixture of Cyclohexane and carbondioxide compared with the experimentally found cross coefficient and the pure coefficients - The experimental values were found in Springer materials (22) and (21)

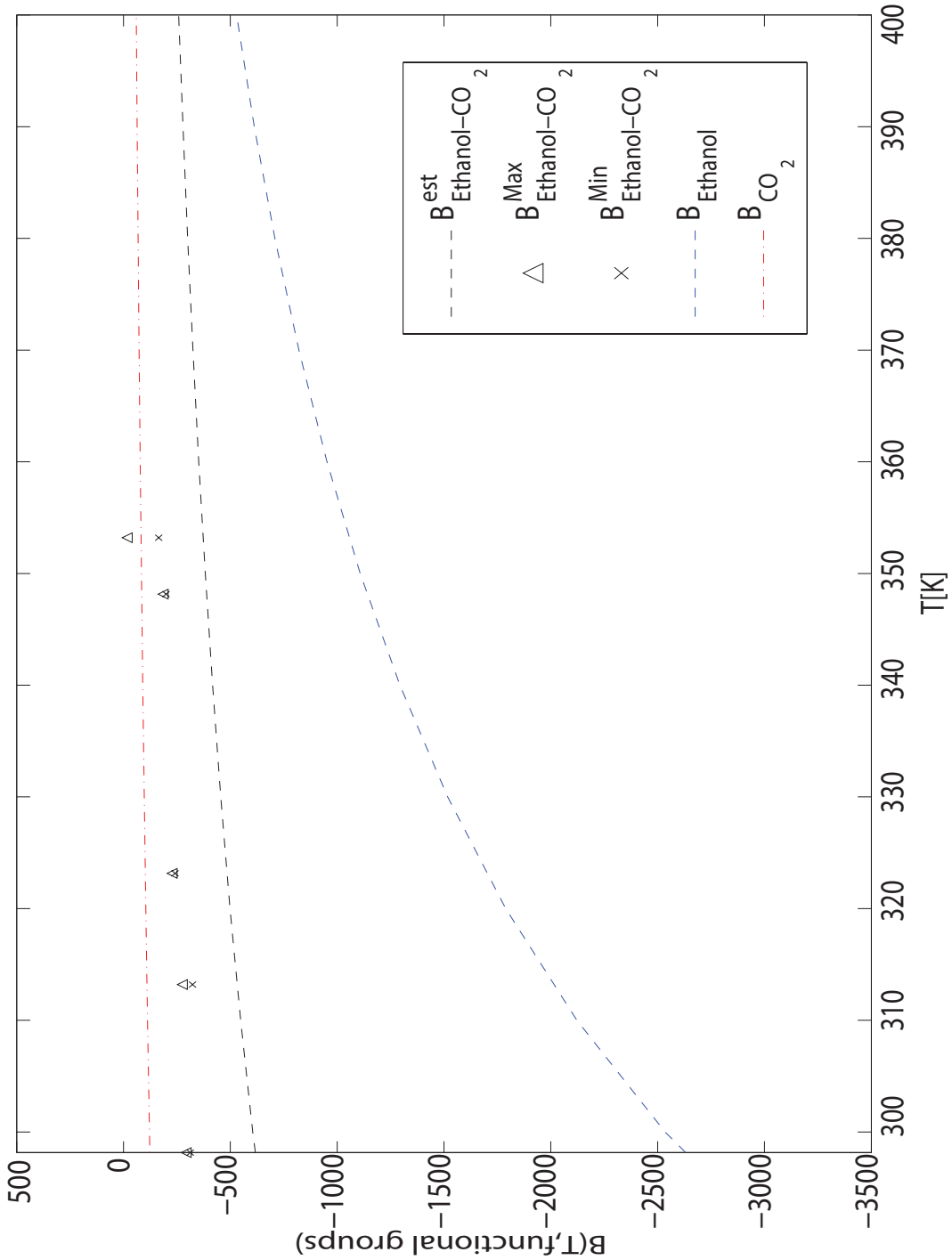

Figure 4.7: Prediction of Cross Second virial coefficient for the mixture of Ethanol and Carbondioxide compared with the experimentally found cross coefficient and the pure coefficients - The experimental values were found in Springer materials (22) and (21)

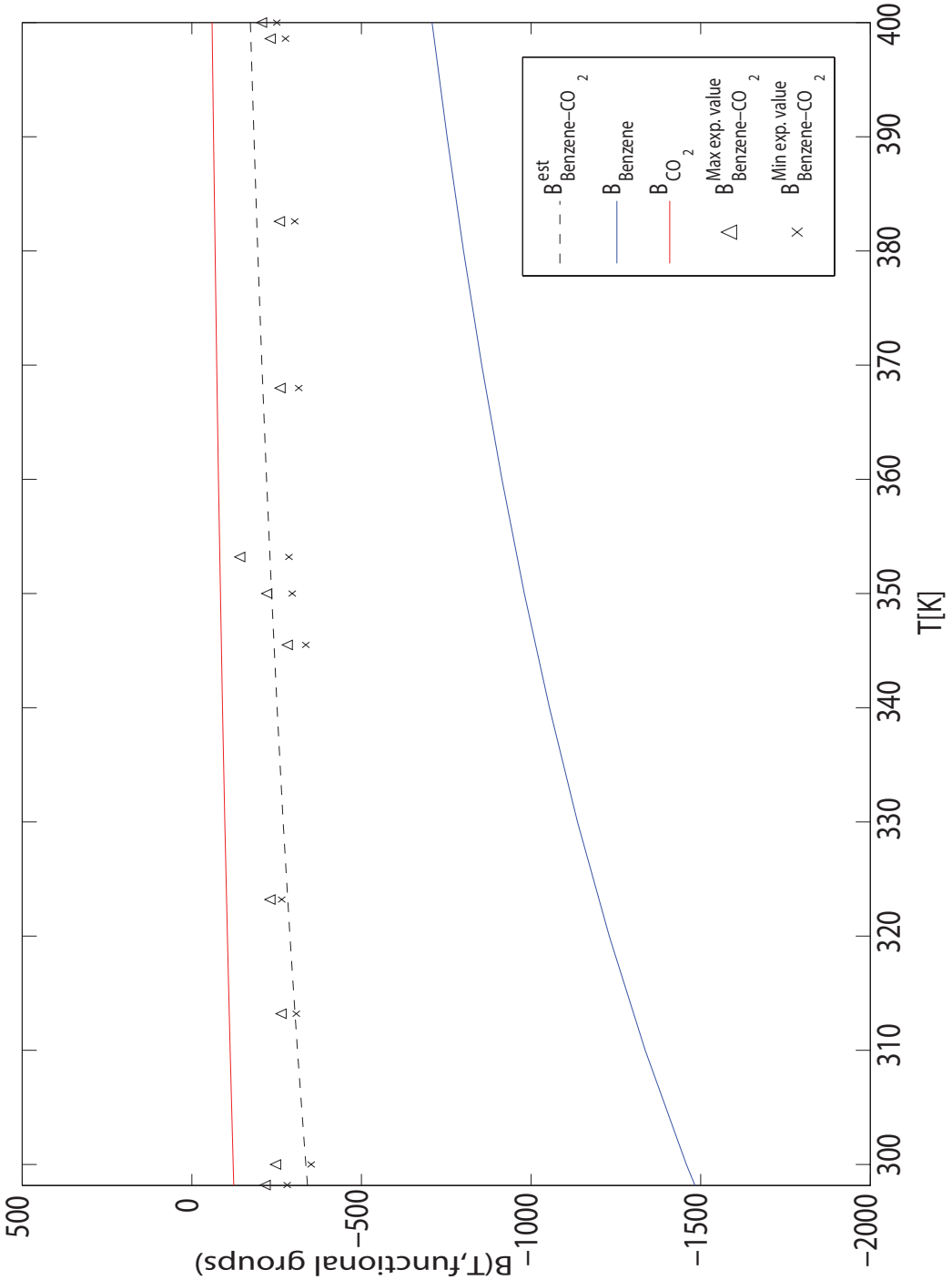

Figure 4.8: Prediction of Cross Second virial coefficient for the mixture of Benzene and Carbondioxide compared with the experimentally found cross coefficient and the pure coefficients - The experimental values were found in Springer materials (22) and (21)

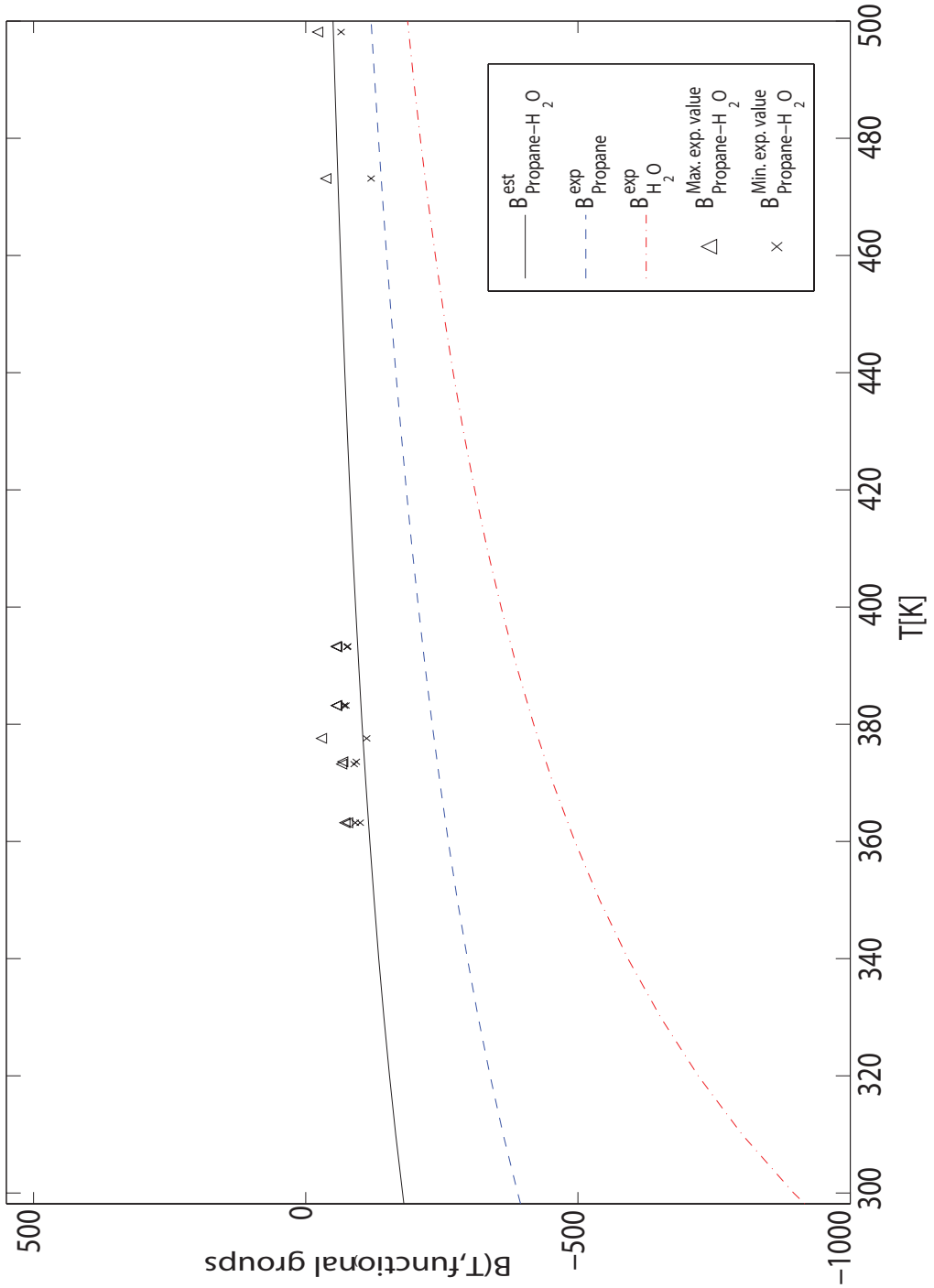

Figure 4.9: Prediction of Cross Second virial coefficient for the mixture of Propane and Water compared with the experimentally found cross coefficient and the pure coefficients - The experimental values were found in Springer materials (22) and (21)

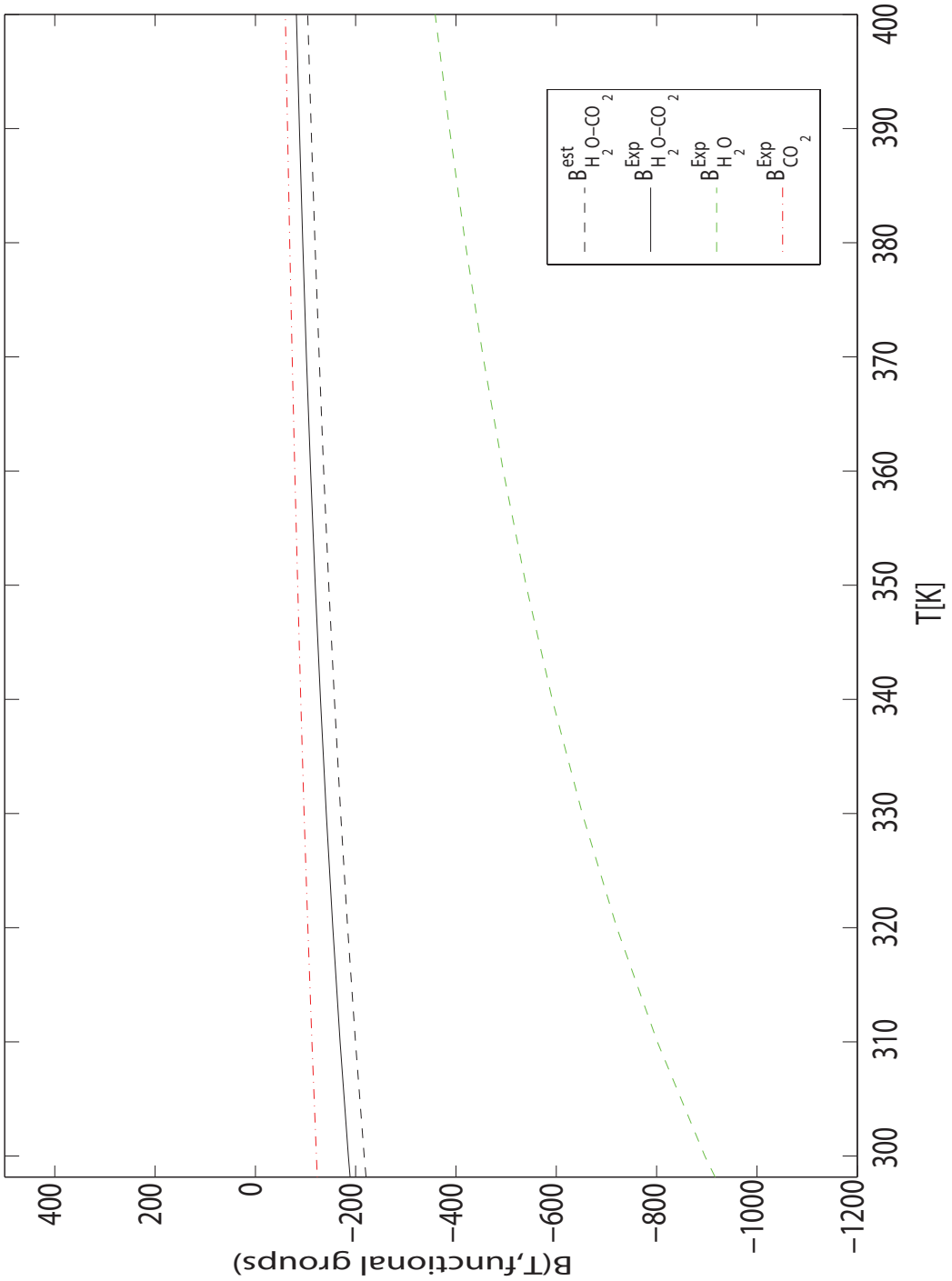

Figure 4.10: Prediction of Cross Second virial coefficient for the mixture of Water and Carbondioxide compared with the experimentally found cross coefficient and the pure coefficients - The experimental values were found in Springer materials (22) and (21)

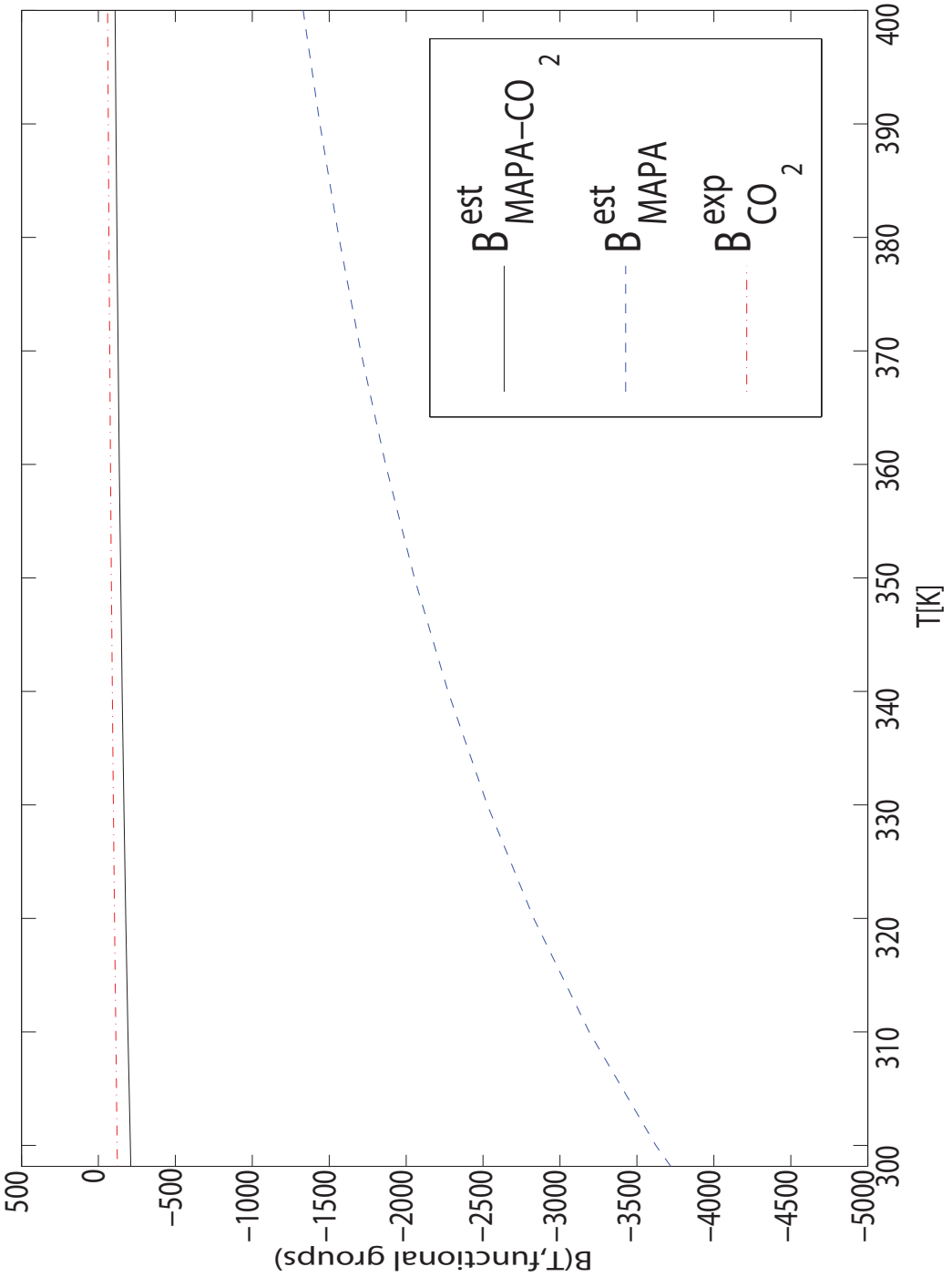

Figure 4.11: Prediction of Cross Second virial coefficient for the mixture of MAPA and Carbondioxide compared with the experimentally found cross coefficient and the pure coefficients - The experimental values were found in Springer materials (22) and (21)

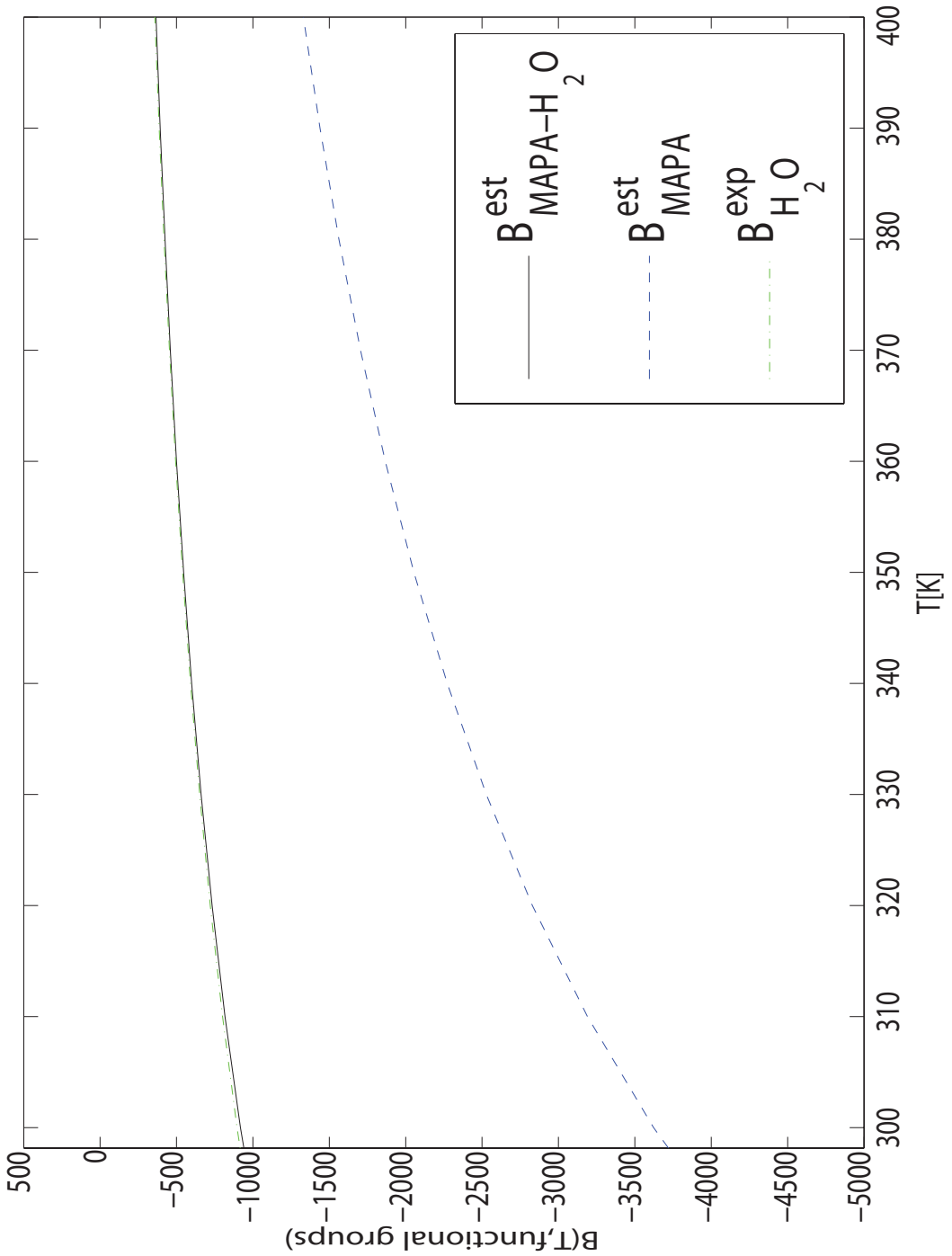

Figure 4.12: Prediction of Cross Second virial coefficient for the mixture of Water and MAPA compared with the experimentally found cross coefficient and the pure coefficients - The experimental values were found in Springer materials (22) and (21)

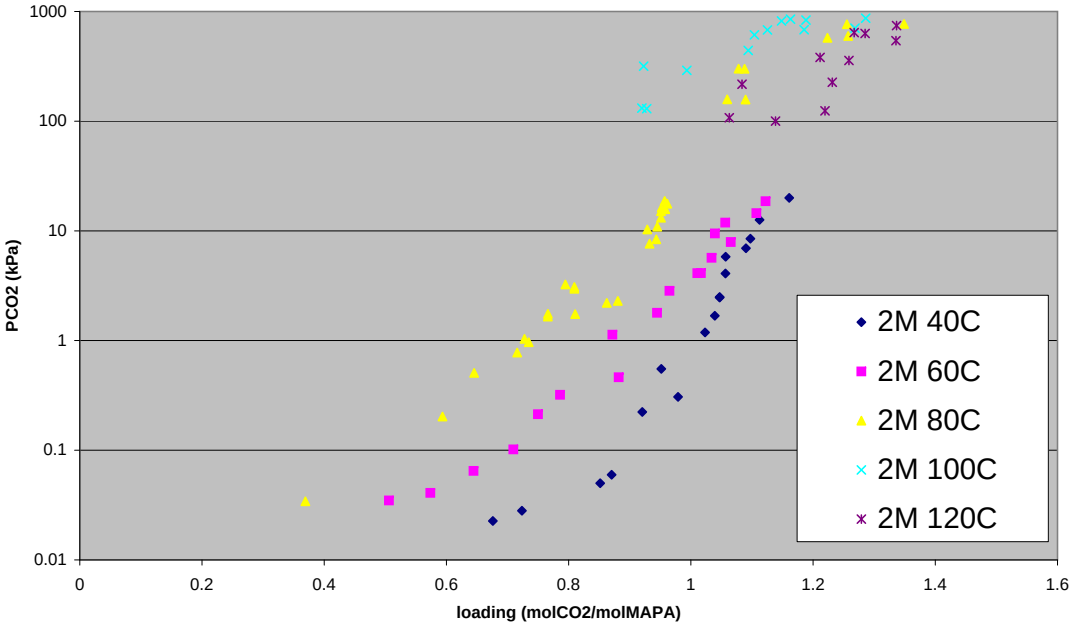

Figure 4.13: The experimental VLE data for the 2M loaded MAPA system -

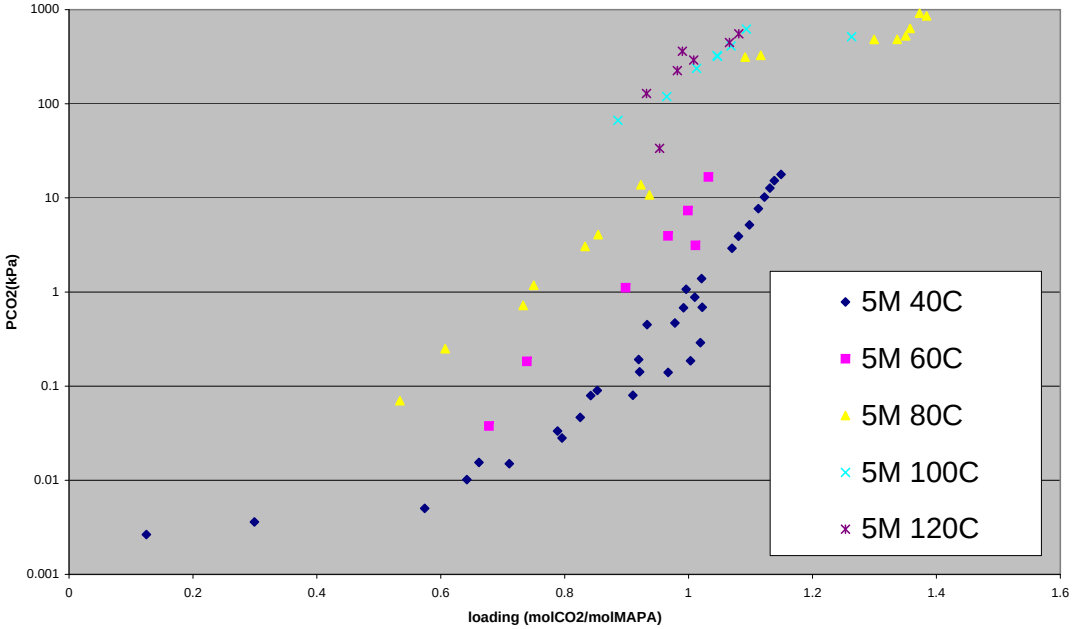

Figure 4.14: The experimental VLE data for the 5M loaded MAPA system -

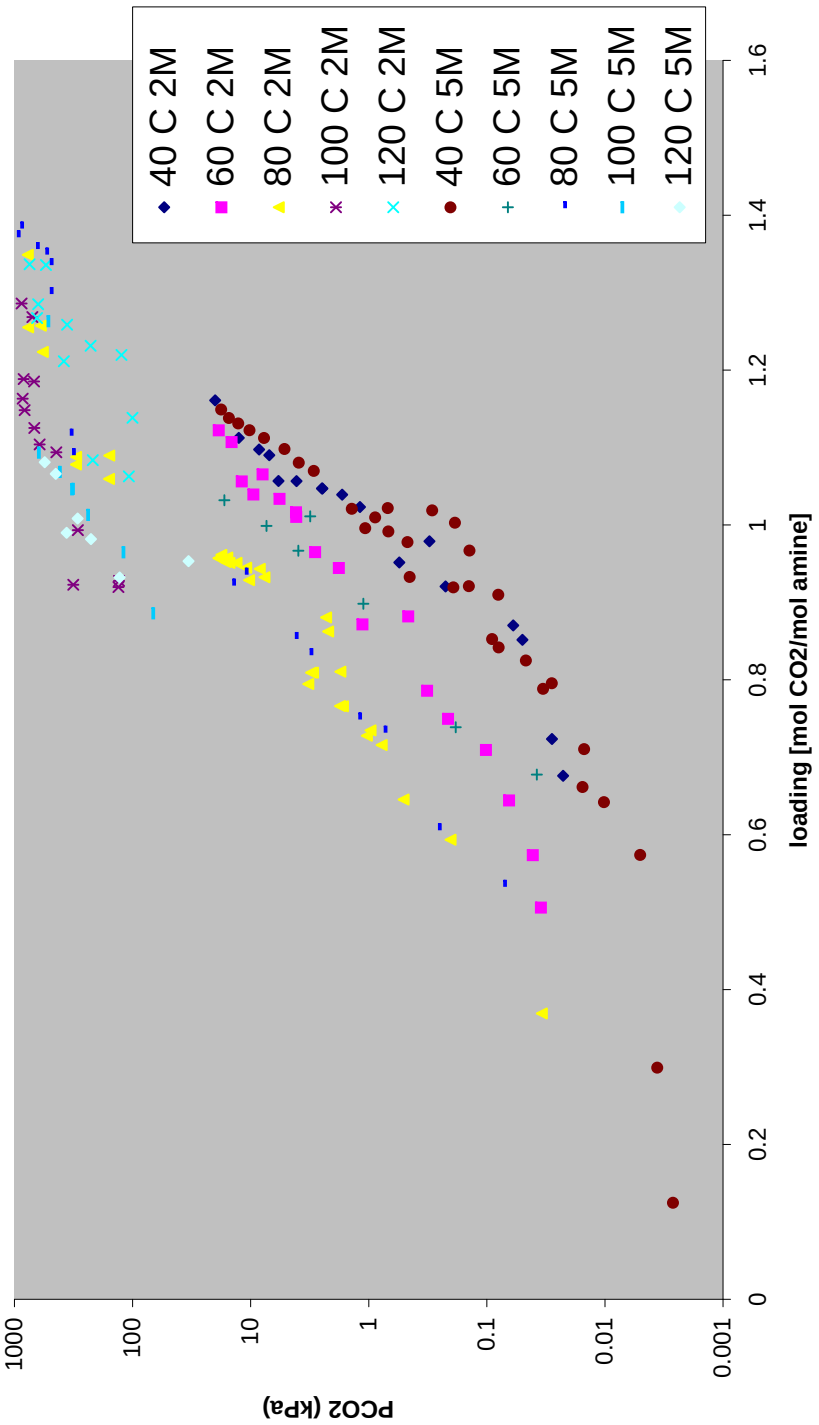

Figure 4.15: 5M and 2M experimental VLE data for the loaded MAPA system -

4.4 Modeling results

The results of the modeling procedure is presented in this section. A problem is that the NMR data does not distinguish between the zwitterion and the carbamate since the only difference between the two is a proton which is to small to detect. Thus two equally viable "scenarios" present them self. One with a high zwitterion stability and one with a high carbamate stability. Both of these "scenarios" are able to predict the VLE - and NMR data at low loading, $\alpha < 1$. However it is possible to change the UNIQUAC parameters in such a way that the model accurately predicts the high loading area, $\alpha > 1$. To do this the UNIQUAC parameters have to be set in a way that result in a very unideal calculated activity coefficients, i.e. that the values of the activity coefficients become very small or very high. These parameters then lead to convergence issues for higher concentrations of amine, since a higher concentration of amine will lead to higher non-idealities in the liquid phase. As discussed in section 3.2 a very very unideal system could cause problems in the iteration procedure. More on this in section 5.2.1. Thus one additional scenario presents itself, namely the scenario that predicts the 2M VLE data at all loadings and temperatures, but which makes the model "crash" for the 5 Molar run.

4.4.1 High zwitterion stability scenario

The high zwitterion stability scenario is presented in the following figures. It's ability to recreate the NMR data is shown in figure 4.18, it's ability to recreate the VLE data is shown in figure 4.17 and 4.16. An example speciation for loaded 5M MAPA system at 40 ° C is presented in figure 4.19. The equilibrium constants that define this scenario are presented in equation 4.1, and the regressed uniquac parameters are presented in tables 4.3 and 4.4.

$$lnK_{MAPACOO_p^-} = 2.27380 + \frac{10007.1}{T} - 7.23890 \cdot lnT \tag{4.1a}$$

$$lnK_{MAPACOO_s^-} = 2.26 + \frac{10407.1}{T} - 7.23910 \cdot lnT \tag{4.1b}$$

$$lnK_{H^+MAPACOO_p^-} = 1250.9 - \frac{61085.0}{T} - 188.54 \cdot lnT \tag{4.1c}$$

$$lnK_{H^+MAPACOO_s^-} = 1251.5 - \frac{60885.0}{T} - 188.44 \cdot lnT \tag{4.1d}$$

$$lnK_{MAPA(COO^-)_2} = 4573.3 - \frac{215550.0}{T} - 675.87 \cdot lnT \tag{4.1e}$$

4.4.2 High carbamate stability scenario

The high carbamate stability scenario is a scenario where the stability of the carbamate is higher when comparing to the high zwitterion stability scenario. In this scenario it's the same case as with the high zwitterion stability scenario; the model has problems predicting the high loading VLE data. The scenario is presented in the following figures. Figure 4.20 shows the experimental and predicted VLE data for the 2M loaded system. The figure 4.21 shows the same but for the 5M loaded system. Figure 4.22 shows the experimental NMR data and its fit to them, figure 4.23 shows an representative speciation for the 5M loaded system at 40°C. The figure 4.24 shows the activity coefficients of CO_2 as a function of loading and temperature predicted from the model for the whole temperature range measured in the experiments, and figure 4.25 shows the activity coefficient of CO_2 as a function of temperature and loading compared to the activity coefficient of CO_2 predicted by the N_2O analogy. The equilibrium parameters that define this scenario are given in equation 4.2. The optimal uniquac parameters for this scenario are given in tables 4.3 and 4.5.

$$lnK_{MAPACOO_p^-} = 4.26 + \frac{11523.75566}{T} - 7.33829 \cdot lnT \tag{4.2a}$$

$$lnK_{MAPACOO_s^-} = 4.97380 + \frac{11766.77023}{T} - 7.63992 \cdot lnT \tag{4.2b}$$

$$lnK_{H^+MAPACOO_p^-} = 1251.9 - \frac{61085.01122}{T} - 187.59824 \cdot lnT \tag{4.2c}$$

Table 4.3: The R and Q parameters for the two different scenarios - where the *emphasized* numbers are from [Arouno et al (1)] and the underlined are from [Thomsen and Rasmussen (29)]. The remaining were used to fit the data.

	High Zwitterion stability scenario		High Carbamate stability scenario	
	R	Q	R	Q
H_2O	0.920	1.400	0.920	1.400
$MAPA$	*7.360*	*6.986*	*7.360*	*6.986*
CO_2	5.741	6.081	5.741	6.081
$H^+MAPACOO_p^-$	0.892	0.486	1.784	0.486
$H^+MAPACOO_s^-$	0.892	0.972	5.353	2.674
H_3O^+	0.138	1e-15	0.138	1e-15
$MAPAH^+$	1.724	2.051	2.299	1.230
$MAPA(H^+)_2$	0.645	6.076	0.753	0.868
OH^-	9.397	8.817	9.397	8.817
HCO_3^-	*4.481*	*2.639*	*4.481*	*2.639*
CO_3^{2-}	*12.994*	*8.615*	*12.994*	*8.615*
$MAPACOO_p^-$	11.306	7.054	1.615	0.882
$MAPACOO_s^-$	9.691	7.054	4.038	3.526
$MAPA(COO^-)_2$	10.828	6.945	4.331	1.736

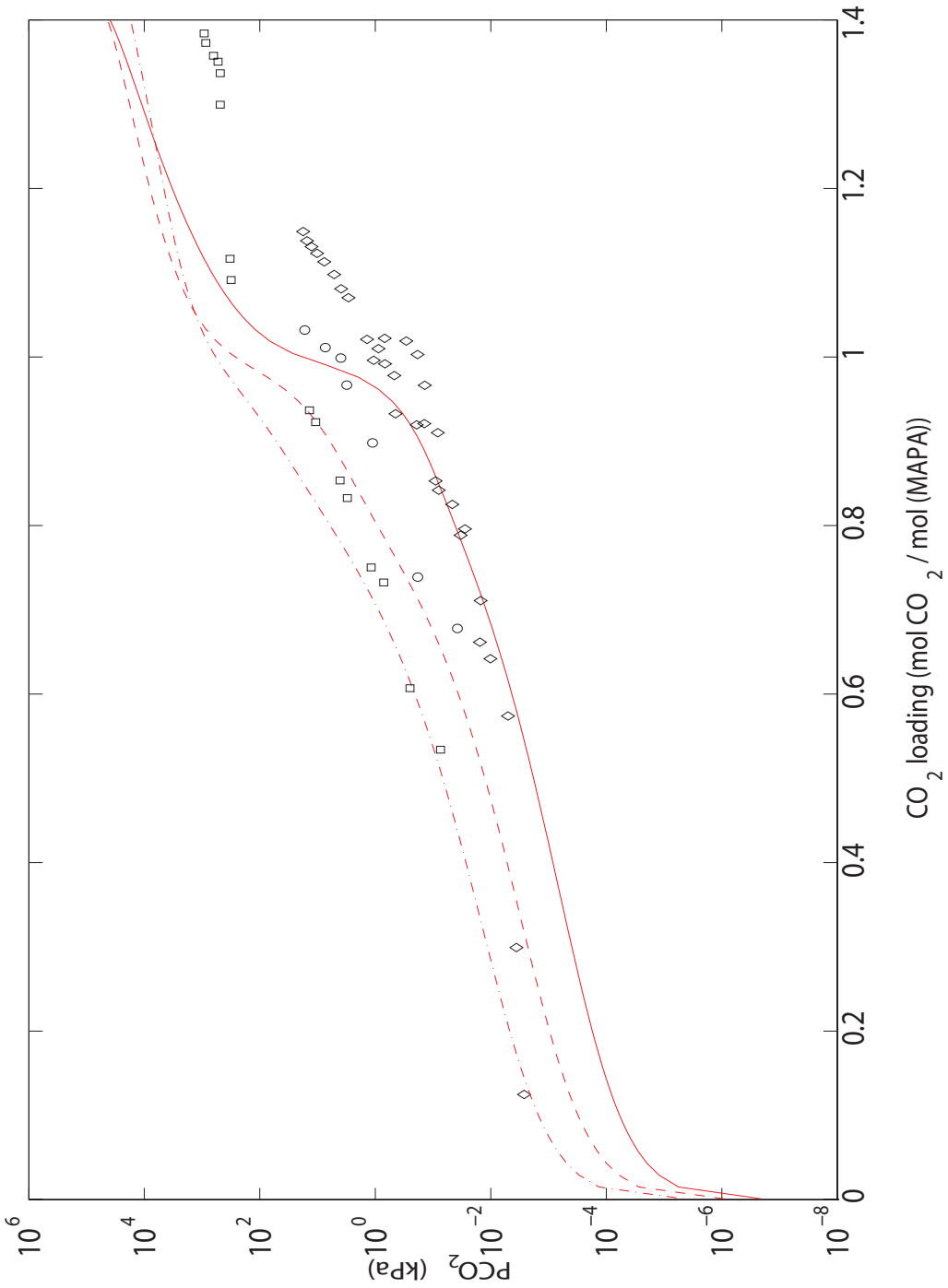

Figure 4.16: Experimentally measured and modeled VLE data for the loaded 5M MAPA system modeled with the "High Zwitterion stability Scenario" - Where the diamonds are for experimental 40° C data, the circles are for experimental 60° C data and the squares are for experimental 80° C data. The lines are the predicted VLE from the model. The solid line is for 40° C, the dashed line is for 60° C and the dash-dot line is for 80° C.

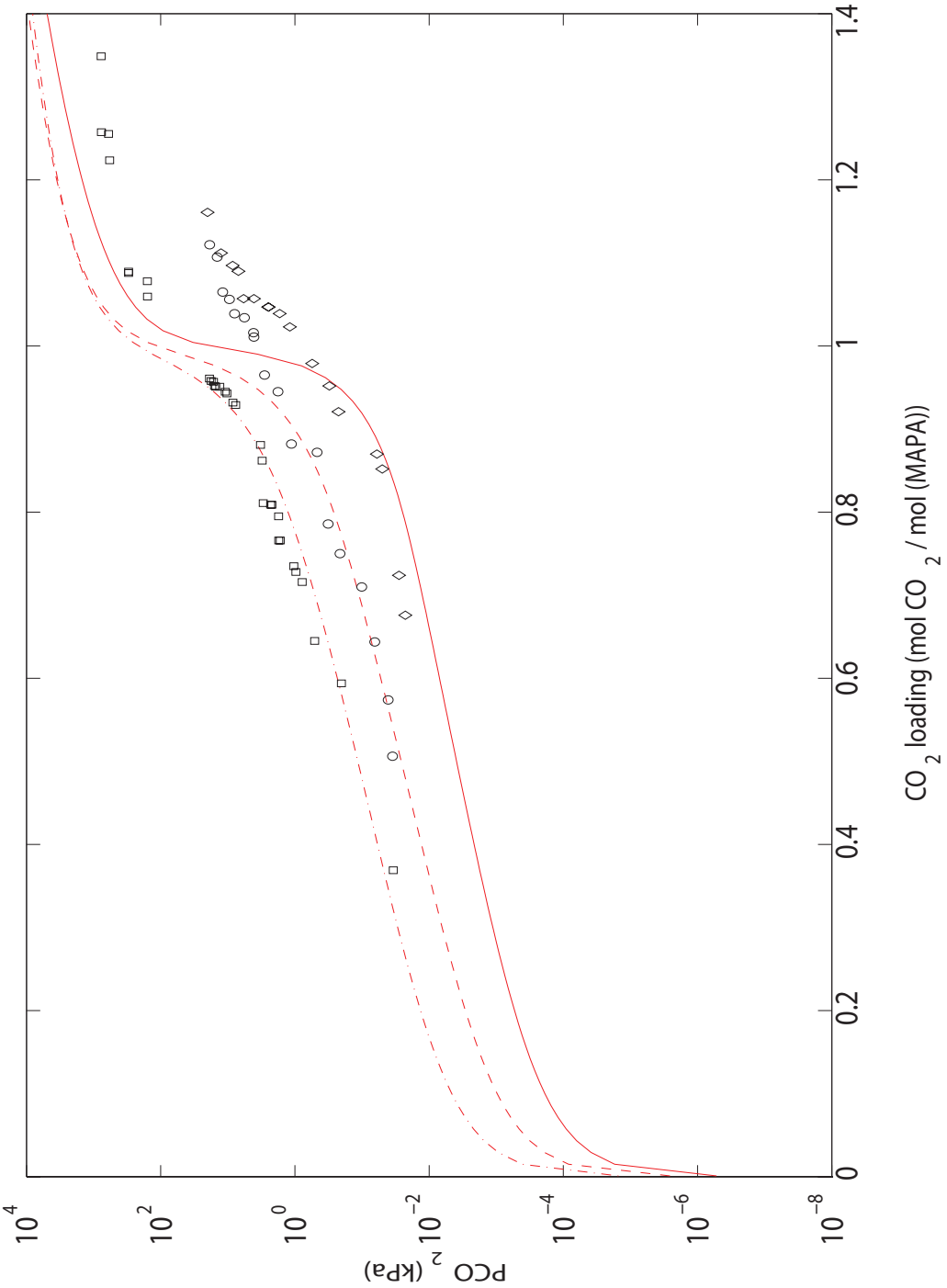

Figure 4.17: Experimentally measured and modeled VLE data for the loaded 2M MAPA system modeled with the "High Zwitterion stability Scenario" - Where the diamonds are for experimental 40° C data, the circles are for experimental 60° C data and the squares are for experimental 80° C data. The lines are the predicted VLE from the model. The solid line is for 40° C, the dashed line is for 60° C and the dash-dot line is for 80° C.

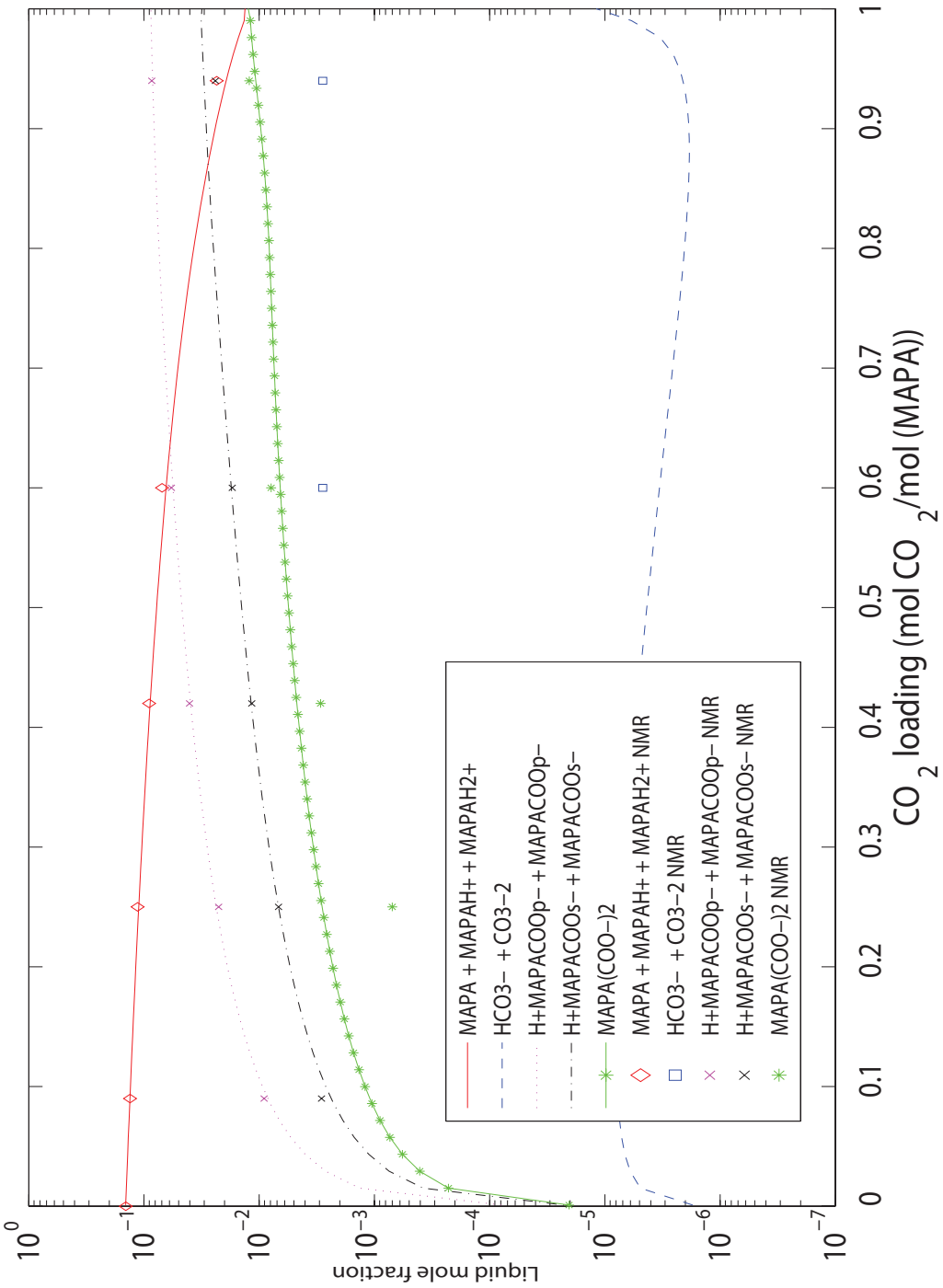

Figure 4.18: The experimental NMR data compared with the model predictions based on the high zwitterion scenario - The legend is in the figure.

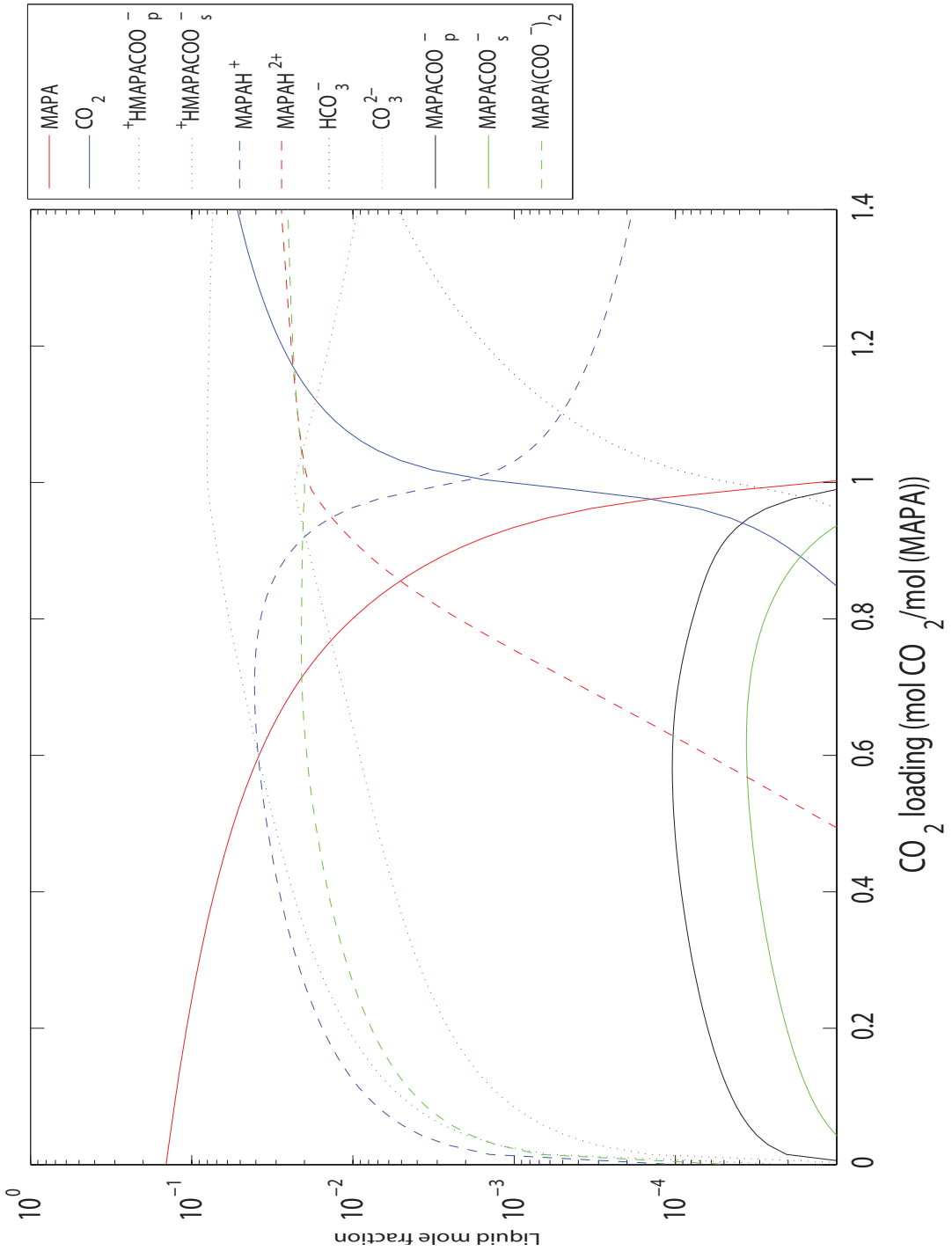

Figure 4.19: Example speciation of the 5M loaded MAPA system at 40° C based on the high zwitterion stability scenario - The legend is in the figure

Table 4.4: UNIQUAC parameter u for the "high zwitterion stability scenario" - Where the grey fields are the parameters from [Aronu et al (1)] and the bold underlined fields are from [Thomsen & Rasmussen (29)]

(a) u0 parameters

u0	H_2O	MAPA	CO_2	$H^+MAPACOO_p^-$	$H^+MAPACOO_s^-$	H_3O^+	$MAPAH^+$	$MAPA(H^+)_2$	OH^-	HCO_3^-	CO_3^{2-}	$MAPACOO_p^-$	$MAPACOO_s^-$	$MAPA(COO)_2$
H_2O	0													
MAPA	196.7549	506.326												
CO_2	-183.0239	-165.1492	**40.52**											
$H^+MAPACOO_p^-$	110.1	2500	-100	-67.27										
$H^+MAPACOO_s^-$	-150	2500	2500	100.1		0								
H_3O^+	**10000.00**	1.00E+09	2500	100	1.00E+09	1.00E+09								
$MAPAH^+$	-154.0887	2500	-113.1662	725	1.00E+09	1.00E+09	0							
$MAPA(H^+)_2$	375.08	2500	2500	314.71	1.00E+09	1.00E+09	1.00E+09	25000						
OH^-	600.4952	1.00E+09	1.00E+09	43	1.00E+09	1.00E+09	1.00E+09	1.00E+09	**1562.88**					
HCO_3^-	**517.0278**	2642.0446	2500	229.99	229.99	1.00E+09	2500	2500	**2.50E+03**	2032.837				
CO_3^{2-}	**361.3877**	1.00E+09	**2500**	2500.1	2500	1.00E+09	1.00E+09	2500	**1.59E+03**	7.99E+02	**1458.34**			
$MAPACOO_p^-$	2500	2500	2500	2500	2500	1.00E+09	1.00E+09	2500	1.00E+09	1.00E+09	1.00E+09	1.50E+03		
$MAPACOO_s^-$	2500	2600	2500	2500	2500	1.00E+09	1.00E+09	2500	1.00E+09	1.00E+09	1.00E+09	1.00E+09	1.50E+03	
$MAPA(COO)_2$	1.00E+09	1.00E+09	2500	2500	2500	1.00E+09	1.00E+09	2500	1.00E+09	1.00E+09	1.00E+09	1.00E+09	1.00E+09	1.50E+03

(b) ut parameters

ut	H_2O	MAPA	CO_2	$H^+MAPACOO_p^-$	$H^+MAPACOO_s^-$	H_3O^+	$MAPAH^+$	$MAPA(H^+)_2$	OH^-	HCO_3^-	CO_3^{2-}	$MAPACOO_p^-$	$MAPACOO_s^-$	$MAPA(COO)_2$
H_2O	0													
MAPA	0.7929	-0.37												
CO_2	6.0908	1.666	**13.63**											
$H^+MAPACOO_p^-$	7.5184	0	0	8.17										
$H^+MAPACOO_s^-$	-2	0	0	0	0									
H_3O^+	**10.91**	0	0	0	0	0								
$MAPAH^+$	-154.0887	0.1213	7.3541	0	0	0	0							
$MAPA(H^+)_2$	-0.3880	100	0	10.00	0	0	0	110						
OH^-	8.5455	0	0	0	0	0	0	0	**5.62**					
HCO_3^-	**6.9504**	15.2488	0	6.24	6.24	0	2.8863	0	**0**	17.114				
CO_3^{2-}	**3.3516**	5	**0**	0	0	0	0	0	**2.75**	2.61	**-1.35**			
$MAPACOO_p^-$	0	0	0	0	0	0	0	0	0	0	0	0		
$MAPACOO_s^-$	0	0	0	0	0	0	0	0	0	0	0	0	0	
$MAPA(COO)_2$	0	0	0	0	0	0	0	100	0	0	0	0	0	0

$$lnK_{H^+MAPACOO_s^-} = 1251.5 - \frac{60885.01122}{T} - 187.25006 \cdot lnT \tag{4.2d}$$

$$lnK_{MAPA(COO^-)_2} = 4560.3 - \frac{219359.91612}{T} - 673.5781 \cdot lnT \tag{4.2e}$$

When considering the equations for the carbamate equilibrium constants it can be seen that the two first parameters on the right hand side in the carbamate stability constant correlation, equations 4.2a and 4.2b, are higher than the same terms in the high zwitterion stability scenario, equations 4.1a and 4.1b. This is the major difference between the two scenarios.

4.4.3 High Carbamate stabiltiy scenario optimized for 2M loaded solution

In this section the last of the three scenarios is presented. This scenario has the same equilibrium constants as the High carbamate stability scenario, equation set 4.2, and it has also the same R and Q parameters as shown in table 4.3. The energetic interaction parameters for CO_2, u_{CO_2-X} have been changed to fit the experimental data, where X represents another arbitrary component in the system. The UNIQUAC parameters for this scenario are shown in table 4.6, and its fit to the VLE data is shown in figures 4.26 and 4.27.

4.4.4 N2O analogy activity results

As described in section 2.5 the experimentally determined solubility was used to find the symmetric activity coefficient of the N_2O analogy system. This coefficient is similar but not the same that would be found for the real system.

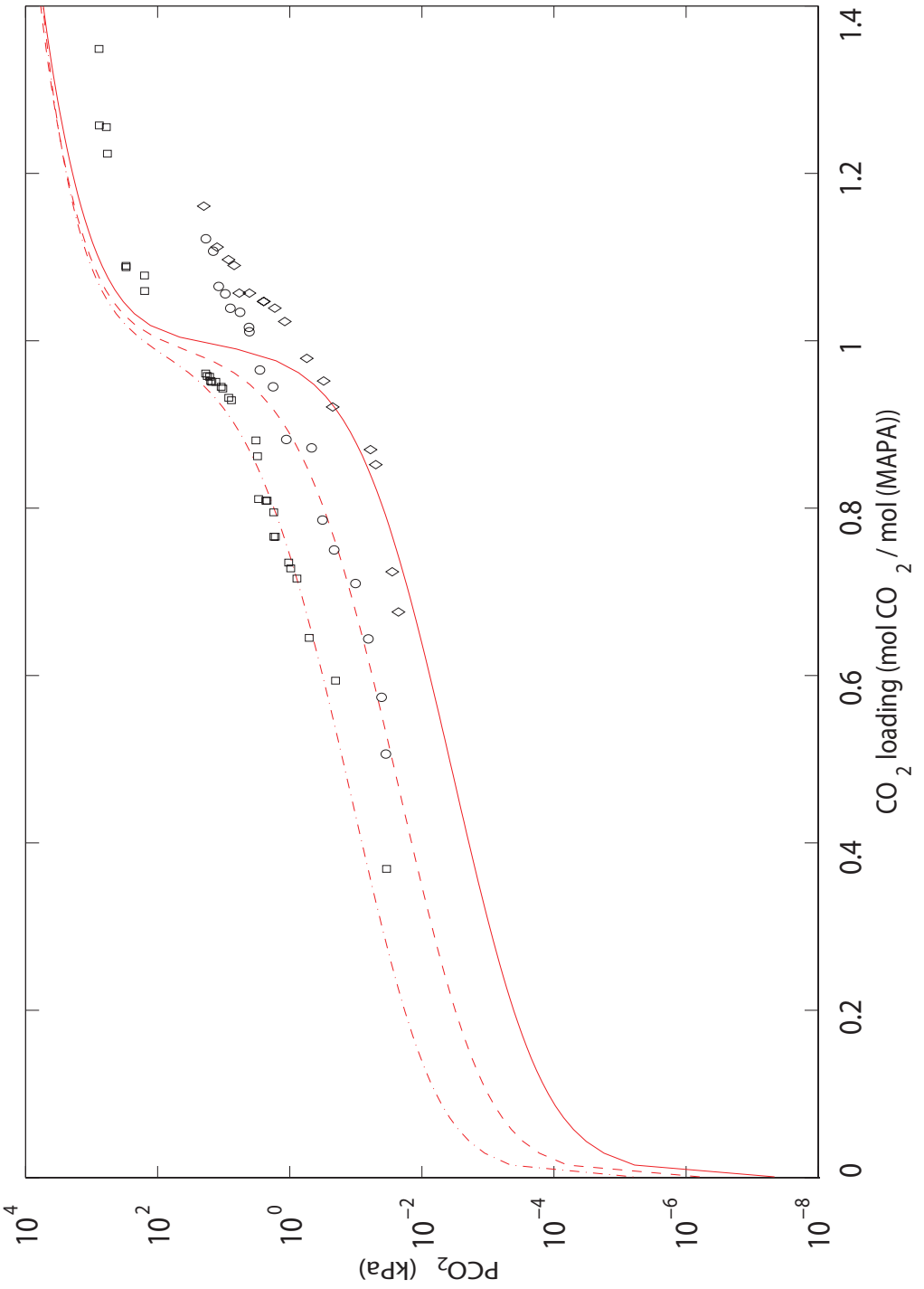

Figure 4.20: The experimental VLE data for the 2M loaded and the predictions from the high carbamate stability scenario - Where the diamonds are for experimental 40° C data, the circles are for experimental 60° C data and the squares are for experimental 80° C data. The lines are the predicted VLE from the model. The solid line is for 40° C, the dashed line is for 60° C and the dash-dot line is for 80° C.

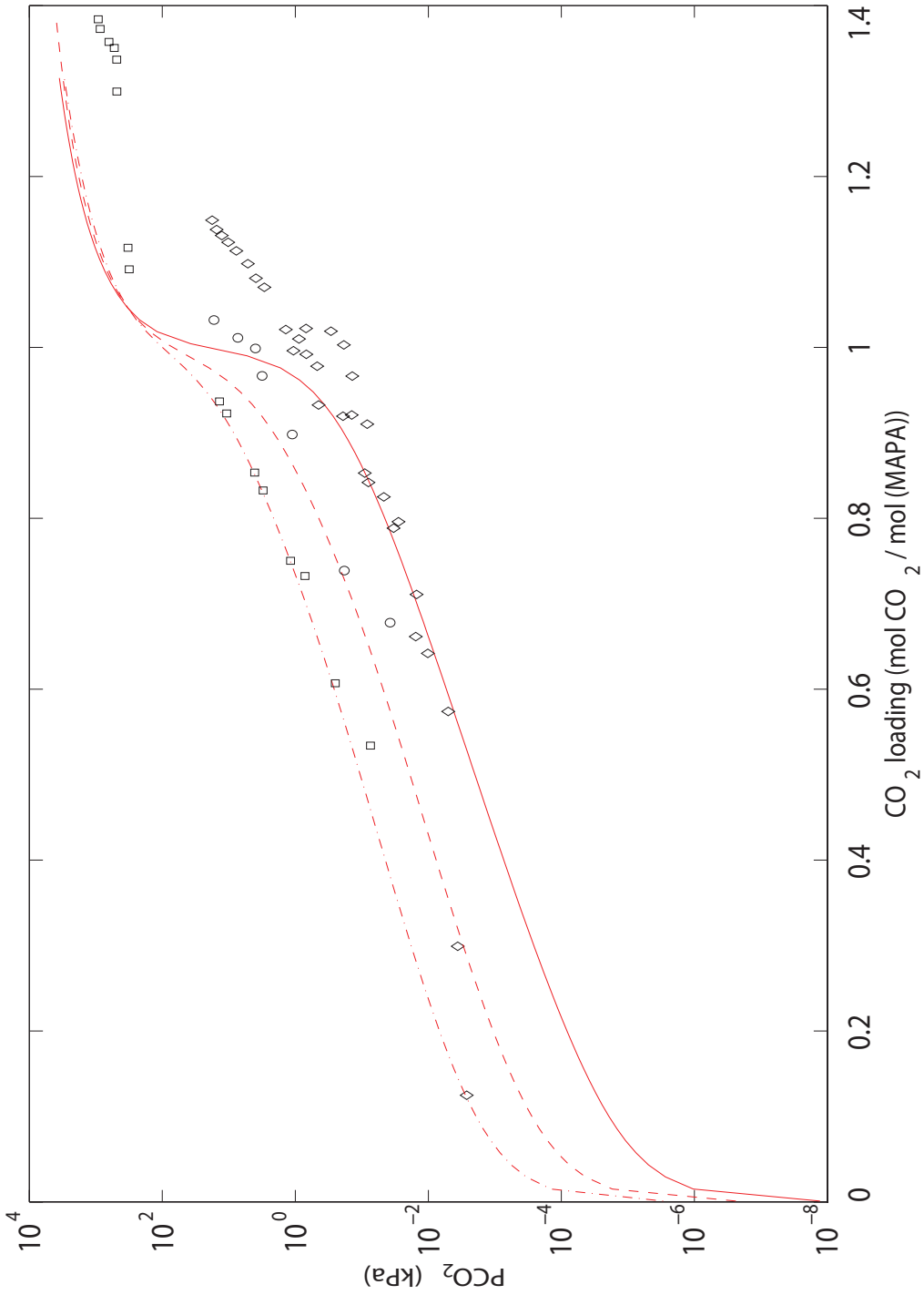

Figure 4.21: The experimental VLE data for the 5M loaded and the predictions from the high carbamate stability scenario - Where the diamonds are for experimental 40° C data, the circles are for experimental 60° C data and the squares are for experimental 80° C data. The lines are the predicted VLE from the model. The solid line is for 40° C, the dashed line is for 60° C and the dash-dot line is for 80° C.

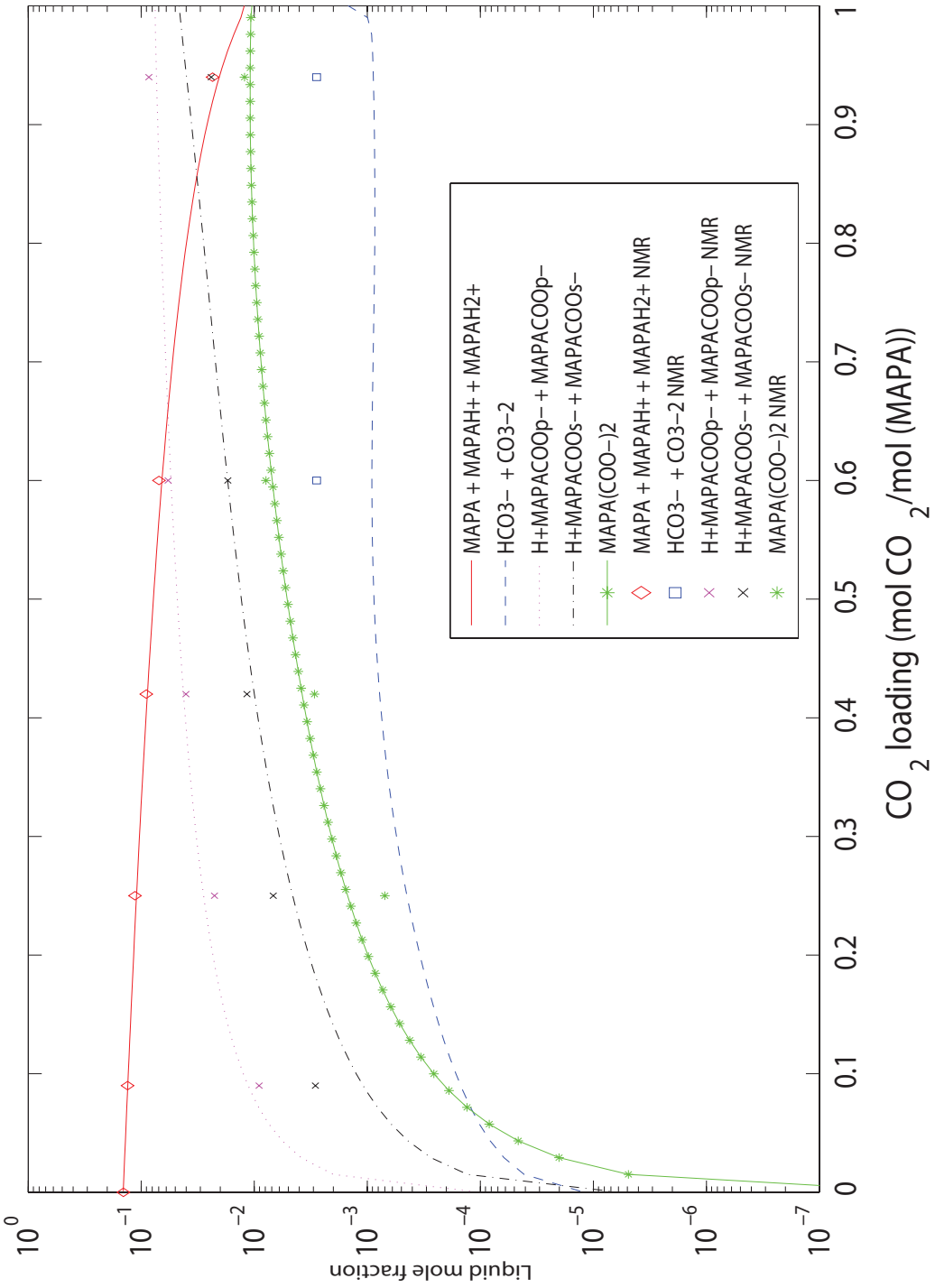

Figure 4.22: The experimental NMR data for the 5M loaded and the predictions from the high carbamate stability scenario - Where the markers are the experimental NMR data and the lines are the predictions from the model

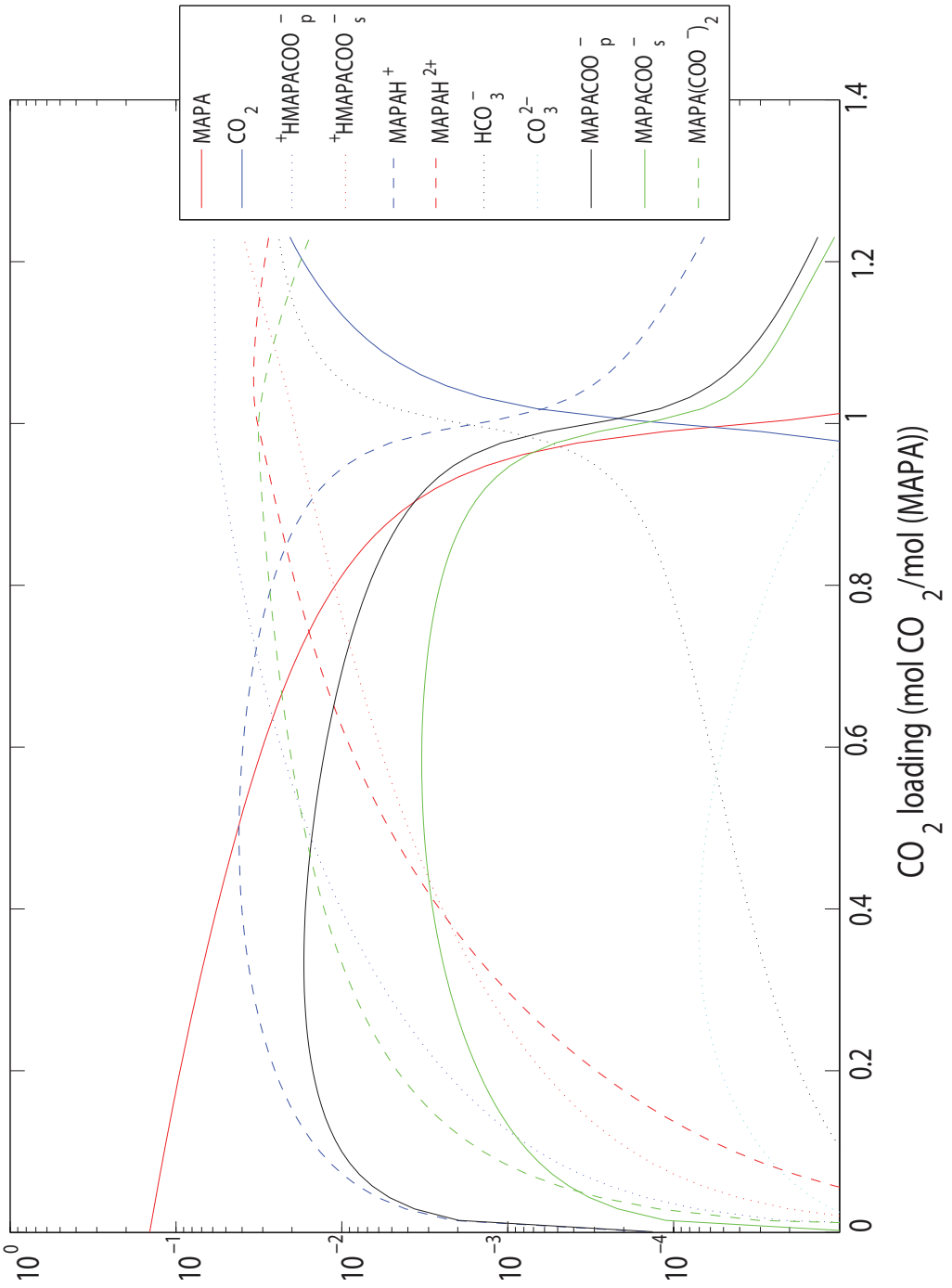

Figure 4.23: Example speciation for the loaded 5M MAPA system at 40°C based on the high carbamate stability scenario -

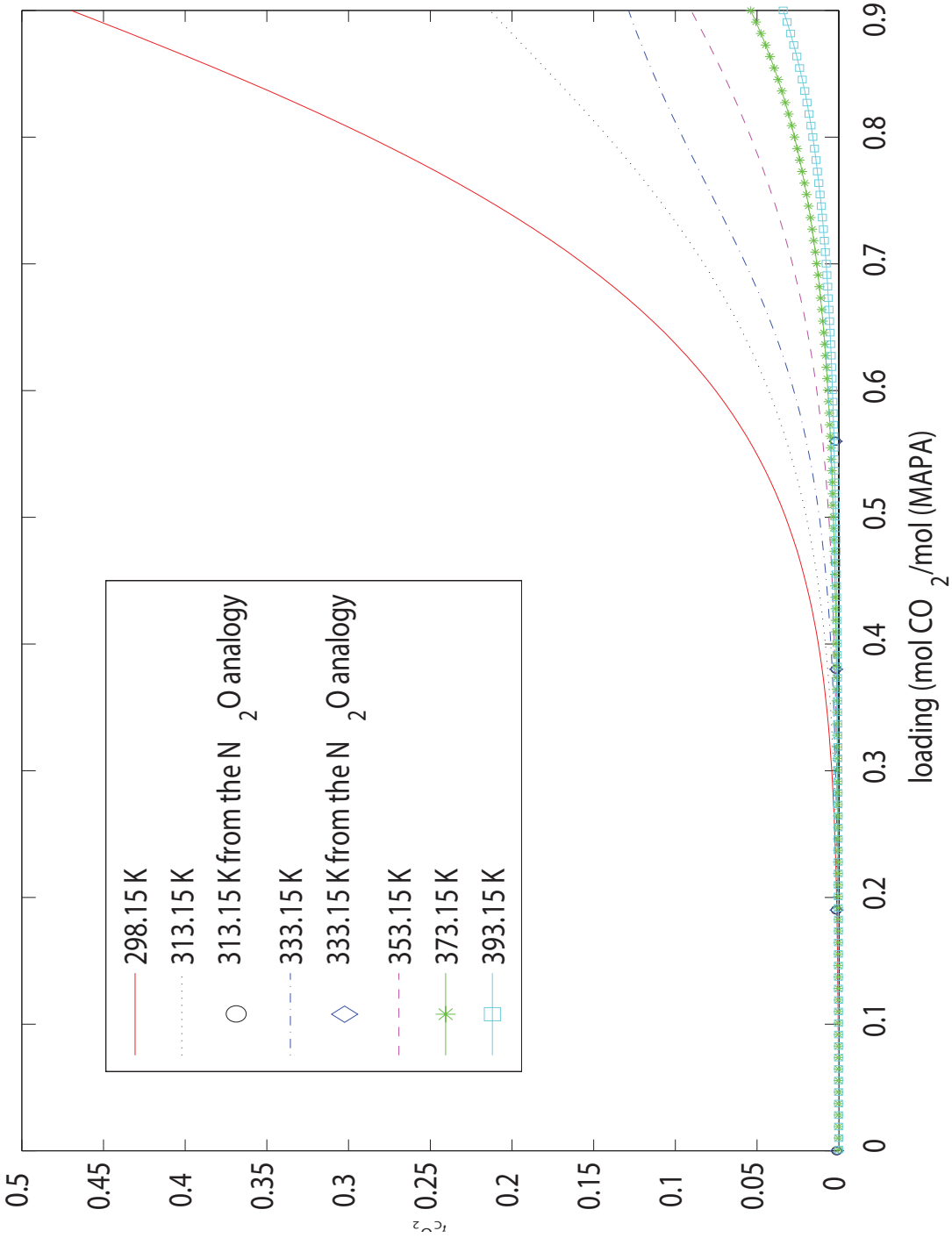

Figure 4.24: The activity coefficient of CO_2 predicted from the model as a function of temperature and loading for the high carbamate stability scenario - The legend is in the figure

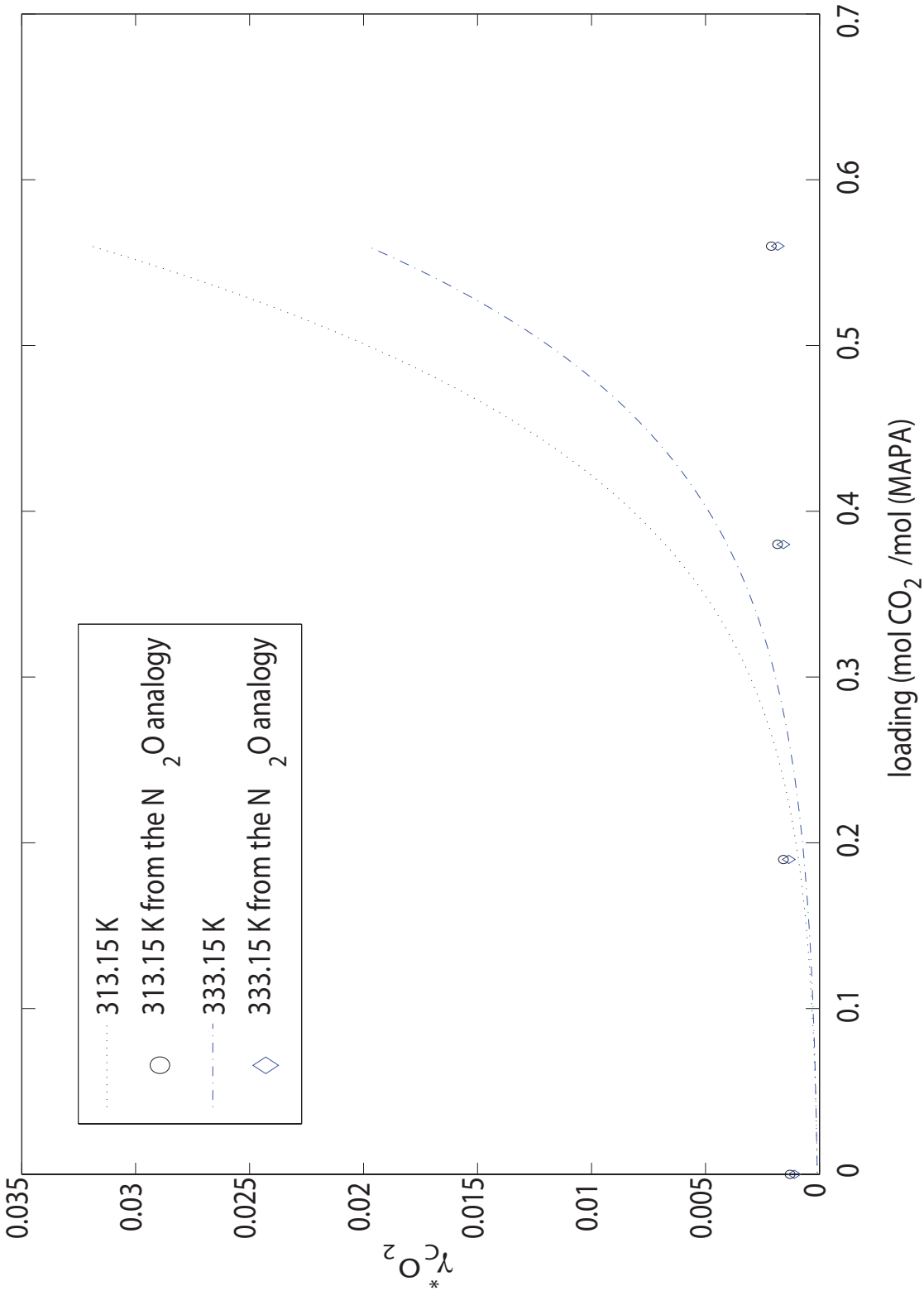

Figure 4.25: The activity coefficient of CO_2 predicted from the model as a function of temperature and loading for the high carbamate stability scenario compared to the experimentally determined activity coefficient of CO_2 from the N_2O analogy - The legend is in the figure

Table 4.5: UNIQUAC parameter u for the "stable carbamate scenario" - Where the grey fields are the parameters from [Aronu et al (1)] and the bold underlined fields are from [Thomsen & Rasmussen (29)]

(a) u0 parameters

u0	H_2O	MAPA	CO_2	$H^+MAPACOO_p^-$	$H^+MAPACOO_s^-$	H_3O^+	$MAPAH^+$	$MAPA(H^+)_2$	OH^-	HCO_3^-	CO_3^{2-}	$MAPACOO_p^-$	$MAPACOO_s^-$	$MAPA(COO^-)_2$
H_2O	**0**													
MAPA	196.7549	506.326												
CO_2	-183.0239	-165.1492	**40.52**											
$H^+MAPACOO_p^-$	110.1	200	-100	-67.27										
$H^+MAPACOO_s^-$	-150	100	-500.1	100.1		0								
H_3O^+	**10000.00**	1.00E+09	-600	100	1.00E+09	1.00E+09								
$MAPAH^+$	-154.0887	400	2500	725	1.00E+09	1.00E+09	0							
$MAPA(H^+)_2$	375.08	150	2500	314.71	1.00E+09	1.00E+09	1.00E+09	25000						
OH^-	600.4952	1.00E+09	1.00E+09	43	1.00E+09	1.00E+09	1.00E+09	1.00E+09	**1562.88**					
HCO_3^-	**517.0278**	-100	2500	429.99	429.99	1.00E+09	2500	100	**2500.00**	2032.8373				
CO_3^{2-}	**361.3877**	200.00	**2500**	-200	-100	1.00E+09	1.00E+09	500	**1588.03**	799.07	**1458.34**			
$MAPACOO_p^-$	0.15	2500	2500	2500	2500	1.00E+09	1.00E+09	2500	1.00E+09	-100.00	-600.00	1500.00		
$MAPACOO_s^-$	100	2600	2500	2500	2500	1.00E+09	1.00E+09	2500	1.00E+09	-100.00	-100.00	1.00E+09	1500.00	
$MAPA(COO^-)_2$	-350.00	-100.00	2500	2500	2500	1.00E+09	1.00E+09	2500	1.00E+09	100.00	100.00	1.00E+09	1.00E+09	2500.00

(b) ut parameters

ut	H_2O	MAPA	CO_2	$H^+MAPACOO_p^-$	$H^+MAPACOO_s^-$	H_3O^+	$MAPAH^+$	$MAPA(H^+)_2$	OH^-	HCO_3^-	CO_3^{2-}	$MAPACOO_p^-$	$MAPACOO_s^-$	$MAPA(COO^-)_2$
H_2O	0													
MAPA	0.7929	-0.37												
CO_2	6.0908	1.666	**13.63**											
$H^+MAPACOO_p^-$	7.5184	0	-6	8.17										
$H^+MAPACOO_s^-$	-2	0	5	0		0								
H_3O^+	**0.00**	0	0	0	0	0								
$MAPAH^+$	10.9052	0.1213	7.3541	0	0	0	0							
$MAPA(H^+)_2$	-0.3880	10	7.3541	10.00	0	0	0	110						
OH^-	8.5455	0	0	0	0	0	0	0	**5.62**					
HCO_3^-	**6.9504**	15.2488	5.8077	6.24	6.24	0	2.8863	0	**0**	17.114				
CO_3^{2-}	**3.3516**	10	**0**	0	10	0	0	10	**2.75**	2.61	**-1.35**			
$MAPACOO_p^-$	0	0	0	0	0	0	0	0	0	0	1	0		
$MAPACOO_s^-$	0	0	0	0	0	0	0	0	0	0	0	0	0	
$MAPA(COO^-)_2$	-9	0	0	0	0	0	0	100	0	0	0	1	0	0

Table 4.6: UNIQUAC parameter u for the "high carbamate stability scenario" optimized for 2M - where the colored values have been changed from the high carabamate stability scenario

(a) u0 parameters

u0	H_2O	MAPA	CO_2	$H^+MAPACOO_p^-$	$H^+MAPACOO_s^-$	H_3O^+	$MAPAH^+$	$MAPA(H^+)_2$	OH^-	HCO_3^-	CO_3^{2-}	$MAPACOO_p^-$	$MAPACOO_s^-$	$MAPA(COO^-)_2$
H_2O	0													
MAPA	196.7549	506.326												
CO_2	-183.0239	-165.1492	40.52											
$H^+MAPACOO_p^-$	110.1	200	887.5	-67.27										
$H^+MAPACOO_s^-$	-150	100	-500.1	100.1		0								
H_3O^+	10000.00	1.00E+09	-600	100	1.00E+09	1.00E+09								
$MAPAH^+$	-154.0887	400	-113.1662	725	1.00E+09	1.00E+09	0							
$MAPA(H^+)_2$	375.08	150	-1106.25	314.71	1.00E+09	1.00E+09	1.00E+09	25000						
OH^-	600.4952	1.00E+09	1.00E+09	43	1.00E+09	1.00E+09	1.00E+09	1.00E+09	1562.88					
HCO_3^-	517.0278	-100	-17.9726	429.99	429.99	1.00E+09	2500	100	2500.0000	2032.8373				
CO_3^{2-}	361.3877	200.0000	2500	-200	-100	1.00E+09	1.00E+09	500	1588.0250	799.0655	1458.34			
$MAPACOO_p^-$	0.15	2500	-100	2500	2500	1.00E+09	1.00E+09	2500	1.00E+09	-100.0000	-600.0000	1500.0000		
$MAPACOO_s^-$	100	2600	2500	2500	2500	1.00E+09	1.00E+09	2500	1.00E+09	-100.0000	-100.0000	1.00E+09	1500.0000	
$MAPA(COO^-)_2$	-350.0000	-100.0000	-1000	2500	2500	1.00E+09	1.00E+09	2500	1.00E+09	100.0000	100.0000	1.00E+09	1.00E+09	2500.0000

(b) ut parameters

ut	H_2O	MAPA	CO_2	$H^+MAPACOO_p^-$	$H^+MAPACOO_s^-$	H_3O^+	$MAPAH^+$	$MAPA(H^+)_2$	OH^-	HCO_3^-	CO_3^{2-}	$MAPACOO_p^-$	$MAPACOO_s^-$	$MAPA(COO^-)_2$
H_2O	0													
MAPA	0.7929	-0.37												
CO_2	6.0908	1.666	13.63											
$H^+MAPACOO_p^-$	7.5184	0	-18.5	8.17										
$H^+MAPACOO_s^-$	-2	0	5	0	0									
H_3O^+	10.91	0	0	0	0	0								
$MAPAH^+$	10	0.1213	7.3541	0	0	0	0							
$MAPA(H^+)_2$	-0.3880	10	9.75	10.00	0	0	0	110						
OH^-	8.5455	0	0	0	0	0	0	0	5.62					
HCO_3^-	6.9504	15.2488	5.8077	6.24	6.24	0	2.8863	0	0	17.114				
CO_3^{2-}	3.3516	10	0	0	10	0	0	10	2.75	2.61	-1.35			
$MAPACOO_p^-$	0	0	0	0	0	0	0	0	0	0	1	0		
$MAPACOO_s^-$	0	0	0	0	0	0	0	0	0	0	0	0	0	
$MAPA(COO^-)_2$	-9	0	0	0	0	0	0	100	0	0	1	0	0	0

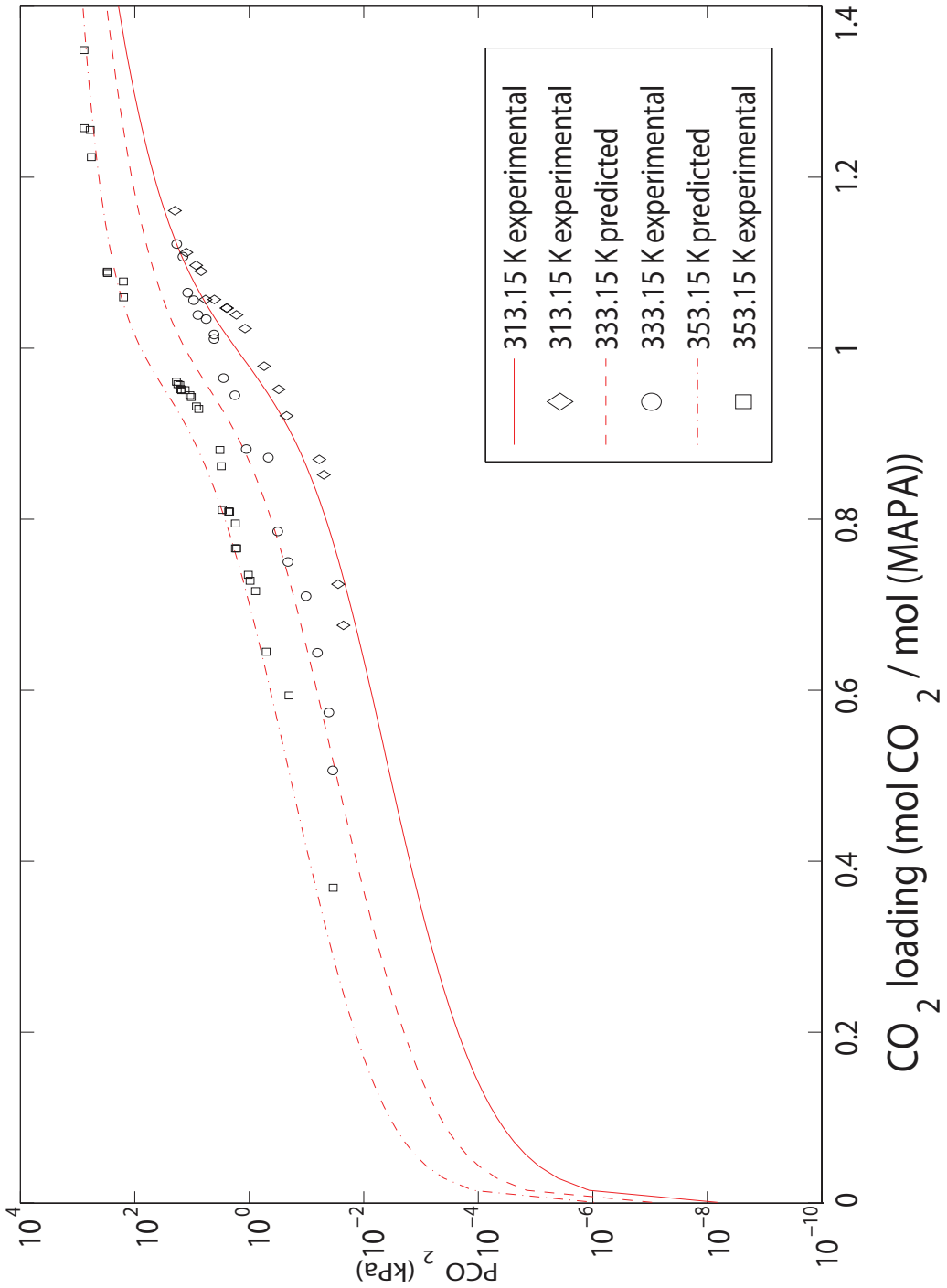

Figure 4.26: The experimental VLE data for the 5M loaded and the predictions from the high carbamate stability scenario - Where the diamonds are for experimental 40° C data, the circles are for experimental 60° C data and the squares are for experimental 80° C data. The lines are the predicted VLE from the model. The solid line is for 40° C, the dashed line is for 60° C and the dash-dot line is for 80° C.

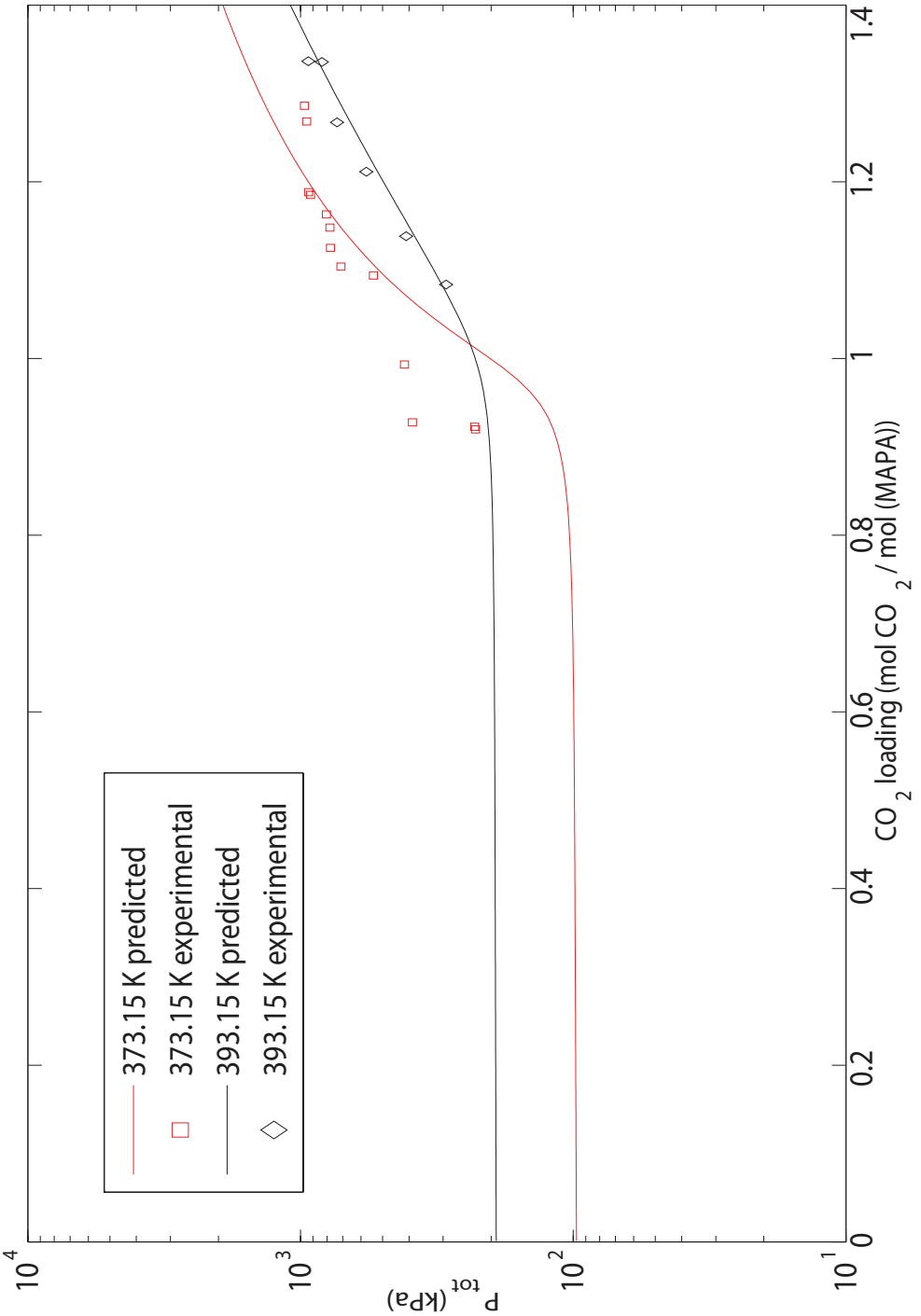

Figure 4.27: The experimental VLE data from the high pressure apparatus and the predictions from the model for the high carbamate stability scenario - The legend is in the figure

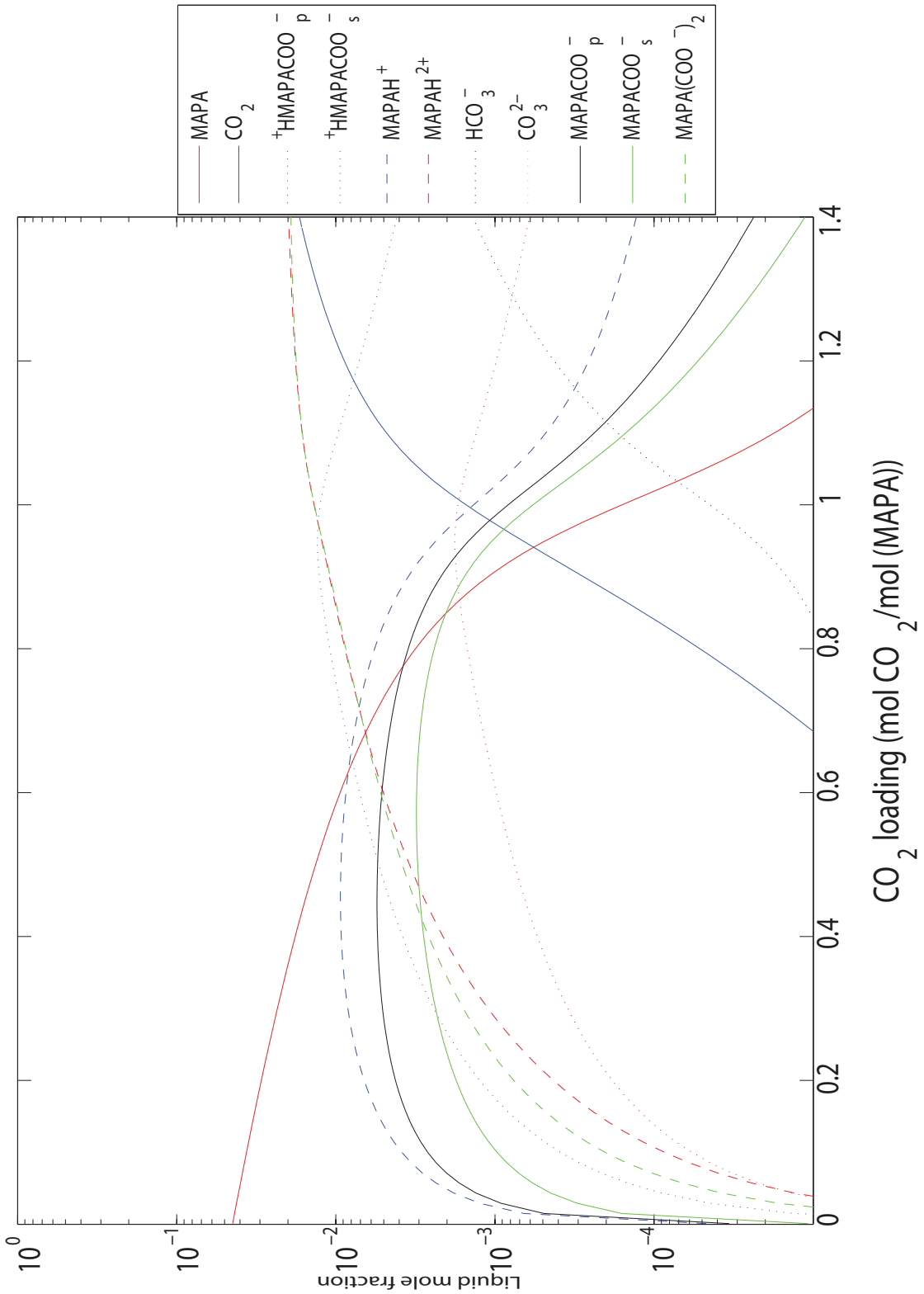

Figure 4.28: Example speciation for the loaded 2M MAPA system at 40°C based on the high carbamate stability scenario optimized for 2M - The legend is in the figure

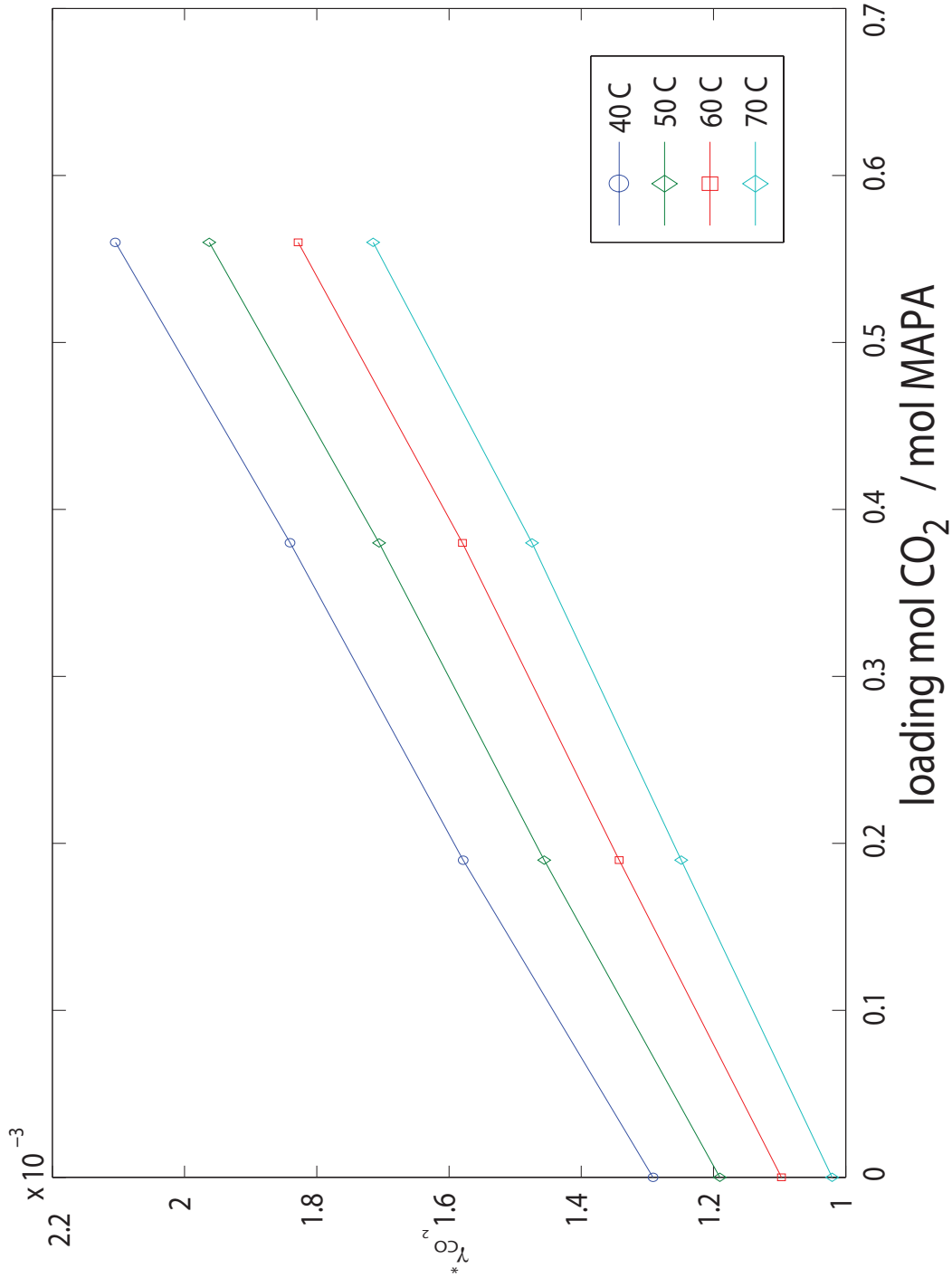

Figure 4.29: The symmetric activity coefficient for CO_2 the loaded 5M MAPA system found from the N_2O analogy - The activity coefficient is a function of both temperature and loading

5

Discussion

5.1 Experimental discussion

5.1.1 On the VLE data

The experimental VLE data for the loaded MAPA system is presented in figures 4.13, 4.14 and 4.15. When considering these figures a few trends become clear; At 40°C, 60°C and 80°C the vle data follow the general trend; when increasing the temperature the capture ability goes down and the partial pressure of CO_2 goes up. At higher temperatures, 100°C and 120°C, however this trend is discontinued. For the 5M case there is no difference in partial pressure of CO_2 between 100°C and 120°C. This is surprising as its thought that a further increasing of temperature should decrease the capture ability. The vle data of the 2M loaded MAPA system are also surprising, here the partial pressures of CO_2 are higher at 100°C than at 120°C. Another interesting effect is that there is no difference in the partial pressure of CO_2 between the two concentrations at 40°C, 60°C and 80°C. This is unusual as for other amines there is a small difference(7). Probably there is a small difference between the two concentrations here aswell, but it is lost in the scatter of the data. If there is no difference it would indicate that there is no effect of water on the partial pressure of CO_2 at these temperatures. At 100°C and 120°C there is a distinct difference between the two concentrations. An explanation for this could be that for the 5M case at these high temperatures and high loadings there are not enough water molecules left to keep the amount

of ions, that would be formed if all the capture ability would be used, completely solvated. For the 2M case this would then not be a problem due to the lesser amount of ions that needs to be kept solvated.
It is worth mentioning that it appears as if the two apparatuses can produce vle data that are consistent with each other, i.e. that the data from the two apparatuses form a continuous line.

5.1.2 On the scatter in the VLE data

As can be seen from the figures 4.13, 4.14 and 4.15, there is considerable scatter in the data. This is the case at all temperatures and concentrations, although some temperatures and concentrations show more scatter than other. The reason for this scatter in the data is unclear. Possible reasons for the scatter could be experimental errors either in the liquid sample analysis or in the pressure measurements. Or it could be a unexplained feature of the loaded MAPA system.
If the pressure measurement is off it would either be an systematic error that don't lead to scatter or a pressure leakage that happened at specific times. Such a leakage would be observed, and it was not. Errors in the liquid sample analysis could include loss of sample, either liquid- or precipitated sample during transfer between glass equipment. This is possible, however four different persons have produced vle data for the loaded MAPA system, and all had scattered results, which decreases the possibility that the scatter is the result of bad laboratory practice. Another loss of CO_2 during the liquid sample analysis could be that during the precipitation of the $BaCO_3(s)$ out of the liquid sample, step 7 in section 3.1.2, not enough heat was supplied so that not all of the capture reactions were completely reversed, leading to not all CO_2 being precipitated out of the solution. The correlation between the amount of CO_2 precipitated and boiling time was investigated more closely and results can be seen in table 4.2. From the table it can be concluded that boiling time it not the reason for the scatter. It is however surprising that there is no correlation between boiling length and amount of CO_2 precipitated. Another explanation could be that the apparatuses were not purged enough leading to oxidative degradation of the amine, this seems

also highly unlikely. The apparatuses used in this work have consistently produced good results for other amines, leading to the conclusion that it's not the experimental method that is the problem. Despite all this it seems highly unlikely that the scatter in the data is the result of an unexplained feature of the loaded MAPA system. It is the authors suggestion that the new apparatus that will be used for measuring the vle in the loading area between the HTA and LTA should be used to produce vle for the loaded MAPA system. If there is less/no scatter then it would indicate that the experimental procedure of the HTA and LTA is the reason for the scatter. It is also recommended to perform the liquid phase analysis in an automatic machine like SINTEF's Apollo to eliminate the human error.

5.2 Modeling discussion

5.2.1 On the model performance

Three scenarios have been presented in this work, the two first scenarios the "high zwitterion stability scenario" and the "high carbamate stability scenario" are two scenarios that predict the NMR data adequately, with exception of CO_3^{2-} and HCO_3^-, as well as the vle data at low loadings, $\alpha < 1$. The "high carbamate stability scenario optimized for 2M" can reproduce the vle data for all loadings and temperatures for the 2M run, it can however not reproduce the NMR data due to convergence problems at 5M. When assessing which scenario that is most likely it could be said none of the above. The inability to describe the high loading vle data is a major flaw which cannot be overlooked. From an speciaition point of view it is more likely that the "high carbamate stability scenario" is the correct one, due to the unlikeliness of the solution containing almost no carbamate as the "high zwitterion stability scenario" predicts.
The high loading prediction problem is likely the result of one of four problems, either there is an unaccounted for reaction which has an influence at high loading, or there is an inconsistency/error/typo in the model. Another possibility is that the solubility representation is not able to predict the actual amount of CO_2 that has been physically solved in the solution. The last possibility could be that the

reactions are correct, but that the correct combination of UNIQUAC parameters and equilibrium constants has not been found.

The first option: Assuming that no completely new compound is formed, there are only limited options for new reactions that could occur at high loadings as the CO_2 has to be stored somehow chemically in the existing species. So either HCO_3^-/CO_3^{2-} is formed in larger quantities, or large quantities of dicarbamate is formed, or somehow the disassembly of the carbamates is hindered in the MAPA system. When considering the difference between the speciation in the "high carbamate stability scenario", figure 4.23, with the speciation of the "high carbamate stability scenario optimized for 2M", figure 4.28, this is partly what happens. Qualitatively, since the one figure is for 2M and the other for 5M, the amount of dicarbamate goes up in the optimized scenario and also the carbamates exist in larger quantities at higher loadings. The speciation of the optimized 2M scenario, figure 4.28 is thought to be more likely than the speciation of the two other scenarios figures 4.23 and 4.19. Especially at higher loadings the sharp drop in concentration of free MAPA and the two carbamates which is displayed on figures 4.23 and 4.19 is thought to be unlikely (7). One could thus argue that the UNIQUAC parameters in the optimized scenario force the components into an speciation which would normally be handled by a reaction that is missing, this can be stated since [Hessen (5)] stated that the main influence on the vle curve are the equilibrium constants, the activity coefficients can only be used to "move" the curve up or down one to two orders of magnitude. When considering the difference between the vle curves of the 2M case of the "high carbamate scenario", figure 4.20, and the vle curves of the 2M optimized scenario, figure 4.28, it becomes clear that the partial pressure curve for the high loading area moves down by much more than just two orders of magnitude. All this points towards a reaction that that is missing in the model, or some other feature that keeps the carbamate from falling apart. One way of determining which of the high zwitterion stability scenario and the high carbamate stability scenario is the correct one, would be to calculate the heat of absorption and to compare it with the heat of absorption measured in [Kim 2009 (17)]. If it is done via Gibbs Helmholtz equation it is dependent on the equilibrium constants. This

was not done in this work due to time constraints.

The second possible reason can never be 100 % disregarded. The model has been searched thoroughly for typo's and inconsistencies, so that it can be stated with some confidence that this should not be the reason. As previously discussed with two different numerical schemes it can be hard to judge if the iteration goes in the correct direction, but as long as it's converging it should not produce erroneous results [Hessen (5)]. One comment on the model. The reason why two numerical schemes were used is because there is no analytical or fast numerical representation for the gradient with regard to the iteration variables. If available this the chemical equilibrium solution routine could be rewritten with only one scheme. This would help with convergence since then a scheme like step length reduction could be employed. From the realization that the speciation of the optimized 2M secario is thought to be the correct one, it could also be stated that the parameters of the optimized 2M scenario are the correct one, but that at higher loadings they become so unideal that the chemical equilibrium calculation routine cannot deal with them. It has to be said however that no other systems seen in the litterature displays so un ideal interaction parameters as the CO_2 parameters in the "high carbamate stability scenario optimized for 2M".

The third possibility is that the current solubility representation, equation 2.18, fails in predicting the amount of CO_2 that is physically solved in the mixture. It is hard to assess the probability this, but it could be the problem. There is one thing that speaks against it, namely the huge quantities of free CO_2 that would have to be solved in the liquid phase, if this was the only reason for the high loading problems.

The last possibility is that the regression done in this work failed to find the optimal configuration of equilibrium constants and UNIQUAC parameters. This is not impossible but the amount of different combinations tested makes this unlikely.

The model also had problems predicting the two points with the lowest loading from Gondal's data. An effort was made to recreate the two data points exper-

imentally. This attempt was not successful. This does not mean that the two data points are invalid, it should be investigated further, due to time constraints this was not done in this work.

5.2.2 On the activity coefficients

When predicting the partial pressures of CO_2 in a gas phase above a loaded solution, the prediction is heavily dependent on both the predicted liquid phase speciation and the predicted solubility of CO_2 in the loaded solution. Since the liquid phase speciation is heavily dependent on the predicted activity coefficients of all the species, especially the activity coefficients of the ions, and the predicted solubility is heavily dependent on the activity coefficient of CO_2, one can state that the predicted partial pressure of CO_2 is heavily dependent on the activity coefficient of CO_2 and the ions in the solution. This makes it an imperative to predict the activity coefficient correctly. The problem is that no experimental data can provide a direct measurement of the activity coefficient of CO_2 and the ions. The only data that was available for regression of the interaction parameters in this work was experimental NMR data and vle data. Thus during the regression the value of the activity coefficients was not constrained but left to vary freely, as the activity coefficients weren't the target of the regression. This means that the configuration of interaction parameters that was found runs the danger of being a "lucky combination". Before it can be claimed that the set of interaction parameters found is the correct one, the parameters have to be tested thoroughly to make sure they are not a lucky combination. Thus it can be stated that any method that can yield the activity coefficient directly is of enormous benefit.

Recently such a method has been postulated. The so called N_2O analogy states that it is possible to measure the activity coefficient of CO_2, by measuring the solubility of N_2O in loaded solutions. [Hartono 2009 (11)] measured the solubility of N_2O in 5M MAPA at different loadings and temperatures. The calculated activity coefficient from this dataset is shown in figure 4.29. The water N_2O solubility was taken from (26). Two trends become clear in this picture.

One, the activity coefficient of CO_2 increases with increasing loading, which is to be expected due to the salting out effect. The other trend which isn't so easy to explain is that the effect of temperature; when the temperature increases the activity coefficient decreases. This is contrary to expectation as a system is thought to be ideal at high temperatures and low pressures. The reason could be that "real" loading was used in the experiments. In other words the amine solution was loaded until the desired loading, then N_2O was addede to measure the CO_2 solubility. This means that the composition of the system is temperature dependent, and thus there is different composition in for each temperature and thus they cannot really be compared. For example the 70°C parallel could contain more of an unideal component, than a parallel of a lower temperature. In [Hartono 2009 (11)] the solubility of CO_2 in neutralized solutions of amine was tested against the calculated solubility of the N_2O anaolgy, and they were found to agree well. This would suggest the anaolgy holds water, at least for the systems tested. The MAPA system was not one of the systems tested. If the N_2O analogy can be verified it would represent an very valuable new reference point for the development of thermodynamic models for electrolyte systems, as the interaction parameters can be regressed against the value of the activity coefficient and not against some physical property that is dependent on the activity coefficient.

The activity coefficients of CO_2 from the "high carbamate stability scenario" are shown in figure 4.24, they show a remarkable smooth trend with regard to temperature. The "nice" trends are not at all expected since, as previously stated, the activity coefficient was left to vary freely during the regression analysis. They also show the same temperature dependency as the N_2O analogy activity coefficient shows, figure 4.29. Figure 4.25 show the comparison between the activity coefficient of CO_2 from the "high carbamate stability scenario" and from the analogy. As expected the model is not capable of predicting the activity coefficient found from the N_2O analogy, as the activity coefficient from the analogy is not added to the regression database.

5.2.3 On the gas phase calculations

When considering the figures 4.3, 4.4 and 4.5, it can be stated that the prediction method adequately can predict the pure second virial coefficient, B_{pure}. The performance of the cross second virial coefficient, B_{cross} prediction method can be assessed by considering figures 4.6,4.7, BenzeneCO2, 4.9 and 4.10. The B_{cross} prediction method also can also adequately predict the experimental data found. From the figures 4.11 and 4.12, which predict the coefficients $B_{MAPA-CO_2}$ and B_{MAPA-H_2O}, one very important conclusion can be drawn. Namely that there is almost no influence of MAPA on the coefficients $B_{MAPA-CO_2}$ and B_{MAPA-H_2O}. This means that even if MAPA would vaporize in significant amounts, which it doesen't [Kim 2009 (17)], it would have little effect on the non ideality of the vapor phase. This is an important realization as it can be used as a basis to justify describing the gas phase of the system when only taking the non-idealities of CO_2 and H_2O into account. This could then be used as an justification for describing the gas phase using the original fugacity coefficient method that was implemented using an Peng Robinson equation of state, where only the non idealities of CO_2 and H_2O were considered. Another reason for using the original Peng Robinson method and not the virial equation approach developed in this work is the consistency with regard to other works that used the this model to regress interaction parameters from experimental vle.

5.2.4 On the parameter regression

As previously stated the regression analysis was very laborious, and in hindsight the author should have used time in the beginning of this work to develop automatic tools to ease the workload. Especially an automatic program that works itself through all the parameters of the extended UNIQUAC model and determines the loading area the different parameters have influence and each parameters significance would save a lot of time.

6

Conclusions & Recommendations

In this work the loaded MAPA system has been thermodynamically characterized. The experimental thermodynamical phase- and chemical equilibrium was measured in the lab as a function of temperature and loading, during several series of experiments. Interaction parameters, based on the extended UNIQUAC framework, and the unknown carbamate equilibrium constants have been determined from a regression analysis. These parameters have been presented and they describe the behavior of the system accurately below loadings of one. Above the model has considerable problems, probably due to reasons discussed.

For future work it should be investigated if it is possible to find the gradients of the activity coefficients with regard to the iteration variables, in either an fast numerical- or an analytical form. The speciation at high loading should also be determined via NMR, as this was critical data that were missing in this work. The scatter of the data should also be investigated in the new vle apparatus that is arriving, and the liquid phase analysis should be carried out automatically in a machine, like SINTEF's Apollo, to eliminate human error. Which of the two scenarios presented in this work, high zwitterion stabiliy or high carbamate stability, is the correct one or whether they both are wrong can theoretically be determined via calculation of heat of absorption. Also it is recommended that the regression analysis is partly or fully automated as it is very time consuming and tedious to do it "manually".

References

[1] Aronu, U.E., Hessen, E.T., Haug-Warberg, T., Hoff, K.A. & Svendsen, H.F. (2011). Vapor-liquid equilibrium in amino acid salt system: Experiments and modeling. *Chemical Engineering Science*, **66**, 2191 – 2198. 38, 58, 63, 71

[2] BASF (2004). *BASF Sicherheitsdatenblatt für Produkt: 3-(Methylamino)propylamin*. 3

[3] Benson, S.W. & Buss, J.H. (1958). Additivity rules for the estimation of molecular properties. thermodynamic properties. *The Journal of Chemical Physics*, **29**, 546–572. 30

[4] correspondence with Dr. Ardi Hartono, E. (2011). 40

[5] correspondence with Dr. Erik T. Hessen, P. (2011). 25, 80, 81

[6] correspondence with PhD candidate Ugochukwu E. Aronu, P. (2011). 37

[7] correspondence with Professor Hallvard F. Svendsen, P. (2011). 6, 77, 80

[8] da Silva, E.F. & Svendsen, H.F. (2004). Ab initio study of the reaction of carbamate formation from co2 and alkanolamines. *Industrial & Engineering Chemistry Research*, **43**, 3413–3418. 6

[9] DIPPR (2004). *The DIPPR Information and Data Evaluation Manager for the Design Institute for Physical Properties. Version 4.1.0*. DIPPR. 4

[10] Faramarzi, L., Kontogeorgis, G.M., Thomsen, K. & Stenby, E.H. (2009). Extended uniquac model for thermodynamic modeling of co2 absorption in aqueous alkanolamine solutions. *Fluid Phase Equilibria*, **282**, 121 – 132. 122

[11] Hartono, A. (2009). *Characterization of diethylentriamine(DEEA) as absorbent for carbon dioxide*. Ph.D. thesis, NTNU. 82, 83

[12] Haug-Warberg, T. (2006). *Den Termodynamiske Arbeidsboken*. Kolofon Forlag As. 12, 13, 124, 126

[13] Hertzberg, T., T. Mejdell (1998). Modfit for matlab. 37

[14] Hessen, E.T. (2010). *Thermodynamic models of CO2 absorption*. Ph.D. thesis, NTNU. 8, 10, 12, 16, 121, 123, 124, 125, 126

[15] Hoff, K.A. (2010). Teknisk Ukeblad 3410. 1

[16] Jens, C.M. (2010). Experimentally determined and modeled enthalpies of protonation for selected amines at elevated temperatures. Project Report, NTNU. 2, 10, 12

[17] Kim, I. (2009). *Heat of reaction and VLE of post combustion CO2 absorbents*. Ph.D. thesis, NTNU. 3, 11, 23, 40, 80, 84

[18] Kim, I. & Svendsen, H.F. (2011). Comparative study of the heats of absorption of post-combustion co2 absorbents. *International Journal of Greenhouse Gas Control*, **5**, 390 – 395, the 5thTrondheim Conference on CO2 Capture, Transport and Storage. 40

[19] Kontogeorgis, G. & Folas, G. (2009). *Thermodynamic models for industrial applications: from classical and advanced mixing rules to association theories*. Wiley. 120, 122

[20] Laurendeau, N. (2005). *Statistical thermodynamics: fundamentals and applications*. Cambridge Univ Press. 13, 34, 36

[21] Materials, S. (2003). *Thermodynamic Properties: Virial Coefficients of Pure Gases and Mixtures*, vol. Virial coefficients of Mixtures: V. 21B. Springer-Verlag. 30, 47, 48, 49, 50, 51, 52, 53

[22] Materials, S. (2003). *Thermodynamic Properties: Virial Coefficients of Pure Gases and Mixtures*, vol. Virial coefficients of Pure components V. 21A. Springer-Verlag. 30, 32, 44, 45, 46, 47, 48, 49, 50, 51, 52, 53

[23] McCann, D.W. & Danner, R.P. (1984). Prediction of second virial coefficients of organic compounds by a group contribution method. *Industrial & Engineering Chemistry Process Design and Development*, **23**, 529–533. 30, 31, 32, 34

[24] Michelsen, M.L. & Mollerup, J. (2007). *Thermodynamic Models: Fundamentals and Computational Aspects*. Tie-Line Publications. 25

[25] Nocedal, J. & Wright, S. (1999). *Numerical optimization*. Springer verlag. 126

[26] Orji, M.E. (2011). *CO2 Solubility in Aqueous solution of MEA by using N2O analogy*. Master's thesis, NTNU. 82

[27] Riazi, M.R., Sahhaf, T.A.A. & Shammari, M.A.A. (1998). A generalized method for estimation of critical constants. *Fluid Phase Equilibria*, **147**, 1 – 6. 32

[28] Sander, B., Rasmussen, P. & Fredenslund, A. (1986). Calculation of vapour-liquid equilibria in nitric acid-water-nitrate salt systems using an extended uniquac equation. *Chemical Engineering Science*, **41**, 1185 – 1195. 121

[29] Thomsen, K. & Rasmussen, P. (1999). Modeling of vapor-liquid-solid equilibrium in gas-aqueous electrolyte systems. *Chemical Engineering Science*, **54**, 1787 – 1802. 11, 12, 58, 63, 71, 121, 123

Appendix A

Experimental method

A.1 LTA procedure

1. Note down the pressure in the room from a barometer.

2. Turn on the fan, set the desired temperature and turn on the heater for the cabinet.

3. Turn on the water bath, and set the desired temperature. Be careful not to open the valve between the water bath and the equilbirum cell before the water bath is on, as the water will flow from the equilibrium cell to the water bath and flood it. Be extra careful when doing experiments at 80 °C as evaporation from the water bath will lead to the error ”low liquid level”, which shuts down the water bath resulting in liquid from the equilibrium cell flowing down into the water bath, flooding it.

4. Remove condensate.

5. Turn on the thermometer which monitors the temperature in the flasks, and in the equilibrium cell.

6. While the temperature is stabilizing the preloaded solution can be made. This is performed by filling the loading apparatus with the desired amine solution, placing the loading apparatus on a scale, connecting the CO_2 gas from a gas bottle and turn it on. This results in the loading of the amine

solution. The amine solution will gain weight, which should be recorded. Since the loading is an exothermic reaction, it is advisable to let the solution cool down, when the weight increase stops, and start the loading procedure again when the temperature of the solution has decreased again.

7. While the solution preloads it self the CO_2 analyzer should be calibrated. The calibration is carried out by setting the valves in such a way that the CO_2 analyzer analyzes a gas with a set CO_2 concentration. Check the response of the CO_2 analyzer for different known concentrations, so that the experimental CO_2 reading can be corrected for.

8. Add the preloaded solution to the flasks, about 150 mL in each flask, via a hand pump.

9. When the temperature in the flasks has reached the desired temperature, $\pm 0.2°C$, start the circulation pump. Open valve V1, slowly to adjust the gas flow from the pump through the amine solution in the flasks. The gas speed should not be to slow, as then the analyzer will have problems, and it should not be to fast either as amine from the solution will be taken into the gas phase, thus changing the concentration of the sample.

10. When acceptable gas speed has been reached, let the system reach equilibrium. This can be seen from the CO_2 analyzer, when the CO_2 content in the gas phase does not vary more than $\pm 0.1\%$. This should not take more than 15 minutes for the higher concentrations, but can take up til 30 minutes for the lower concentrations.

11. Write down the gas phase CO_2 concentration, the temperature of the sample, the temperature of the condensate and stop the pump. Quickly take a liquid sample from the first flask. This liquid sample can then be analyzed as described in section 3.1.2.

12. Dilute the rest of the solution with unloaded amine, in order to decrease the loading.

13. Repeat from point 7.

14. When the experiment is finished for the day, the water bath, heater, fan and circulation pump should be turned off. The next day the procedure starts at point 1 again, with exception that it might not be necessary to preload a new solution.

A.2 HTA procedure

1. When starting the apparatus for the first time with a new solvent, the autoclave should be washed with water several times, dried, and then washed with the desired amine solution.

2. Before use each day it should be flushed, this is carried out by keeping the autoclave pressurized at 5-6 bara with pure CO_2 while opening the bottom valve to let off the overpressure.

3. Start the logging of temperature and pressure on the connected computer.

4. Turn on the fan and heater of the termoset, turn on the oilbath and open the circulation valve.

5. Adjust the CO_2 pressure in the autoclave to 5-6 bara.

6. Add 200 mL of unloaded amine solution with the piston pump, the pressure will gradually be reduced til about 1-3 bara as the CO_2 is absorbed in the amine solution.

7. Adjust the pressure to the desired total pressure via the pressure reduction valve on the gas flasks.

8. Let the autoclave stay pressurized while reaching equilibrium for at least 2 hours.

9. Turn of the pressure and let the apparatus reach equilibrium, this should also take about 2-3 hours. Equilibrium is defined as temperature- and pressure variation of respectively ± 0.2°C and ± 0.01bar over at least 30 minutes.

10. While the apparatus reaches equilibrium the sampling is prepared. To avoid loss of CO_2 from the solution, a 75 mL sampling cylinder which is evacuated and filled with unloaded amine solution is used. It is important to weigh the cylinder while evacuated and with unloaded solution. It is very important that the cylinder does not contain residual amine solution or water from previous samples or washings, this can be prevented by leaving the sampling cylinder in a heating cabinet while the apparatus reaches equilibrium and by flushing the sample cylinder with pressurized air.

11. When the apparatus has reached equilibrium the total pressure and temperature is noted down. The sample cylinder is securely connected to the autoclave and filled up with the sample. Weigh the cylinder afterwards, but wait until the cylinder has cooled down to room temperature before transfering the sample solution from inside the cylinder to a sample glass.

12. Flush the apparatus and refill it with new amine solution so that the experiment can be repeated

A.3 Liquid sample analysis procedure

A.3.1 CO_2 titration procedure

1. Take a 250 mL Erlenmeyer flask and dispense 25ml of 0.5 M $BaCl_2$ and 50mL of 0.1 M NaOH into it.

2. Weigh the flask and tare the scale.

3. Use an automatic pipette and dispense 1 ml of sample into the same Erlenmeyer flask.

4. Record the weight of the added sample.

5. Seal the flask with a stopper with vapor tube.

6. Place the flask on the heater and heat it up until it boils.

7. Boil the content of the Erlenmeyer flask for about 4 minutes[1].
8. After letting the solution boil for 4 minutes transfer it to a cooling tray and let it cool down to room temperature. Replace the stopper with a square of para film and seal the flask.
9. Take a silicone filter and place it in the center of the vacuum filter.
10. Start the vacuum filter.
11. Wet the filter with some distilled water.
12. Place the glass top on top of the filter and clamp it together.
13. Pour you cooled solution into the middle of the filter.
14. Use distilled water to get the last drops from the Erlenmeyer flask into the filter, and go through 3x100 mL washings of the flask, where the water from the washing goes into the vacuum filter.
15. Carefully take of the top of the vacuum filter.
16. Remove the filter paper with the white powder and place it into a 100 mL beaker.
17. Place the top of the vacuum filter on top of the 100 mL beaker and rinse the top with 25 mL of distilled water.
18. Turn of the suction of the vacuum filter.
19. Weigh the beaker with the filter paper and tare the scale.
20. Dispense 40 mL of 0.1 M HCl solution into the beaker with the original solution.
21. Barium carbonate will react with the hydrocloric acid liberating the CO_2 into the solution.
22. Record the weight of the added hydrocloric acid.

[1]This point is discussed further in section 5.1.2

23. Add a magnet to the beaker and put the beaker on a magnetic stirrer to allow the bariumcloride to dissolve completely.

24. Rinse the electrode and NaOH dispenser of the auto titrator with distilled water, then dry it with a paper towel.

25. When the $BaCO_3$ has completely dissolved place the flask on the auto titrator and push start, becareful not to let the electrode or base dispenser touch the stirrer magnet.

26. After the automatic titration has finished remove the beaker and note down the amount of 0.1 M NaOH used.

27. Wash the equipment used.

A.3.2 Amine analysis procedure

1. Take a 100 mL beaker and dispense 60 mL of distilled water into it.

2. Weigh the beaker and tare the scale.

3. Use an automatic pipette to dispense 0.5 mL of sample into the beaker and note the weight increase.

4. Place the beaker on the auto titrator with a magnetic stir rode in the bottom of the beaker.

5. Rinse the electrode and H_2SO_4 dispenser with distilled water and dry with a paper towel.

6. Lower the electrode and dispenser into the solution in the beaker, be careful that the magnetic stir rode does not touch the electrode or dispenser.

7. Start the auto titration.

8. After the titration is finished, note down the amount of H_2SO_4 used.

A.4 Example calculations

Figures A.1, A.2 and A.3 show example calculations based based on the method explained in section 3.1.3.

A.5 Experimental results

The experimental VLE data for the loaded MAPA system available are shown in tables A.1 and A.2. In these tables the data from Peter Bruder, Shahla Gondal are displayed together with the data from this work.

45 wt% MEA		Prøve 13
Type amin:		MAPA 45wt% 80 C
Date:	mmddåå	19.01.2011
WH20	g water	1100.7
WMEA	g Amine	907
Concentration:	Wt. %	45.2
nH20	mol water	61.09
nMEA	mol Amine	10.29
XH2O	molfraction water	0.86
XMEA	molfraction Amine	0.14
CMEA	Amine (mol/kg)	5.12
Gas Phase		
Total pressure	bara	3.696
Temperature	oC	80
Temperature	K	353.15
P (H2O)	bar	0.41
P (amin)	bar	0.01697
P (CO2)	bar	3.27
P (CO2)	kPa	327.34
Liquid sample		
Weight empty	g	1655
Weight empty + unloaded	g	1725.7
weight empty + unloaded + loaded	g	1819.8
Amine Analysis		
Total weight sample	g	164.8
Weight unloaded sample	g	70.7
Weight loaded sample	g	94.1
	CO2 Analysis	Prøve 13
Dato:	mmddåå	24.01.2011
Parallell 1:		
Sample weight	g	0.964
HCl	g	61.483
NaOH	ml	10.958
pH:		
CO2 conc (unloaded + loaded)	mol/kg	2.5917
CO2 conc (loaded sample)	mol/kg	4.5389
Parallell 2:		
Sample weight	g	0.907
HCl	g=ml	61.631
NaOH	g=ml	13.39
pH:		
CO2 conc (unloaded + loaded)	mol/kg	2.6287
CO2 conc (loaded sample)	mol/kg	4.6037
Blind Sample		
HCl	g=ml	40.271
NaOH	g=ml	39.714
pH:		5.25
Blindverdi:	g=ml	0.557
Avg CO2 conc (loaded sample)	mol/kg	4.5713
% difference	%	-1.41
Beregnet aminkons(approx amine conc):	mol/kg ladet løsn	4.0941
Loading basert på ber. Amin	mol CO2/mol amin	1.1166

Figure A.1: Example calculations for the HTA experiments -

FORSØK		A 31	A 32
Dato	ddmmåå		
ID			
Lufttrykk	mm Hg		
Pressure	mbar	997.1	997.1
Tetthet 20C loadet løsning	kg/l		
LIKEVEKTSMÅLING:			
Temperatur, vannbad (T1)	C		
Temp. celle 3 (T2)	C	80	79.9
Temperatur, kondensat	C	15.1	15.8
Kanal	%	19.7000	17.7000
Avlest signal CO2-analysator	mA	19.950	18.170
Kalibrering a		1.2420	1.2420
Kalibrering b		-4.8630	-4.8630
Volum% CO2, analysator	**vol %**	**19.9149**	**17.7041**
VÆSKEANALYSE:			
pH			
Prøve nr		**A 31**	**A 32**
Parallell 1:			
Vekt prøve	g	0.531	0.521
Vekt HCl tilsatt	g	31.021	30.451
NaOH v/titr.	ml	11.856	11.998
CO2 konsentrasjon	**mol/kg**	**1.778**	**1.744**
Parallell 2:			
Vekt tilsatt prøve	g	0.529	0.551
Vekt HCl tilsatt	g	32.543	30.151
NaOH v/titr.	ml	13.434	10.112
CO2 konsentrasjon	**mol/kg**	**1.780**	**1.793**
Blindprøve:			
Vekt HCl tilsatt	g	**22.482**	**22.482**
NaOH v/titr.	ml	**22.202**	**22.202**
Blindverdi	ml	0.280	0.280
Kons CO2 etter forsøk, titrering (middel	**mol/kg**	**1.779**	**1.769**
Appolo:			
Vekt prøve (+ omtrentlig tetthetsmåling)	g (kg/l)		
Appolo middel	ppm		
Justering ppm	ppm		
Justering til titreringsverdier	%		

Figure A.2: Example calculations for the LTA experiments part one

-

Kons CO2 etter forsøk, Apollo	mol/kg		
Kons CO2 etter forsøk, totalt	**mol/kg**	**1.779**	**1.769**
Aminanalyse			
Aminkons. fra GC/titrering	mol/kg		
Tetthet	kg/l		
Molar aminkons. fra GC/titrering 1	mol/L	2.221	2.223
Molar aminkons. fra GC/titrering 2	mol/L	2.178	2.219
Average of 2 runs	mol/L	**2.1995**	**2.221**
Kommentarer:	.		
% Difference		1.95498977	0.180099054
		0.193885925	0.19578115
Beregning av partialtrykk og loading ved likevekt:			
Væskefasen:			
Vektfraksjon CO2		7.83 %	7.78 %
Loading		**0.964**	**0.958**
Temperatur, likevektscelle	K	353.15	353.05
Temperatur, kondensator	K	288.3	288.95
Dampfasen:			
Damptrykk, rent vann	kPa	47.368	47.177
Damptrykk, ren MAPA	kPa	11.775	11.724
Damptrykk, ren	kPa	0.001	0.001
Damptrykk, vann over kondensat	kPa	1.716	1.795
CO2-konsentrasjon, målt	vol %	19.91	17.70
Totaltrykk, P(tot)	kPa	99.71	99.71
Partialtrykk vann, P(H2O)	kPa	1.06	1.05
Partialtrykk, MAPA	kPa	11.51	11.4620
Partialtrykk,	kPa	0.00	0.00
Partialtrykk CO2, P(CO2)	**kPa**	**17.695834**	**15.755025**

Figure A.3: Example calculations for the LTA experiments part two -

Table A.1: Experimental 2M VLE data - The data is plotted in graph 4.13

2M MAPA												
VLE 40°C		VLE 60°C		VLE 80°C		VLE 100°C			VLE 120°C			
Loading	p_{CO2} [kPa]	Loading	p_{CO2} [kPa]	Loading	p_{CO2} [kPa]	Loading	p_{CO2} [kPa]	Ptot [bar]	Loading	p_{CO2} [kPa]	Ptot [bar]	
0.676	0.023	0.506	0.035	0.369	0.034	0.920	131.686	2.297	1.063	107.372	2.997	
0.724	0.028	0.574	0.041	0.594	0.203	0.923	317.417	4.155	1.084	217.387	4.097	
0.852	0.050	0.644	0.065	0.645	0.507	0.928	130.119	2.282	1.138	100.087	2.924	
0.870	0.060	0.710	0.102	0.716	0.777	0.993	290.517	3.886	1.212	381.387	5.737	
0.921	0.223	0.750	0.213	0.728	1.038	1.094	441.990	5.401	1.220	124.234	3.164	
0.952	0.551	0.786	0.320	0.735	0.966	1.104	612.490	7.106	1.232	226.334	4.185	
0.979	0.306	0.872	1.130	0.766	1.655	1.125	678.517	7.766	1.259	357.934	5.501	
1.023	1.187	0.882	0.463	0.766	1.753	1.148	820.600	9.187	1.267	642.672	8.35	
1.039	1.681	0.945	1.789	0.795	3.251	1.163	851.400	9.496	1.285	630.234	8.224	
1.047	2.467	0.965	2.843	0.809	3.081	1.185	681.600	7.797	1.336	541.887	7.342	
1.047	2.491	1.011	4.109	0.809	2.969	1.188	836.100	9.343	1.337	743.672	9.36	
1.057	4.090	1.016	4.122	0.811	1.741	1.269	704.900	8.031				
1.057	5.812	1.034	5.682	0.862	2.207	1.286	869.600	9.677				
1.090	6.946	1.039	9.472	0.881	2.299							
1.097	8.477	1.056	11.893	0.929	10.308							
1.112	12.601	1.065	7.912	0.932	7.635							
1.161	19.977	1.107	14.492	0.943	8.380							
		1.122	18.615	0.945	10.919							
				0.951	15.123							
				0.951	13.193							
				0.952	16.352							
				0.957	18.755							
				0.958	15.755							
				0.964	17.696							
				1.059	158.189							
				1.078	301.439							
				1.088	300.689							
				1.090	157.469							
				1.224	575.139							
				1.255	765.689							
				1.257	598.439							
				1.349	770.539							

Table A.2: Experimental 5M VLE data - The data is plotted in graph 4.14

5M MAPA												
VLE 40°C		VLE 60°C		VLE 80°C		VLE 100°C			VLE 120°C			
Loading	p_{CO2} [kPa]	Loading	p_{CO2} [kPa]	Loading	p_{CO2} [kPa]	Loading	p_{CO2} [kPa]	Ptot [bar]	Loading	p_{CO2} [kPa]	Ptot [bar]	
0.125	0.003	0.678	0.038	0.534	0.074	0.886	66.683	1.573	0.644	0.000	1.658	
0.299	0.004	0.739	0.183	0.607	0.251	0.965	119.193	2.098	0.932	128.651	3.062	
0.574	0.005	0.898	1.111	0.733	0.716	1.013	237.413	3.275	0.953	33.592	2.105	
0.642	0.010	0.967	3.947	0.750	1.180	1.046	325.093	4.157	0.982	224.974	4.025	
0.662	0.015	0.999	7.336	0.833	3.045	1.047	319.164	4.098	0.990	361.848	5.4	
0.711	0.015	1.011	3.129	0.854	4.072	1.069	411.464	5.02	1.008	291.441	4.689	
0.789	0.033	1.032	16.682	0.923	13.778	1.093	621.029	7.113	1.066	447.276	6.254	
0.796	0.028			0.937	10.780	1.263	515.568	6.06	1.081	554.687	7.32	
0.825	0.047			1.091	313.339							
0.842	0.079			1.117	327.339							
0.853	0.090			1.300	482.839							
0.910	0.080			1.337	483.633							
0.920	0.192			1.351	527.739							
0.921	0.142			1.358	632.639							
0.933	0.450			1.373	919.233							
0.967	0.140			1.384	860.133							
0.978	0.469											
0.992	0.681											
0.996	1.070											
1.003	0.186											
1.010	0.881											
1.019	0.290											
1.021	1.390											
1.022	0.689											
1.070	2.918											
1.081	3.909											
1.098	5.169											
1.113	7.688											
1.123	10.208											
1.131	12.726											
1.138	15.245											
1.149	17.763											

Appendix B

Matlab code

B.1 Chemical- and phase equilibrium calculation routine

```
[gam,GAMMAINF]=uniquacMAPA(x,T,c,varargin);



maxit           = 2000;
nl              = n;
errp            = 1;
tolp            = 1e-6;
toly            = 1e-6;
iterp           = 0;
pm              = 0;

% Total pressure is unknown, pressure est. loop
while errp > tolp && iterp < maxit ;
    pp   = x.*gam.*K';
    p    = sum(pp);
    errp = abs(p-pm)/p;
    pm    = p;
    iterp = iterp + 1;
end

errp = 0;
iterp= 0;

pps   = psvec;
ps    = sum(pp);
```

```
y     = pp/p;  % Initial estimate of y
ys      = pps/ps % molefractions of saturated mixture.
errp  = 1;
erry  = 1;
itp   = 0;
it    = 0;
ntots = sum(ys);
ns = ys.*ntots;

while erry>toly && it < maxit
    ym   = y;
    ntot= sum(y);
    n=y.*ntot;

     %phi  = phi_virial(T,p,n,c);   % New fugacity calculation routine ↩
         developed in this work
     %phis = phi_virial(T,ps,ns,c);
     [phi,phis]  = fugcoeff(T,x,ym,p,ps,'vapour',c); % Original fugacity ↩
         calculation routine


    while errp > tolp && itp < maxit; % Internal loop to find total
    %pressure
        pfac  = exp(vi.*(p-psvec)/(c.r*T));% Poynting factor
        pp    = x.*gam.*K'.*pfac'.*phis./phi;
        p     = sum(pp);
        errp  = abs(p-pm)/p;
        pm    = p;
        itp = itp + 1;
    end

    y = pp/p;
    erry = max(abs(y-ym)./y);
    errp = 1; itp = 0;
    it = it + 1;
end
```

B.2 Gas phase calculation

B.2.1 fugacity calculation routine

```
%Function that calculates the fugacity coefficients, phi, and phi_sat for
%a given gas phase based on the Virial equation of state. Based on
%procedure from "Den Termodynamiske Arbeidsboken - Haug-Warberg T. -
%Allkopi 2006 - Chapter 12 pages 136-137".
%
```

```
%INPUT: - Only usable for the MAPA(g)-H2O(g)-CO2(g) system at the moment
%
%       1-Mapa 2-H20 3-CO2
%n = [   n1     n2     n3    ] [mol]
%T [K]
%p [Pa]
%c - struct with physical data
%
%Output: fugacity coefficient - phi [dimless], if the aim is to produce phi
%and phi sat, run the function twice with first the actual pressures and
%then with the saturated pressures.
%
%Implemented by Christian M. Jens, 14-03-2011 - Trondheim

function product = phi_virial(T,p,ps,n,c)

    ntot = sum(n);
    x = n/ntot;
    Amine = 'MAPA';



      % Calculating the second virial coefficients

        B_MAPA = B2(T,c.Tc,Amine);
        B_CO2 = B2(T,c.Tc,'CO2');
        B_H2O = B2(T,c.Tc,'H2O');

        temp = Bcrosstore(T,Amine,c);
        B_CO2_MAPA = temp(1);
        B_H2O_MAPA = temp(2);
        B_CO2_H2O = B2_Mix_Real(T,'H2O-CO2');

    Bij = [ B_MAPA B_H2O_MAPA B_CO2_MAPA ;
            B_H2O_MAPA B_H2O B_CO2_H2O   ;
            B_CO2_MAPA B_CO2_H2O B_CO2]  ;

    %Calculating the "B"s
    %RT*ln phi =p*( 2*Bk/ntot - B )
    B=0;
    for i = 1:length(n)
        for j = 1:length(n)
            B =B + x(i)*x(j)*Bij(i,j);
        end
    end

    Bk = zeros(length(n),1);
    for i = 1:length(n)
        for j=1:length(n)
            Bk(j) =Bk(j) + x(i)*Bij(i,j);
        end
```

```
    end

    Bk = Bk*10^(-6);      %change units to atm
    B  = ntot*B*10^(-6); %change units to atm

    phi = exp( (p*(2*Bk)-B/ntot)/(c.r*T));

product = phi;

end

% A function which finds the cross B's for a system of H_2O, CO_2 and a
% specified component, based on the Pure B's for the above specified components.
%
% Method: the function firsly regresses the experimentally found PURE B's into
% the square well potential equation of B^SWP = B^HS [1+
% (lambda^3-1)(1-exp(eps/kT)], meaning B^SWP, B^HS, lambda^3 and eps are found
% for each component. Then to find for example B_H2O-CO2 the function
% averages the four parameters above with different averaging techniques
% which have been determined by testing prediction against known
% experimentally determined cross B's.


% Input: T[K], comp: name of the third component in the gas phase that contains
% CO2 and H2O, c: struct with physical data.

function Ans = Bcrosstore(T,Comp,c)

    %Estimation of Cross Virial coefficient.
        BHS= zeros(3,1);
        Eps= zeros(3,1);
        B= zeros(3,1);
        BHScross= zeros(3,1);
        BSWcross= zeros(3,1);
        alpha3=zeros(3,1);
        v=zeros(3,1);
        BSW=zeros(3,1);
        Epscross=zeros(3,1);
        alpha3cross=zeros(3,1);


            if strcmp(Comp,'MAPA')
                Tc=c.Tc;
                a=3*240;

            elseif strcmp(Comp,'Benzene')
                Tc=c.Tcbenzene;
                a=3*240;

            elseif strcmp(Comp,'Ethane')
```

```
    Tc= c.Tcethane;
    a=3*240;

elseif strcmp(Comp,'Ethanol')
    Tc= c.Tcethanol;
    a=3*200;

elseif strcmp(Comp,'Propane')
    Tc= c.Tcpropane;
    a=3*240;

elseif strcmp(Comp,'Cyclohexane')
    Tc= c.Tccyclohexane;
    a=3*240;
end
    %a = (3/1.69)*Tc;

    t = [a 0.5*a (1/3)*a];


    %Calculate B(T1), B(T2) and B(T3)

    for i = 1:length(t)
        Tr=t(i)/Tc;
        B(1,i) = B2(t(i),Tr,Comp); % B2 pure component
        B(2,i) = B2(t(i),Tr,'H2O');% B2 pure H2O
        B(3,i) = B2(t(i),Tr,'CO2');% B2 pure CO2
    end


    for i=1:3 %go over number of components - COMPONENT SPECIFIC ↩
        PARAMETERS
        BHS(i)      = B(i,1)+((B(i,1)-B(i,2))^2)/(B(i,2)-B(i,3)↩
            );
        Eps(i)      = c.r*a*log((B(i,2)-B(i,3))/(B(i,1)-B(i,2))↩
            );


    end

    for i=1:3
        v(i)        = exp(Eps(i)/(c.k_boltzmann*t(i)));
        alpha3(i)   = (B(i,1)-BHS(i)*v(i))/(BHS(i)-BHS(i)*v(i))↩
            ;
        alpha(i)    = (alpha3(i))^(1/3);
        q           = exp( Eps(i)/(c.k_boltzmann*T));
        BSW(i)      = BHS(i)*(1+(alpha3(i)-1)*(1-q));
    end


        BHScross(1) = sqrt(BHS(1)*BHS(2)); %Amine H2O
```

```
                        BHScross(2) = sqrt(BHS(1)*BHS(3)); %Amine CO2
                        BHScross(3) = sqrt(BHS(2)*BHS(3)); %Water H2O


                        alpha3cross(1) = (1/512)*((alpha3(1)^(1/9)+alpha3↩
                            (2)^(1/9))^9); %Amine H2O
                        alpha3cross(2) = (1/512)*((alpha3(1)^(1/9)+alpha3↩
                            (3)^(1/9))^9); %Amine CO2
                        alpha3cross(3) = (1/512)*((alpha3(2)^(1/9)+alpha3↩
                            (3)^(1/9))^9); %Water CO2


                        Epscross(1) = sqrt(Eps(1)*Eps(2)); % Amine H2O
                        Epscross(2) = sqrt(Eps(1)*Eps(3)); % Amine CO2
                        Epscross(3) = sqrt(Eps(2)*Eps(3)); % Water CO2

                        q1 = exp( Epscross(1)/(c.k_boltzmann*T)); % Amine ↩
                            H2O
                        q2 = exp( Epscross(2)/(c.k_boltzmann*T)); % Amine ↩
                            CO2
                        q3 = exp( Epscross(3)/(c.k_boltzmann*T)); % H2O-CO2

                        BSWcross(1)= BHScross(1)*(1+(alpha3cross(1)-1)*(1-↩
                            q1)); % Amine H2O
                        BSWcross(2)= BHScross(2)*(1+(alpha3cross(2)-1)*(1-↩
                            q2)); % Amine CO2
                        BSWcross(3)= BHScross(3)*(1+(alpha3cross(3)-1)*(1-↩
                            q3)); % H2O-CO2

Ans = [BSWcross BHS BHScross BSW Eps Epscross alpha3 alpha3cross B(:,1) B(:,2) ↩
    B(:,3)  ];
end

%Function that gives the second virial coefficient of a specified compond.
%
%
%Input required is the Reduced Temperature= T/Tc, and specify which
%compound.
%

function Ans = B2(T,Tr,compound)



    if strcmp(compound,'MAPA') % predicted
        Ans = 189.18 - 458.19./Tr - 251.464./(Tr.^3) -11.8756./(Tr.^7);

    elseif strcmp(compound,'Pyridine') % found from Springer Materials
        Ans = 3.4839 *10^3 -2.4252*10^6/T + 2.6800*10^8/(T^2);

    elseif strcmp(compound,'H2O') % found from Springer Materials
```

```
        Ans = 1.5883*10^2 - (3.0107*10^5)./T + (1.8189*10^8)./(T.^2)...
            -(5.6932*10^10)./(T.^3); % real from pure gases

    elseif strcmp(compound,'CO2') % found from Springer Materials
        Ans = 5.7400*10-(3.8829*10^4)./T + (4.2899*10^5)./(T.^2) -(1.4661*10^9)...
            ./(T.^3); % real from pure gases

    elseif strcmp(compound,'2-Propanol') % found from Springer Materials
        Ans= 1.0296*10^4 -1.4140*10^7/T + 6.4638*10^9/(T^2) -1.0248*10^12/(T^3)...
            ;

    elseif strcmp(compound,'Propene') % found from Springer Materials
        Ans = 1.0101*10^2 -7.5735*10^4/T -7.9502*10^6/(T^2) -2.7987*10^9/(T^3);

    elseif strcmp(compound,'Ethane') % found from Springer Materials
        Ans =-2.8002*10^3 + 2.4580*10^6/T -7.2439*10^8/(T^2) + 6.8408*10^10/(T...
            ^3);

    elseif strcmp(compound,'Benzene') % found from Springer Materials
        Ans = 4.7946*10^2-6.8047*10^5/T + 2.3851*10^8/(T^2) -6.2693*10^10/(T^3)...
            ;

    elseif strcmp(compound,'Ethanol') % found from Springer Materials
        Ans = 9.6838*10^3-1.3575*10^7/(T) + 6.3248*10^9/(T^2)-1.0114*10^12/(T...
            ^3);

     elseif strcmp(compound,'Propane') % found from Springer Materials
      Ans =  1.0971*10^2 -8.4673*10^4/(T)-8.1215*10^6/(T^2) -3.4382*10^9/(T^3);

     elseif strcmp(compound,'Cyclohexane')  % found from Springer Materials
      Ans = 7.3023*10 -1.2813*10^5/T -1.3635*10^7/(T^2) -2.8581*10^10/(T^3);

    end

end

%Function that gives the cross second virial coefficient of a specified compond...
    .
%
%
%Input required is the Reduced Temperature= T/Tc, and specify which
%compound mix.

function Ans= B2_Mix_Real(T,mix)

    if strcmp(mix,'H2O-CO2') % found from springer Materials
        Ans = -1.0744*10^(2)+(1.1123*10^5)./T-(4.0394*10^(7))./(T.^2);
    elseif strcmp(mix,'Ethanol-H2O') % found from springer Materials
        Ans =-1.6626*10^3 + 1.6933*10^6/T -4.7847*10^8/(T^2);
    elseif strcmp(mix,'Propane-H2O') % found from springer Materials
        Ans = 1.9447*10^2-1.0179*10^5/T ;
```

```
    elseif strcmp(mix,'Benzene-CO2') % found from springer Materials
        Ans = -1.7625*10 - 8.5149*10^4/T;
    elseif strcmp(mix,'Ethane-CO2') % found from springer Materials
        Ans = -2.8002*10^3 + 2.4580*10^6/T -7.2439*10^8/(T^2) + 6.8408*10^10/(T↩
            ^3);
    elseif strcmp(mix,'Cyclohexane-CO2') % found from springer Materials
        Ans = -1.9488*10^2 + 3.9274*10^5/T -2.4825*10^8/(T^2) + 3.8182*10^10/(T↩
            ^3);
    end

end
```

B.2.2 Critical properties prediction

```
%Function that predicts Critical Temperature, Volume and Pressure based
% on "A generalized method for estimation of critical constants"
% -Fluid Phase Equilibria 147, 1998. 1Ű6 - Mohammad R. Riazi ),
%Taher A. Al-Sahhaf, Mutlaq A. Al-Shammari.
%
%The function gives back a vector Ans = [Tc(K) Vc(cm3/g) Pc(MPa)]
%and the input needed is M = Molecular mass(g/mol), rho(g/cm3) =
%density of the  pure component at 20C and Tb(K) = Boiling
%temperature at atmospheric pressure.
%
%Implemented by Christian M. Jens, 11-03-2011 - Trondheim
%


function Ans = Critical_properties_Riazi(M,rho,Tb)

% Parameters for Critical Temperature
    a_tc = 1.60193;
    b_tc = 0.00558;
    c_tc = -0.00112;
    d_tc = -0.52398;
    e_tc = 0.00104;
    f_tc = -0.06403;
    g_tc = 0.93857;
    h_tc = -0.00085;
    i_tc = 0.28290;

% Parameters for Critical Volume
    a_vc = 10.74145;
    b_vc = 0.07434;
    c_vc = -0.00047;
    d_vc = -2.10482;
    e_vc = 0.00508;
```

```
    f_vc =  -1.18869;
    g_vc =  -0.66773;
    h_vc = -0.01154;
    i_vc =  1.53161;

% Parameters for Critical Pressure
    a_pc = -8.84800;
    b_pc = -0.03632;
    c_pc = -0.00547;
    d_pc = 0.16629;
    e_pc = -0.00028;
    f_pc =  0.04660;
    g_pc =  -2.00241;
    h_pc = 0.00587;
    i_pc =  -0.96608;




Ans(1) = exp(a_tc+b_tc*M+c_tc*Tb+d_tc*rho+ e_tc*Tb*rho)*(M^f_tc)*
(Tb^(g_tc+h_tc*M)*(rho^(i_tc)));
Ans(2) = exp(a_vc+b_vc*M+c_vc*Tb+d_vc*rho+ e_vc*Tb*rho)*(M^f_vc)*
(Tb^(g_vc+h_vc*M)*(rho^(i_vc)));
Ans(3) = exp(a_pc+b_pc*M+c_pc*Tb+d_pc*rho+ e_pc*Tb*rho)*(M^f_pc)*
(Tb^(g_pc+h_pc*M)*(rho^(i_pc)));
```

B.3 Setup of modfit

```
format long;
%
%% FILE UNIQUACMODMAPA
%
% Heading text
% Fyll inn navn
HEAD{1}='Calculation of interaction parameters for';
HEAD{2}='the UNIQUAC model of MAPA';
HEAD{3}='';
HEAD{4}='';
HEAD{5}='';

% Call file with data
MAPAdata
c=dataMAPA;

% Responses
```

```
Y = pexp;
YNL{1}='CO2 Partial Pressure';  % name of respons 1 (langt navn)
YNK{1}='pco2';  % kort navn (symbol) for responsen

% Independent variables
X = [alfaco2 T wam];
XNL{1}='CO2 loading';  % name of independent var
XNL{2}='Temperature';   % NL = langt navn
XNL{3}='Amine1 weight fraction';
XNK{1}='alfaco2';  % name of independent var
XNK{2}='T'; % NK = kort navn
XNK{3}='wam';


% Defines function to be called by Modfit
USERFUN='uniquacmodMAPA'; % Navn på fil som definerer modellen

% Parameter setup
% Upper and lower boundaries

BMAX = [

          330; ... %u0(3,4)
          100; ... %ut(3,4)
          1d+10; ... %u0(3,5)
          100; ... %ut(3,5)
          1d+10; ... %u0(3,7)
          100; ... ut(3,7)
          1d+10; ... %u0(3,8)
          100; ... %ut*(3,8)
          1d+10; ... %u0(3,10)
          100; ... %ut(3,10)
          1d+10; ... %u0(3,14)
          100; ... % ut(3,14)
       ]';

BMIN = [

          -800; ... %u0(3,4)
          -10; ... %ut(3,4)
          -800; ... %u0(3,5)
          -10; ... %ut(3,5)
          -500; ... %u0(3,7)
          -10; ... ut(3,7)
          -50; ... %u0(3,8)
          -100; ... %ut*(3,8)
          -830; ... %u0(3,10)
          -100; ... %ut(3,10)
          -850; ...     %u0(3,14)
         -100; ...     %ut(3,14)
```

```
];

% Initial values
%Uniquac parameterts


% CO2 interactions
B0(1)  = -150;      %u0(3,4)
B0(2)  = -6.3;     %ut(3,4)
B0(3)  = -500.1;      %u0(3,5)
B0(4)  = 5;        %ut(3,5)
B0(5)  = -600;   % u0(3,6)
B0(6)  = 0.00001;        % ut(3,6)
B0(7)  = -600.1662;      % u0(3,8)
B0(8)  = 10.3541;         %ut(3,8)
B0(9)  = -600;%;  %u0(3,10)
B0(10) = 0.00001;          %ut(3,10)
B0(11) = -600*1.5;       % u0(3,14)
B0(12) = -5.260001;       % ut(3,14)

% Consistency check
Btest = [B0 BMAX BMIN];

% Parameter names (long)
BNL{1}='beta1';   % name of parameter 1 kalles gjerne beta1, beta2 osv.
BNL{2}='beta2';   % name of parameter 2
BNL{3}='beta3';   % name of parameter 3
BNL{4}='beta4';   % name of parameter 3
BNL{5}='beta5';
BNL{6}='beta6';   % name of parameter 2
BNL{7}='beta7';
BNL{8}='beta8';   % name of parameter 2
BNL{9}='beta9';   % name of parameter 2
BNL{10}='beta10';   % name of parameter 3
BNL{11}='beta11';
BNL{12}='beta12';   % name of parameter 2
%BNL{13}='beta13';
%BNL{14}='beta14';    % name of parameter 2
%BNL{15}='beta15';    % name of parameter 2
%BNL{16}='beta15';    % name of parameter 2
% BNL{17}='beta15';    % name of parameter 2
% BNL{18}='beta15';    % name of parameter 2
% BNL{19}='beta15';    % name of parameter 2
% BNL{20}='beta15';    % name of parameter 2
% BNL{21}='beta15';    % name of parameter 2
% BNL{22}='beta15';    % name of parameter 2
% BNL{23}='beta15';    % name of parameter 2
% BNL{24}='beta15';    % name of parameter 2
% BNL{25}='beta15';    % name of parameter 2
% BNL{26}='beta15';    % name of parameter 2
```

```
% Parameter names (short)
BNK={'B1';'B2';'B3';'B4';'B5';'B6';'B7';'B8';'B9';'B10';'B11';'B12';'B13';'B14'↩
    ;'B15';'B16'};%;'B17';'B18';'B19';'B20';'B21';'B22';'B23';'B24';'B25';'B26↩
    '...

% Select parameters that are to be refitted
% 1 -> refit, 0 -> do not fit
%     1  2  3  4  5  6  7  8  9  10  11  12  13  14  15  16  17  18  19  20  ↩
    21  22  23  24  25  26  27  28  29  30  31  32  33  34
BIN=[ 0  1  0  1  0  1  0  1  0  1  0  1 ];%  0  1  1  1  0  0  0 ↩
      0  0  1  1  1  1  1  0

% Regression setup
CRIT=3;             % optimization criteria
ITMAX=200;          % Max number of iterations
FCRIT=0.01;         % Function termination criteria
```

```
function Y = uniquacmodMAPA(beta,X,dat,FLAGG)

% Independent variables
alfaco2 = X(:,1);
T = X(:,2);
wam = X(:,3);
loading = alfaco2;

% mem = uniquac_init;
% s = uniquac_init('struct');
c = dataMAPA;   % Call file with data

 beta

for i=1:length(T)
    [phist(:,i),nhist,gamhist,phihist] = eqmodelMAPA(loading(i),wam(i),T(i),'↩
        UNIQUAC',c,beta);
end

for i=1:length(T)
    if FLAGG(i)==0
        Y(i) = phist(3,i);
    elseif FLAGG(i)==1
        Y(i) = sum(phist(:,i));
    end
end

Y=Y';
```

```
%
%% FILE MAPA DATA

%% 0.452 WT% MAPA DATA

% T=40C data
alfa11 = [0.12483 0.29920 0.66163 0.78857 0.82512 0.91950 0.84199...%Shahla
        1.02226 1.07047 0.93262 0.99612 1.01897 0.96650 0.91028];   %Peter
pexp11 = [0.002651 0.003602 0.015450 0.033342 0.046604 0.191951 0.079436...%↩
    Shahla
        0.68929 2.91780 0.44757 1.06961 0.29060 0.13910 0.08295];   %Peter ↩
                %pCO2
alfa1 = alfa11; %sort(alfa11); B = sort(A) sorts the elements along different ↩
    dimensions of an array, and arranges those elements in ascending order.
pexp1 = pexp11; %sort(pexp11);
T1    = (40 + 273.15)*ones(1,length(alfa1));
wam1  = 0.452*ones(1,length(alfa1));
f1 = 0*ones(1,length(alfa1)); % 0 --> pco2


% T=60C data
alfa22  = [0.89832 0.96676 0.99888 1.03198 0.73885 0.67772 1.01114];
pexp22  = [1.11051 3.94738 7.33619 16.68244 0.18321 0.03771 3.12941];       %↩
    pCO2
alfa2 = sort(alfa22);
pexp2 = sort(pexp22);
T2     = (60 + 273.15)*ones(1,length(alfa2));
wam2  = 0.452*ones(1,length(alfa2));
f2 = 0*ones(1,length(alfa2)); % 0 --> pco2


% T=80C data
alfa33  = [0.92279 0.75034 0.83262 0.85350 0.93679 0.73256 0.60706 0.53400];
pexp33  = [13.77793 1.17997 3.04527 4.07226 10.78022 0.71645 0.25070 0.07420]; ↩
    %pCO2
alfa3 = sort(alfa33);
pexp3 = sort(pexp33);
T3     = (80 + 273.15)*ones(1,length(alfa3));
wam3  = 0.452*ones(1,length(alfa3));
f3 = 0*ones(1,length(alfa3)); % 0 --> pco2


% T=100C data
alfa44  = [0.88593 0.96478 1.01299 1.04668 1.06861 1.26326 1.09335 ];
pexp44  = [157.3 209.8 327.5 409.8 502.0 606.0 711.3];      %ptot
alfa4 = sort(alfa44);
pexp4 = sort(pexp44);
T4     = (100 + 273.15)*ones(1,length(alfa4));
wam4  = 0.452*ones(1,length(alfa4));
f4 = 1*ones(1,length(alfa4)); % 1 --> ptot
```

```
% T=120C data
alfa55  = [0.64428  0.95325 0.93216 0.98181 1.00830 0.98996 1.06604 1.08105];
pexp55  = [165.8 210.5 306.2 402.5 468.9 540.0 625.4 732.0];    %ptot
alfa5   = sort(alfa55);
pexp5   = sort(pexp55);
T5      = (120 + 273.15)*ones(1,length(alfa5));
wam5    = 0.452*ones(1,length(alfa5));
f5 = 1*ones(1,length(alfa5)); % 1 --> ptot

%% for 18.6 wt%

% T=40C data
alfa11 = [ 1.161    1.112   1.097   1.090   1.057   1.057   1.047   1.047   ↩
    1.039   1.023   0.952   0.979   0.921   0.852   0.870   0.724   0.676 ];
pexp11 = [ 19.977449    12.601048   8.477375    6.945504    5.811616    ↩
    4.089923    2.467308    2.490837    1.680685    1.186688    0.551148    ↩
    0.306383    0.223469    0.049975    0.059783    0.028069    0.022629]; ↩
            %pCO2
alfa6 = alfa11; %sort(alfa11); B = sort(A) sorts the elements along different ↩
    dimensions of an array, and arranges those elements in ascending order.
pexp6 = pexp11; %sort(pexp11);
T6    = (40 + 273.15)*ones(1,length(alfa6));
wam6  = 0.186*ones(1,length(alfa6));
f6 = 0*ones(1,length(alfa6)); % 0 --> pco2


% T=60C data
alfa22  = [1.122    1.107   1.056   1.039   1.065   1.034   1.016   1.011   ↩
    0.965   0.945   0.872   0.882   0.786   0.750   0.710   0.644   0.574   ↩
    0.506];
pexp22  = [18.614943    14.492319   11.893128   9.471661    7.912365    ↩
    5.681832    4.122046    4.108678    2.842544    1.789333    1.130388    ↩
    0.463004    0.320364    0.212694    0.101618    0.064720    0.040819    ↩
    0.034839];      %pCO2
alfa7 = sort(alfa22);
pexp7 = sort(pexp22);
T7     = (60 + 273.15)*ones(1,length(alfa7));
wam7  = 0.186*ones(1,length(alfa7));
f7 = 0*ones(1,length(alfa7)); % 0 --> pco2


% T=80C data
alfa33  = [0.961    0.958   0.951   0.943   0.951   0.957   0.952   0.929   ↩
    0.945   0.862   0.932   0.881   0.809   0.809   0.795   0.811   0.766   ↩
    0.766   0.728   0.735   0.716   0.645   0.594   0.369];
pexp33  = [17.695834    15.755025   13.193447   8.380003    15.122527   ↩
    18.754985   16.352015   10.308495   10.918872   2.207362    7.635338    ↩
    2.299357    3.081271    2.968779    3.251284    1.741318    1.752659    ↩
    1.655355    1.037553    0.966179    0.776944    0.507492    0.203117    ↩
    0.034229]; %pCO2
```

```
alfa8 = sort(alfa33);
pexp8 = sort(pexp33);
T8     = (80 + 273.15)*ones(1,length(alfa8));
wam8  = 0.186*ones(1,length(alfa8));
f8 = 0*ones(1,length(alfa8)); % 0 --> pco2


% T=80C high loading data from vippe
alfa33  = [1.0781   1.0880   1.0595   1.0896   1.2236   1.2574   1.3488   1.2553 ];
pexp33  = [3.473    3.4655   2.0405   2.0333   6.21     6.443    8.164    8.1155 ↩
    ]*10^2; %ptot
alfa9 = sort(alfa33);
pexp9 = sort(pexp33);
T9     = (80 + 273.15)*ones(1,length(alfa9));
wam9  = 0.186*ones(1,length(alfa9));
f9 = 1*ones(1,length(alfa9)); % 1 --> ptot


% T=100C  data
alfa33  = [1.0939   1.1041   1.2685   1.1884   1.1631   0.9228   0.9933   1.1253  ↩
    1.1853   1.1483   1.2861   0.9278   0.9199 ];
pexp33  = [5.401    7.106    8.031    9.343    9.496    4.155    3.886    7.766   ↩
    7.797    9.187    9.677    2.282    2.297]*10^2; %ptot
alfa10 = sort(alfa33);
pexp10 = sort(pexp33);
T10     = (100 + 273.15)*ones(1,length(alfa10));
wam10  = 0.186*ones(1,length(alfa10));
f10 = 1*ones(1,length(alfa10)); % 1 --> ptot

% T=120C  data
alfa33  = [1.1385   1.0838   1.2115       1.3357   1.2673   1.3366];
pexp33  = [2.924    4.097    5.737    7.342    8.35     9.36]*10^2; %ptot
alfa11 = sort(alfa33);
pexp11 = sort(pexp33);
T11     = (120 + 273.15)*ones(1,length(alfa11));
wam11  = 0.186*ones(1,length(alfa11));
f11 = 1*ones(1,length(alfa11)); % 1 --> ptot




%% setter opp for modfit
alfaco2 =   [alfa1,alfa2,alfa3,alfa4,alfa5,alfa6,alfa7,alfa8,alfa9,alfa10,↩
    alfa11]';
T       =   [T1,T2,T3,T4,T5,T6,T7,T8,T9,T10,T11]';
wam     =   [wam1,wam2,wam3,wam4,wam5,wam6,wam7,wam8,wam9,wam10,wam11]';
pexp    =   [pexp1,pexp2,pexp3,pexp,4,pexp5,pexp6,pexp7,pexp8,pexp9,pexp10,↩
    pexp11]';
F       =   [f1,f2,f3,f4,f5,f6,f7,f8,f9,f10,f11]';
X       =   [alfaco2 T wam];
Y       =   pexp;
```

```
% weights      =  [w1,w2,w3,w4,w5,w6]';%,w7,w8,w9]';
%semilogy(alfaco2,pexp,'o')
```

Appendix C

Chemical equilibrium solver

C.1 Excess Gibbs energy models

One of the most common ways to describe the thermodynamics of an electrolyte system is through a ”excess gibbs energy model”, these models often contain an long range Debye Hückel term and a short range term. The different Excess gibbs energy models differ in how to describe this ”short range term”[1]

The Excess Gibbs energy is then the sum of the short range and the long range term, as shown in equation C.1, and how it is transformed into the activity coefficient equation is shown in equation C.2.

$$G^E = G^E_{LR} + G^E_{SR} \tag{C.1}$$

$$ln\gamma_i = \left[\frac{\partial \frac{nG^E}{RT}}{\partial n_i}\right]_{P,T,n_{j\neq i}} \tag{C.2}$$

C.1.1 Local composition models

There are two kinds of activity based models, local composition and random mixing models. The random mixing models utilize, as their name indicates,

[1]Can sometimes also be a medium range term

random mixing rules. However, since any real mixing process will be influenced by "intermolecular" forces, any real mixing process will not adequately be described by entirely random mixing rules. Therefore any model which takes this "non-randomness" into account should theoretically be able produce better predictions then the models that only utilize the random mixing. The first equation which took this "non randomness" into account was the Wilson equation in 1964. In general the so called "local composition" models have radically improved the amount of liquid systems which are applicable to modeling. The models who take "non randomness" into account are radically different from the random mixing models, due to their completely different basis. The local composition models are named so because they employ local compositions which are the results of the short range forces in the liquid phase. Local composition models are also more easily extended from binary systems to multicomponent systems [Kontogeorgis (19)].

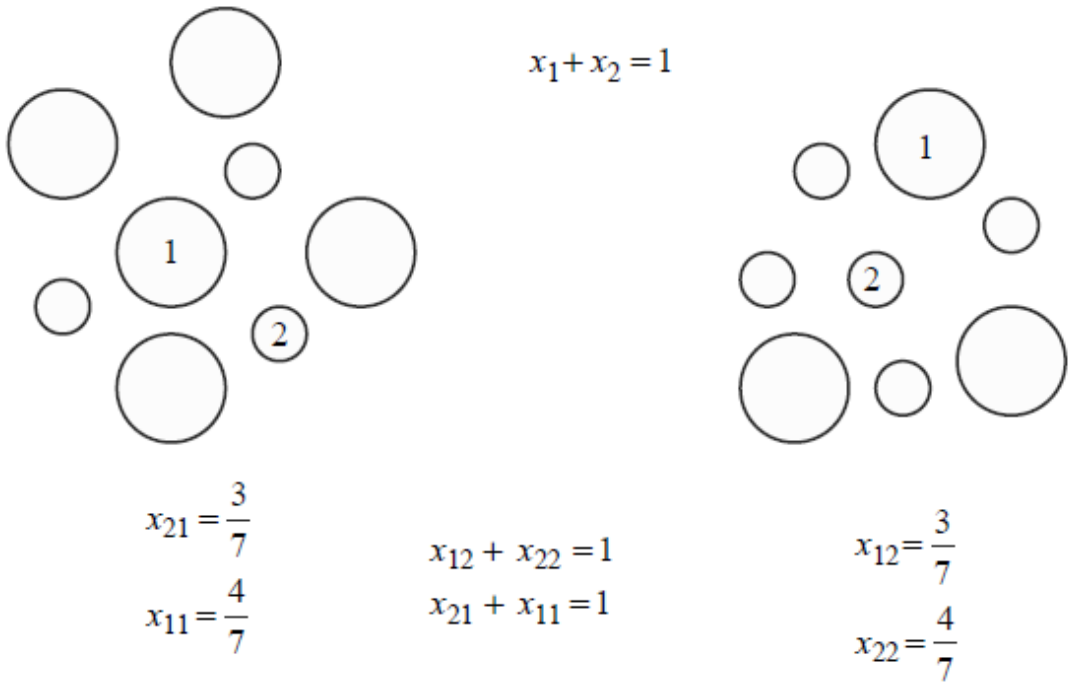

Figure C.1: Illustration of the principle of the local composition model - Where two molecules of different size mix differently in two situations in the same phase [Kontogeorgis (19)]

Arguably the most known local composition models are, NRTL, UNIQAUC and the Wilson equation. In this work the UNIQUAC model was chosen, because the ext. UNIQUAC model is easier to implement than the NRTL model, and because it was thought that the parameters of the UNIQUAC model are easier understood, than the parameters of the other models.

C.1.2 The extended UNIQUAC model

The original UNIQAC model was extended to include an electrostatic term by Sander et al (28). Thus the model includes an electrostatic Debye Hückel term in addition to the original combinatorial- and residual term.The model used in this work is the model of Thomsen and Rasmussen (29). Equation C.3 shows how the different terms of the UNIQAC model are added together.

$$g^{Excess} = g^{Excess}_{combinatorial} + g^{Excess}_{residual} + g^{Excess}_{ext.Debye-Hückel} \tag{C.3}$$

The combinatorial term, equation C.4, accounts for the mixing based on the differences in size between the molecules, the residual term, equation C.5 accounts for the mixing based on the energetic interactions from the nearest neighbors and the Debye Hückel term accounts mixing based on the long range forces [Hessen (14)].

$$\frac{g^E_c}{RT} = \sum x_i ln \frac{\phi_i}{x_i} - \frac{z}{2} \sum (q_i x_i) ln \frac{\phi_i}{\theta_i} \tag{C.4}$$

Here z is the coordination factor, e.g. Z=10 for liquid phase

$$\frac{g^E_r}{RT} = -\sum_i x_i q_i ln \left(\sum_k \theta_k \Psi_{kl} \right) \tag{C.5}$$

Where ϕ_i and θ_i are defined in equations, C.6 and C.7.

$$\phi_i = \frac{x_i r_i}{\sum_i x_i r_i} \tag{C.6}$$

$$\theta_i = \frac{x_i q_i}{\sum_i x_i q_i} \tag{C.7}$$

. Where Ψ_{kl} is defined in equation C.8 and the parameters q and r are the molecular surface area and volume, the so called "Van der Waals volume and area". They can be estimated by for example an least square minimization to experimental VLE or LLE data, as done in Famarazi et al (10).

$$\Psi_{kl} = exp(\frac{u_{kl} - u_{ll}}{T}) \tag{C.8}$$

Where u_{ij} is the binary interaction parameter between molecule "i" and molecule "j", for instance MDEA and water. u_{ij} is assumed to be temperature dependent(10) as equation C.9shows

$$u_{ij} = u_{ij}^0 + u_{ij}^t(T - 298.15) \tag{C.9}$$

Together with the van der Waals volume and area the binary interaction parameter are the main adjustable parameters, of the extended UNIQAC model[1]. It is worth to mention that when the UNIQAC model is derived an term containing $\frac{z}{2}$ appears in the exponential part containing the interaction energies, equation C.8. This is ignored [Kontogeorgis (19)] as it's a far to strong correction for non randomness. It is then rectified when the interaction parameters are fitted to experimental data, as it can be assumed that the z-factor is incorporated into the values for the energy parameters.

The activity coefficient expressions are found by using equation C.2, and the results shown below in equations C.10 and C.11

$$ln\gamma_i^c = ln(\frac{\phi_i}{x_i}) + 1 - \frac{\phi_i}{x_i} - \frac{zq_i}{2}\left(ln(\frac{\phi_i}{\theta_i}) + 1 - \frac{\phi_i}{\theta_i}\right) \tag{C.10}$$

[1]For the original UNIQAC model only the binary interaction parameters are adjustable, as r_i and q_i are functions of the functional groups of the molecule i

$$ln\gamma_i^r = q_i \left[1 - ln\left(\sum_k \theta_k \Psi_{ki}\right) - \sum_k \frac{\theta_k \Psi_k}{\sum_l \theta_l \Psi_{lk}}\right] \tag{C.11}$$

Equation C.12 shows the contribution from the Debye Hückel term:

$$ln\gamma_i^{DH} = -A_{DH} \frac{z_i^2 \sqrt{I}}{1 + b\sqrt{I}} \tag{C.12}$$

Where A_{DH} is the so called Debye Hückel parameter [Hessen (14)], which is defined in equation C.13

$$A_{DH} = \frac{F^2}{8\pi RTN_A} \sqrt{\frac{2F^2}{\varepsilon_0 \varepsilon_r RT}} \tag{C.13}$$

Where b is an constant factor, as shown in equation C.14, and I is the ionic strength, as shown in equation C.15

$$b = 1.50 \left[\frac{1}{kgmol^{1/2}}\right] \tag{C.14}$$

$$I = \frac{1}{2} \sum m_i z_i \left[\frac{mol}{kgH_2O}\right] \tag{C.15}$$

If $T\epsilon[273.15K, 383.15K]$, A_DH can be approximated as a temperature dependent polynomials, equation C.16 [Thomsen (29)]. This was done in this work.

$$A = [1.131 + 1.335 \cdot 10^{-3} \cdot (T - 273.15) + 1.164 \cdot (T - 273.15)^2] \left[\frac{kg^{1/2}}{mol^{1/2}}\right] \tag{C.16}$$

When adding the Debye Hückel term it is important to remember that the combinatorial- and residual terms are the based on the symmetric activity coefficient. The result is that equations C.19, C.17 and C.18 have to be used.

$$ln\gamma_i^{c,\infty} = ln(\frac{r_i}{r_w}) + 1 - \frac{r_i}{r_w} - \frac{zq_i}{2} \left(ln(\frac{r_i q_w}{r_w q_i}) + 1 - \frac{r_i q_w}{r_w q_i}\right) \tag{C.17}$$

$$ln\gamma_i^{r,\infty} = q_i(1 - ln\Psi_{wi} - \Psi_{iw}) \tag{C.18}$$

where the subscript "w" indicates water, assuming the mixture is an aqueous solution. This translates into equation for an ion "i" C.19 and equation for the solvent C.20, water.

$$\gamma_i^* = \frac{\gamma_i^c}{\gamma_i^{c,\infty}} \frac{\gamma_i^r}{\gamma_i^{r,\infty}} \gamma_i^{*,DH} \tag{C.19}$$

$$\gamma_w = \gamma_w^r \gamma_w^c \gamma_w^{DH} \tag{C.20}$$

For a more in depth and thorough explanation of the Debye Hückel theory the reader is referred to the pHd thesis of Erik T. Hessen(14)

C.1.3 Gibbs energy minimization routine

Any Excess Gibbs energy model has to be coupled with an Gibbs energy minimization routine, ie. a chemical equilibrium solver. The following section will describe the equilibrium solver for this model.

Formulation the problem

For a closed system with constant temperature and pressure, the Gibbs energy function is given in equation C.21 as stated in [T. Warberg (12)].

$$G_{eq} = \min_{\mathbf{n}} G(T, p, \mathbf{n}) \tag{C.21}$$

This is subject to some constraints, conservation of mass equation C.22, that no negative moles numbers are calculated equation C.23 and the electro negativity constraint, equation C.24. A constraint means an equation or inequality that has to be fulfilled at any given point.

$$\mathbf{An} = \mathbf{b} \tag{C.22}$$

$$n_i \geq 0 \tag{C.23}$$

$$\sum_i n_i z_i = 0 \tag{C.24}$$

Where A is mass conservation matrix the [1], $\mathbf{n}$ is the composition vector [2] and $\mathbf{b}$ is the vector which contains the total amount of elements in the mass conservation matrix. The problem is to formulate the Gibbs energy as a function of $\mathbf{n}$ and to find the composition vector $\mathbf{n}^{'}$ that minimizes $\mathbf{G}$. This can be rewritten as equation C.25, where all the constraints have been written into equation C.22[3]

$$G_{eq} = \min_{\mathbf{An=b}} G(\mathbf{n}) \tag{C.25}$$

Equation C.25 is now an constrained optimization problem and [Hessen (14)] solves this by using Lagrangian multipliers. Thus equation C.25 can then be rewritten as equation C.26

$$L(\lambda, \mathbf{n}) = G(\mathbf{n}) - \lambda^{\mathbf{T}}(\mathbf{An} - \mathbf{b}) \tag{C.26}$$

Taking the derivative of C.26 and recognizing $d\mathbf{G}/d\mathbf{n} = \mu$ and $d\mathbf{G}/d\lambda = 0$, yields equations C.27 and C.28

$$\frac{\mathrm{d}L}{\mathrm{d}n} = \mu - \lambda^T \mathbf{A} = 0 \tag{C.27}$$

$$\frac{\mathrm{d}L}{\mathrm{d}\lambda} = -\left(\mathbf{An} - \mathbf{b}\right) = 0 \tag{C.28}$$

[1] atom matrix, $\mathbf{A} \in \mathbb{R}^{mxn}$,m = number of elements,n = number of species

[2] $\mathbf{n}, \mathbf{b} \in \mathbb{R}^n$

[3]Sometimes it is not necessary to add the electro negativity constraint to equation C.22. It could be implicitly included in the original constraint equation C.22.

The Gibbs energy an now be written as equation C.29

$$G_{min} = \mathbf{n}\mu^T = \mathbf{n}\mathbf{A}^T\lambda = \mathbf{b}^T\lambda \tag{C.29}$$

For every system that the Lagrangian multiplier method is applied on, the physical meaning of the Lagrangian multiplier changes. Thus in this system the Lagrangian multiplier is the same as the "chemical potential of the elements" [Hessen (14)]. This can be realized from considering equation C.27. The equation for the chemical potential can be rewritten as equationC.30

$$\frac{\mu}{RT} = \frac{\mu^0}{RT} + \ln\gamma + \ln\mathbf{x} \tag{C.30}$$

$$\ln\,\mathbf{x} = \frac{\mathbf{A}\lambda}{RT} - \frac{\mu^0}{RT} - \ln\,\gamma \tag{C.31}$$

In equation C.31 the composition of the system is related to the Lagrangian multiplier. Equation C.32 is an "objective function[2]" [Hessen (14)]. This objective function has been constructed from equation C.29 and contains no new information, as $\sum_i x_i - 1 = 0$, thus reducing the equation to equation C.29.

$$\mathbf{Q}(n_t, \lambda) = n_t\left(\sum_i x_i - 1\right) + \mathbf{b}^T\lambda \tag{C.32}$$

There are many different ways of putting up the equations for the chemical equilibrium, for example the Q function, equation C.32 would is not the only way of doing it. [Haug-Warberg (12)] describes several other ways that could be equally viable.

Solving the problem

The equation set that has been presented cannot be solved analytically, thus a numerical method has to be employed. [Hessen (14)] used an Newton Raphson

[2]dual transformation based on optimization theory, see [Nocedal & Wright](25)

method[1]. The Newton Raphson method is based upon a Taylor expansion of the selected equation/equation set. In this case a Taylor expansion of the objective function Q is the basis for the newton routine, equation C.33.

$$\bigtriangledown \mathbf{Q} + \bigtriangledown^2 \mathbf{Q}\ \mathrm{d}\mathbf{y} = 0 \tag{C.33}$$

Where $\mathbf{y} = [\mathrm{d}\mathbf{n}\ \mathrm{d}\boldsymbol{\lambda}]^T$ is the update vector, i.e. the vector that is being changed when doing a step in the Newton Raphson method. Equation C.33 can be solved for the update vector, this gives equation C.34.

$$\mathrm{d}\mathbf{y} = [\bigtriangledown^2 Q]^{-1} \bigtriangledown Q = H^{-1} g \tag{C.34}$$

Where $\mathbf{H}$ is the Hessian, equation C.36, and $\mathbf{g}$ is the gradient,equation C.35 , of $\mathbf{Q}$.

$$\mathbf{g} = \begin{bmatrix} n_t(\mathbf{Ax} - \mathbf{b}) \\ \sum_i (x_i - 1) \end{bmatrix} \tag{C.35}$$

$$\mathbf{H} = \begin{bmatrix} \frac{\partial^2 \mathbf{Q}}{\partial \lambda \partial \lambda} & \frac{\partial^2 \mathbf{Q}}{\partial \lambda \partial n_t} \\ \frac{\partial^2 \mathbf{Q}}{\partial n_t \partial \lambda} & \frac{\partial^2 \mathbf{Q}}{\partial n_t \partial n_t} \end{bmatrix} = \begin{bmatrix} n_t \mathbf{A}\mathbf{A}^T\mathbf{x} & \mathbf{Ax} \\ \mathbf{Ax} & 0 \end{bmatrix} \tag{C.36}$$

The solver works by calculating the update vector, equation C.34. A step it then introduced in the Lagrangian multiplier, equation C.37, and in the total mole, equation C.38, based on the values of the update vector. The new update vector, $\mathrm{d}y^{k+1}$ is calculated and the error is checked by summing the absolute value of the update vector C.39.

$$\lambda^{k+1} = \lambda^k + \Delta\lambda^k \tag{C.37}$$

$$n_t^{k+1} = n_t^k + \Delta n_t^k \tag{C.38}$$

[1] A numerical scheme for finding approximations for the roots of a real valued function

Where Δn_t and $\Delta \boldsymbol{\lambda}$ are the elements of the update vector,dy^k

$$error = \sum_i |\mathrm{d}y_i| \tag{C.39}$$

The magnitude of the update vector becomes a smaller and smaller as the newton routine closes in on the correct composition, the error then becomes smaller, equation C.39, until its satisfactory small, i.e. the routine ends, yielding the correct equilibrium concentration of the species.

Initiation of the Newton Raphson iteration scheme

When using the Newton Raphson scheme it is important that the initial values are chosen correctly. If this is not done properly convergence of the iteration can be difficult. Recall that the physical meaning of the Lagrangian multiplier is the chemical potential of the elements[1]. The initial "guess" of the Lagrangian multiplier can thus be defined as the standard state chemical potential of the elements. It is a much better parameter to step in then for instance equilibrium composition as there often is no clear initial guess of the equilibrium composition, and a bad guess could easily lead to the iteration not converging. The standard state chemical potential was calculated from the equilibrium constant data. Equations C.40and C.41 shows their calculation. It is very important before using equation C.40, to check the reference state for the reaction. It could be necessary to to change the reference state by multiplying the equilibrium constant with the activity coefficient at infinite dilution.

$$RTln\mathbf{K} = -\ \boldsymbol{\nu}\ \boldsymbol{\mu^0} \tag{C.40}$$

Where $\mathbf{K}$ is a vector with the equilibrium constants of the different reactions, $\boldsymbol{\nu}$ is a matrix with the stoichiometric coefficients of the different reactions, and $\boldsymbol{\mu^0}$ is a vector that contains the standard state chemical potentials. As there are nine species and only four reactions in the modeled system equation C.40 is underspecified. This can be solved by rearranging the equation into the form of

[1]Hydrogen, Carbon, Nitrogen, Oxygen, Potassium and Chlorine

equation C.41. Here the **E** is a matrix that has 1 on the diagonal and 0 on the rest of the elements. The other term added, in the equation, is the " $0/\ \boldsymbol{\mu^0}\ (RT)^{-1}$ " term. This basically states that the value of vector element is either the standard state chemical potential if available in the literature or zero. This is ok as it will be the chemical potential that the solver will step in, so that resulting value at equilibrium will not be zero. The net effect of these two additions is that the equation C.40 has been made solvable.

$$\mu^0 = -RT \begin{pmatrix} \mathbf{N}^T \\ \mathbf{E} \end{pmatrix}^{-1} \qquad \begin{pmatrix} ln\mathbf{K} \\ 0/\mu_0(RT)^{-1} \end{pmatrix} \tag{C.41}$$

Equation C.41 only gives the standard chemical potential of the species[1] and not of the elements[2] which is the starting value for the "Lagrangian multiplier". The standard state chemical potential of the elements is calculated in equation C.42.

$$\boldsymbol{\lambda}_0 = \frac{\mathbf{A}\boldsymbol{\mu}^0}{RT\mathbf{A}\mathbf{A}^{'}} \tag{C.42}$$

As previously stated equation C.42 gives an initial guess of the Lagrangian multiplier, the guess is not however good enough to use as a initial guess in the iteration. Therefore an ideal solution is calculated first, where the total moles are fixed, hence equation C.38 is not used, rather $n_t^{k+1} = n_t^k$, and the step is only applied in the Lagrangian multiplier, equation C.37.

The ideal solution also ignores the activity coefficient. Thus $\boldsymbol{\lambda}_{ideal}$ is calculated which is good enough as a first guess for the real solution iteration, which yields the real composition at the given conditions.

[1] H_2O, MEA, etc
[2] H,O, etc